Implementation of Multiconfiguration Time-Dependent Hartree-Fock for polyatomic molecules

Daniel J. Haxton
Department of Physics, University of California, Berkeley
Workshop *"The Electronic-Structure Problem in Theoretical Strong-Field Physics"*
ITAMP, Harvard, Oct 12 2016

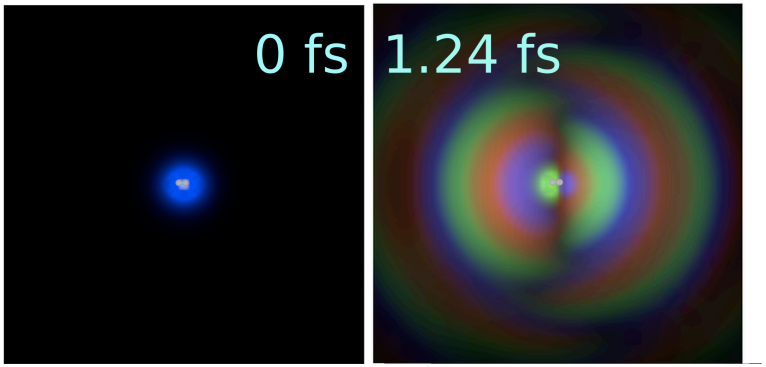

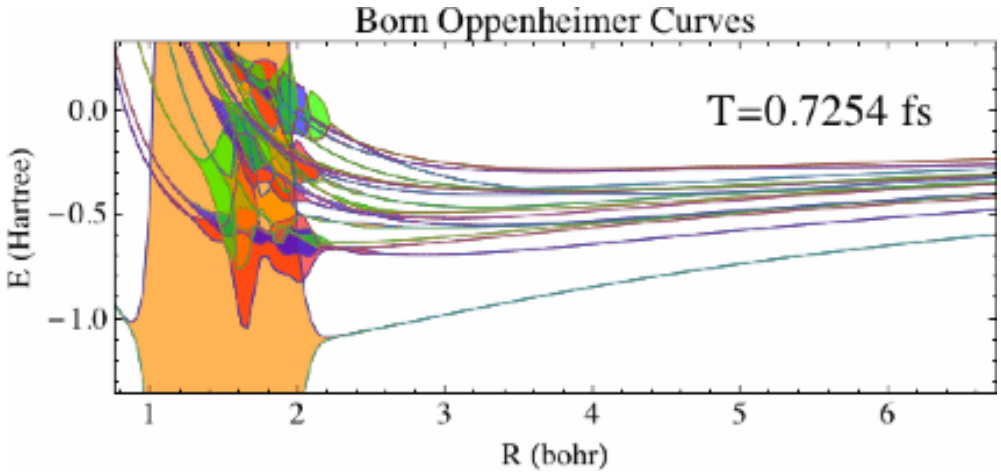

All results here were calculated on LBL's Lawrencium supercluster, **scs.lbl.gov**
with the open-source LBNL-AMO-MCTDHF code, **https://github.com/LBNL-AMO-MCTDHF**

http://danhax.us/ITAMP2016.pdf

U.S. DEPARTMENT OF ENERGY

Schrodinger equation

$$i\hbar\frac{\partial}{\partial t}\Psi(\vec{q},t) = H\Psi(\vec{q},t)$$

Schrodinger equation is linear in ψ.

For applications in ultrafast, nonlinear laser physics of molecules we want to solve this equation with all (or many) electrons active, allowing multiple ionization and all other effects like AC stark shifts.

Interested in

- Transient absorption
- Wave mixing
- Multidimensional spectroscopies

MCTDHF = time-dependent MCSCF

Time-dependent configuration interaction + time-dependent orbitals

MULTICONFIGURATION TIME DEPENDENT HARTREE-FOCK

IS NOT HARTREE-FOCK

ON THE CONTRARY

IT IS MULTICONFIGURATION

Nuclear motion too: *a lot* for diatomics, *a little* for polyatomics

General attack on the several-electron problem

MCTDHF wave function

Time-dependent linear combination of Slater determinants for *f* electrons made from time-dependent orbitals

$$|\Psi(t)\rangle = \sum_{\vec{n}} A_{\vec{n}}(t)|\vec{n}(t)\rangle$$

$$|\vec{n}(t)\rangle = a^{\dagger}_{n_1}(t)a^{\dagger}_{n_2}(t)...a^{\dagger}_{n_f}(t)|0\rangle$$

$$\langle\vec{r}|a^{\dagger}_{\alpha}(t)|0\rangle = \phi_{\alpha}(x,y,z,t) = \sum_{i} c_{i\alpha}(t)\chi_i(x,y,z)$$

Nonlinear MCTDHF equations

$$i\frac{\partial}{\partial t}\vec{A} = (H-\tau)\vec{A}$$

$$i\frac{\partial}{\partial t}\vec{\phi} = \left[(1-P)\left(\rho^{-1}\mathbf{W}+h_0\right)+g\right]\vec{\phi}$$

$$H_{\vec{n}\vec{m}} = \langle\vec{n}|H|\vec{m}\rangle \quad \tau_{\vec{n}\vec{m}} = \langle\vec{n}|\sum_{\alpha\beta} g_{\alpha\beta}a^\dagger_\alpha a_\beta|\vec{m}\rangle$$

$$\mathbf{W}_{\alpha\beta} = \sum_{\gamma\delta}\Gamma^{\gamma\delta}_{\alpha\beta}\mathbf{w}_{\gamma\delta} \quad \rho_{\alpha\beta} = \sum_{\vec{n}\vec{m}} A^*_{\vec{n}}A_{\vec{m}}\langle\vec{n}|a^\dagger_\alpha a_\beta|\vec{m}\rangle$$

$$\mathbf{w}_{\gamma\delta}(\vec{r}) = \int d^3r' \frac{\phi_\gamma(\vec{r'})^*\phi_\delta(\vec{r'})}{|\vec{r}-\vec{r'}|} \qquad P = \sum_\alpha |\phi_\alpha\rangle\langle\phi_\alpha|$$

Code is available open-source

github.com/LBNL-AMO-MCTDHF

Sign up as an official user to get access to the examples

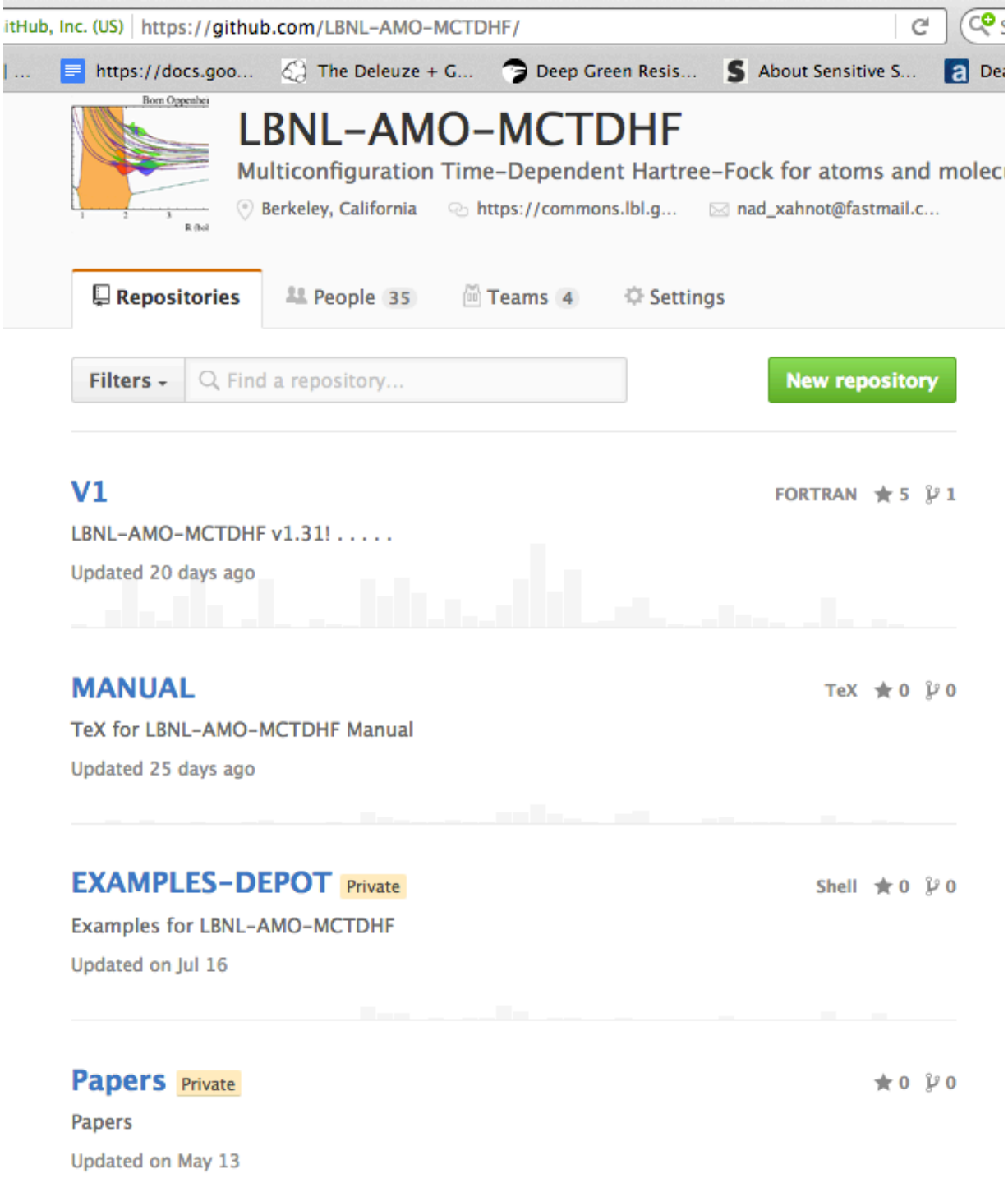

GitHub.com page for LBNL-AMO-MCTDHF organization

35 users in the LBNL-AMO-MCTDHF organization

Main code
Manual tex
Examples
Papers

Code layout

MCTDH.SRC	main program
MCTDH.SRC/H2PROJECT	diatomic subroutines
MCTDH.SRC/HEPROJECT	atomic subroutines
MCTDH.SRC/SINCDVR	polyatomic subroutines
MCTDH.SRC/SINC1D	1d subroutines

Add new coordinate systems easily. Complied as e.g.

COMPDIRS/BIN.ecs.hermnorm/chmctdhf_atom	Usual version:
COMPDIRS/BIN.ecs.hermnorm/chmctdhf_diatom	complex scaling,
COMPDIRS/BIN.ecs.hermnorm/chmctdhf_sinc	Hermitian norm
COMPDIRS/BIN.ecs.cnorm/cmctdhf_atom	Versions with
COMPDIRS/BIN.ecs.cnorm/cmctdhf_diatom	complex scaling,
COMPDIRS/BIN.ecs.cnorm/cmctdhf_sinc	c-norm

Well-behaved solution of TD Schrodinger equation for highly nonlinear pulses

Rabi flopping in CN radical, C 1s ←→ 5σ

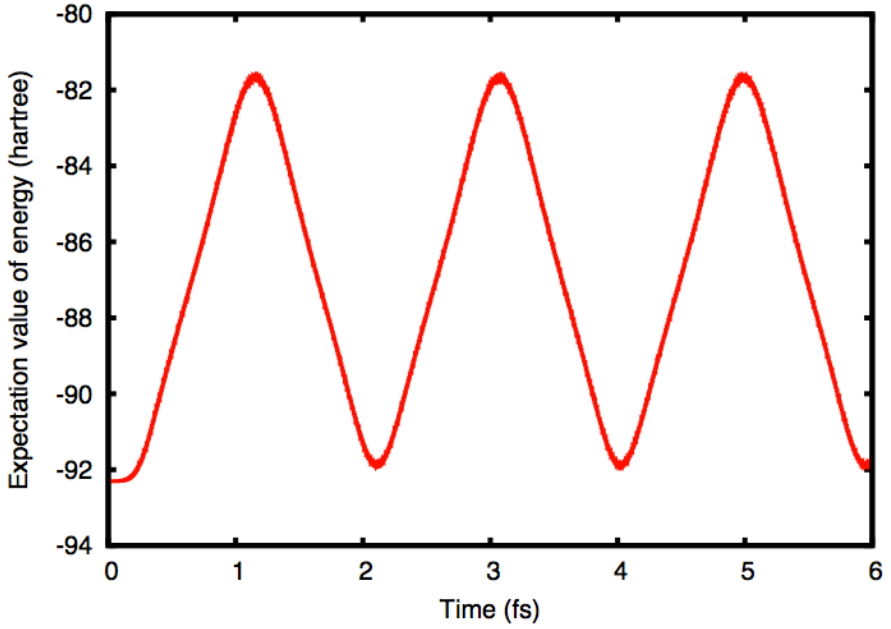

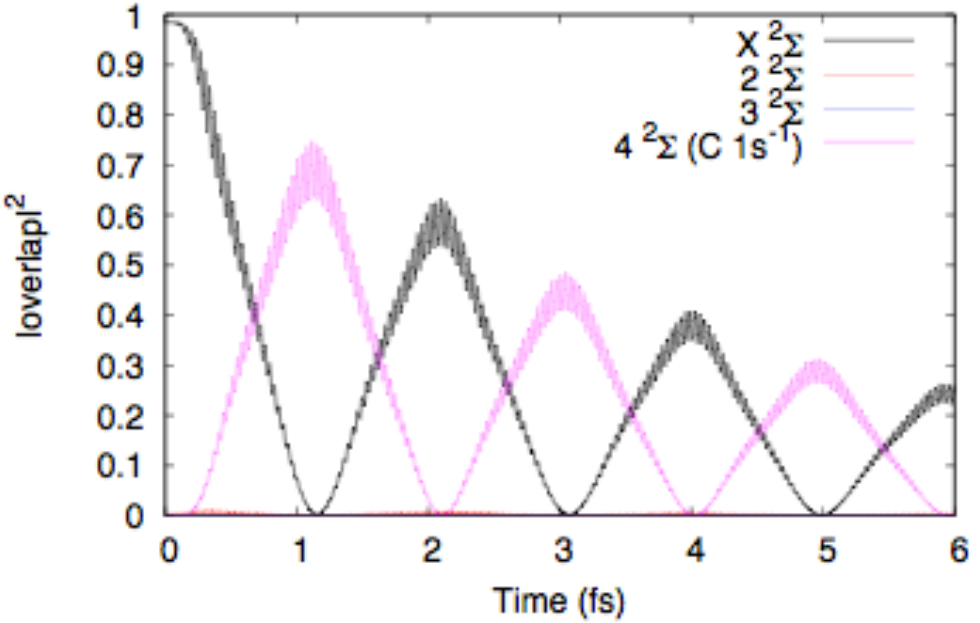

POLYATOMIC LBNL-AMO-MCTDHF (chmctdhf_sinc) **HURDLES OVERCOME**

1) Unconditionally stable predictor-corrector algorithm for propagation of orbitals and configuration coefficients separately **Phys. Rev. A. 83, 063416 (2011)**

2) Treatment of matrix elements between wave functions with different orbitals (e.g. orbitals of ψ(t) at different times) **Phys. Rev. A. 83, 063416 (2011)**

$$\mathbf{S}\vec{B} = \vec{A} \rightarrow \vec{B} = \exp(-\ln\ \mathbf{S})\vec{A}$$ **!**

3) Cartesian polyatomic representation using (A) Poisson method, following Rescigno's method in spherical coordinates, and (B) Triple Toeplitz Matrix-vector multiplication for two-electron matrix elements; giving O(N log N) scaling not $O(N^4)$, $N=n^3$ for cubic grids **arxiv 1507.03324**

4) Original derivation of complete MCTDHF equations of motion for arbitrary Slater determinant lists. Three versions, MacLachlan and Lagrangian stationary principles and also density matrix constraint. No restriction to full CI nor any other. **Phys. Rev. A 91, 012509 (2015)**

Current method for propagating MCTDHF equation

4-step Linear Mean Field predictor-corrector method

Orbitals and Slater determinants propagated independently each step

1) Slater determinants only (CI step)
2) Slater determinants (1^{st} order Magnus) and orbitals (LMF)
3) Slater determinants (1^{st} order Magnus) and orbitals (LMF)
4) Slater determinants only (1^{st} order Magnus) (2^{nd} order better?)

Polyatomic grid method using sinc basis functions

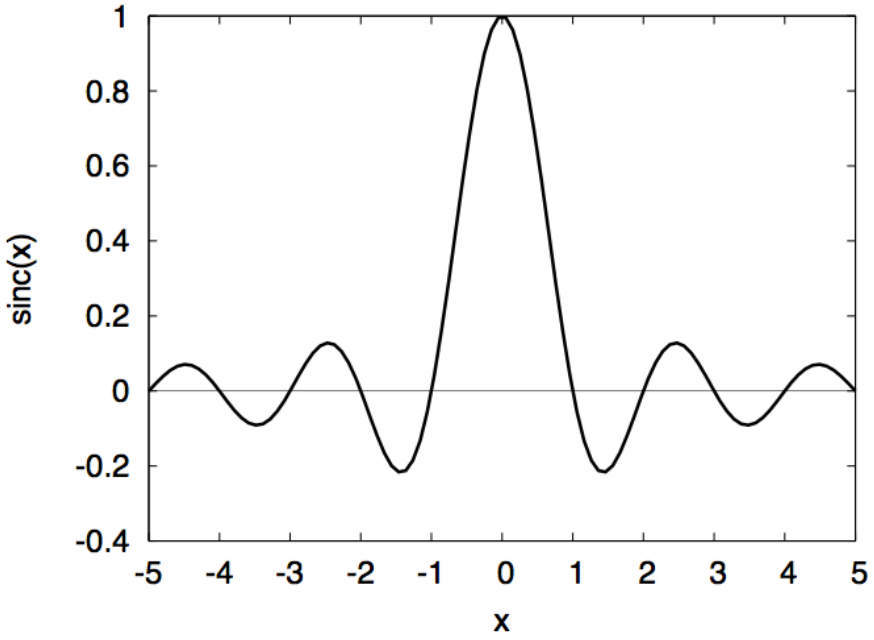

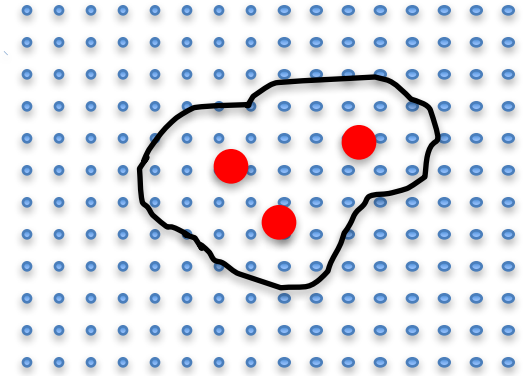

$$\mathrm{sinc}(x) \equiv \frac{\sin(\pi x)}{\pi x}$$

$$\phi_{i_1 i_2 i_3}(x, y, z) = \mathrm{sinc}(x/\Delta - i_1)\mathrm{sinc}(y/\Delta - i_2)\mathrm{sinc}(z/\Delta - i_3)$$

Polyatomic grid method using sinc basis functions

Use Poisson's equation to obtain sparse representation of $1/r_{12}$ via kinetic energy

$$\langle \vec{i}\vec{j}| \frac{1}{r_{12}} |\vec{k}\vec{l}\rangle \approx \delta^3_{\vec{i}\vec{k}} \delta^3_{\vec{j}\vec{l}} \, 2\pi \Delta^{-3} (T^{-1})_{\vec{i}\vec{j}}$$

Limit of matrix inverse as size of matrix goes to infinity

An ideal resolution-of-the-identity approximation in which the auxilliary basis, the basis in which the density is expanded, is the same as the basis used in the calculation.

Following McCurdy, Baertschy, and Rescigno, J. Phys. B, 37, R137 (2004)
See http://arxiv.org/abs/1507.03324, to appear in Mol. Phys.

Fully parallel polyatomic implementation, OpenMP/MPI for both orbitals and configuration coefficents, O(N log N) method for polyatomic version

Millions of Slater determinants and millions of sinc basis functions.

Orientation-averaged calculations on NO_2 take ~10,000 CPU-hours per data point. (grid 55x55x55 with 121 CPUs, 7 calculations, 12 hours each)

Parallelization of MCTDHF method

Three aspects:

1) Slater determinants
2) Different orbitals, different processors atom & diatomic
3) Every orbital divided among all processors polyatomics

$$i\frac{\partial}{\partial t}\vec{A} = (H - \tau)\vec{A}$$

$$i\frac{\partial}{\partial t}\vec{\phi} = \left[(1 - P)\left(\rho^{-1}\mathbf{W} + h_0\right) + g\right]\vec{\phi}$$

$$\mathbf{W}_{\alpha\beta} = \sum\nolimits_{\gamma\delta} \Gamma^{\gamma\delta}_{\alpha\beta}\mathbf{w}_{\gamma\delta}$$

Analysis Capabilities

A) Can project on eigenfunctions to obtain **populations**

$$\langle \psi_i | \Psi(t) \rangle$$

B) Can calculate **absorption/emission**

C) Can calculate **photoionization yields** (with final state of cation, and angular for atoms and diatomic molecules)

Photoabsorption

Calculate response function S from Fourier transform of induced dipole D and input field E

$$S(\omega) = 2\ \mathrm{Im}\left(D(\omega)E(\omega)^*\right)$$

Total change in energy

$$\Delta E = \hbar \int d\omega\ \omega S(\omega)$$

Cross section or generalized cross section obtained as

$$\sigma(\hbar\omega) = 4\pi\alpha\omega \frac{S(\omega)}{|E(\omega)|^2}$$

Lithium 15 orbitals

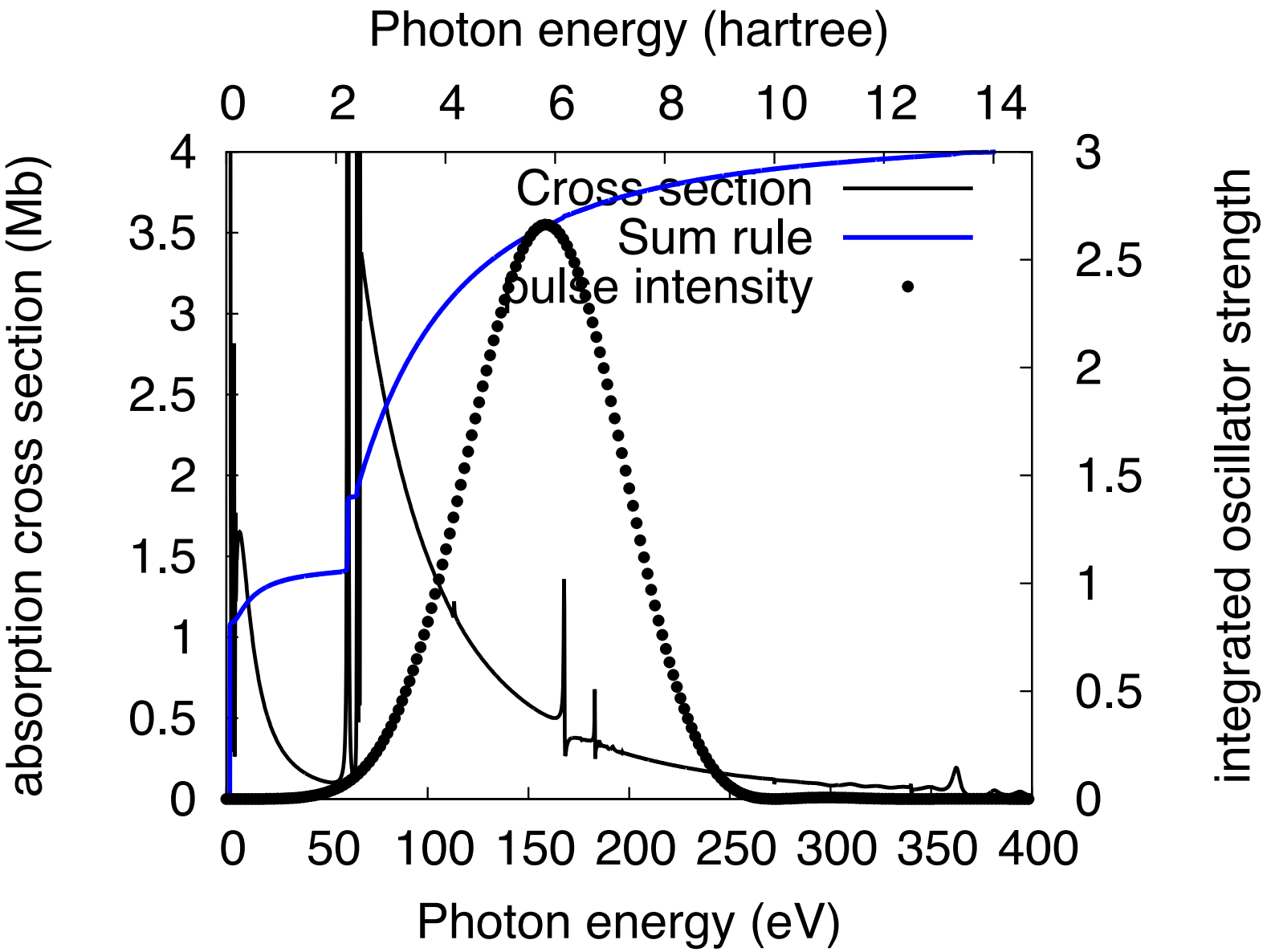

Photoionization

Formalism of Heidelberg group: Jäckle and Meyer, *Time-dependent calculation of reactive flux employing complex absorbing potentials: General aspects and application within MCTDH*, JCP 105, 6778 (1996)

Antihermitian part of ECS hamiltonian

$$f(E) = \int_0^\infty dt \int_0^\infty dt' \, e^{iE(t-t')} \left\langle \Psi(t') \left| i(\hat{H} - \hat{H}^\dagger) \right| \Psi(t) \right\rangle$$

Based on the fact that the antihermitian part of the Hamiltonian causes absorption in the asymptotic region.

With nuclear motion, dissociative excitation may be distinguished from ionization by using different parts of the antihermitian part of the Hamiltonian.

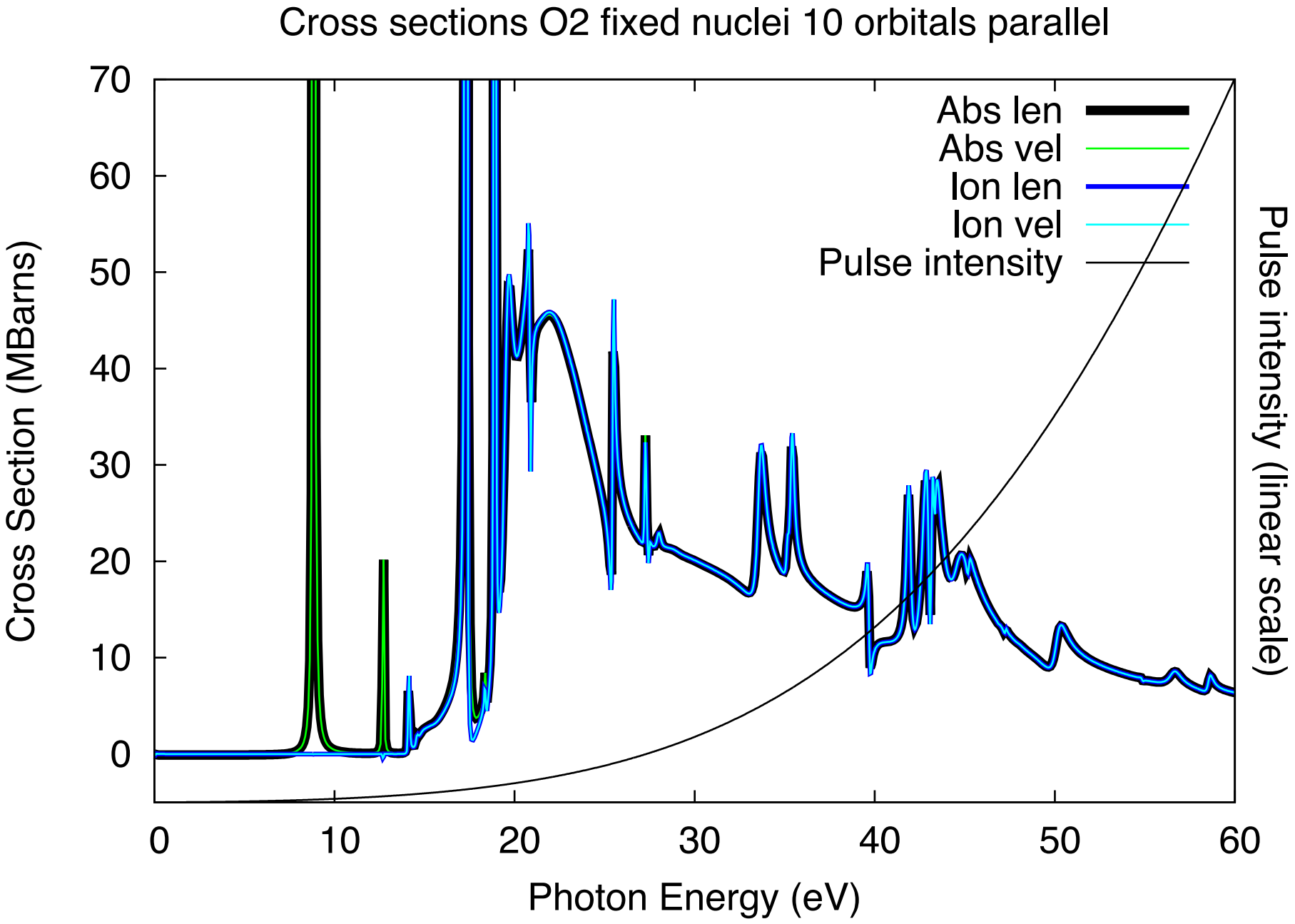
Cross sections O2 fixed nuclei 10 orbitals parallel
Abs len
Abs vel
Ion len
Ion vel
Pulse intensity
Cross Section (MBarns)
Pulse intensity (linear scale)
Photon Energy (eV)
0
10
20
30
40
50
60
70

Partial photoionization flux O_2: integrals dt and dE agree

(Nontrivial, different formulas)

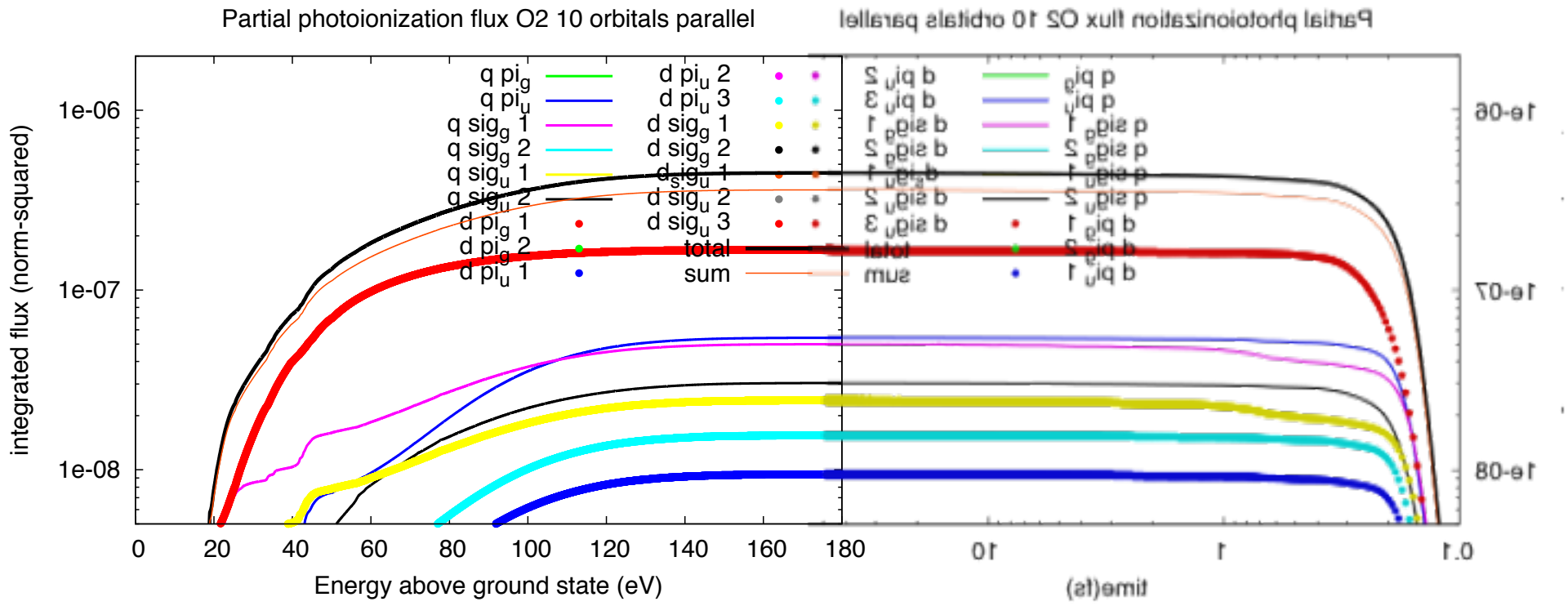

Flux integral dE

Flux integral dt

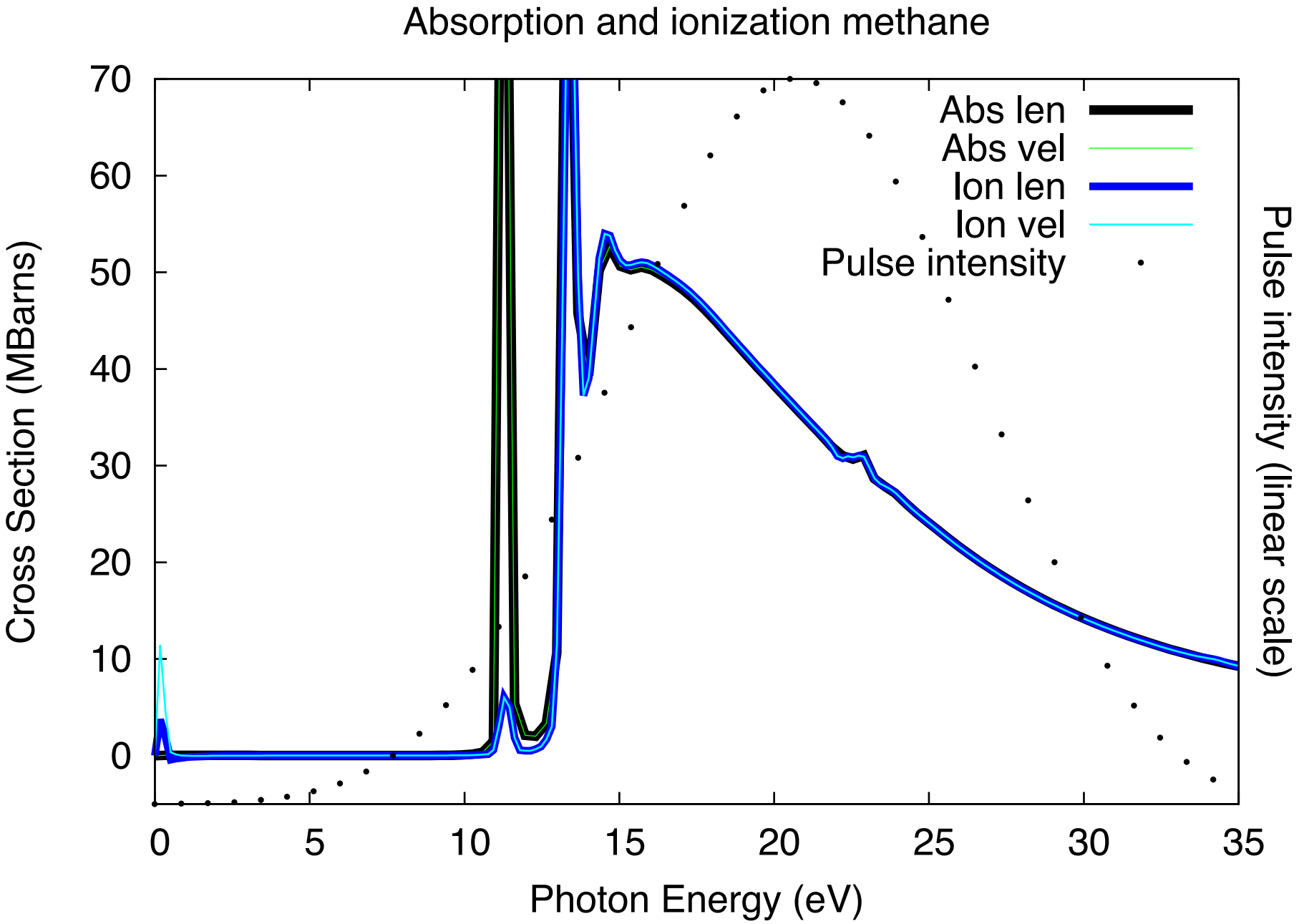

63x63x63 points, 0.4 bohr spacing, scaling at 8 bohr

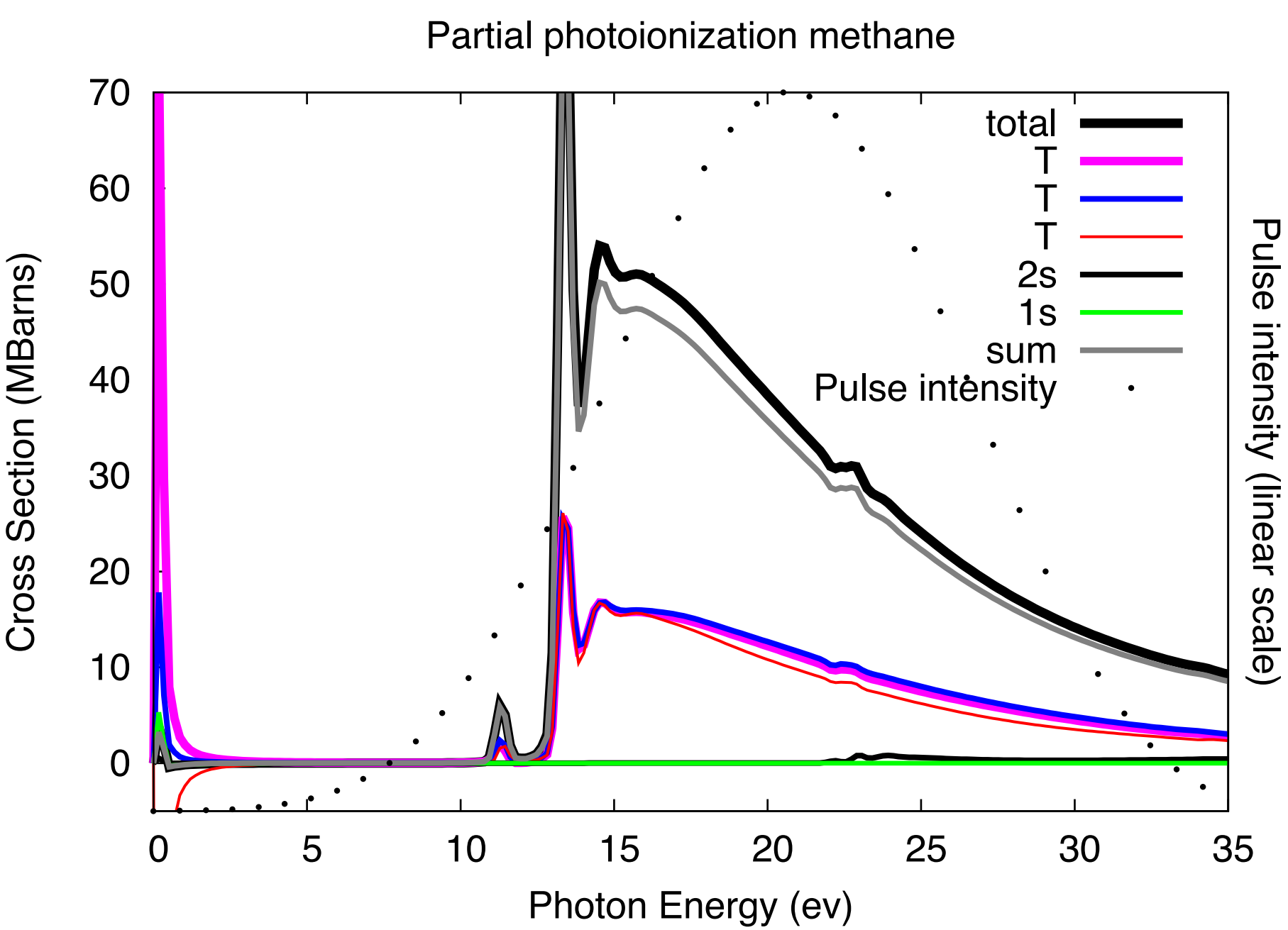

63x63x63 points, 0.4 bohr spacing, scaling at 8 bohr

Benzene $\Delta=0.47a_0$ $x_0=9a_0$

Configuration interaction representation appropriate for double core excited physics. 42 electrons, 24 orbitals, double excitations allowed from first 18 to last 6 orbitals (CISD particle-hole conjugate), approximately 100,000 spin adapted configurations or 650,000 Slater determinants.

64x64x64 points (10^{176} primitive Slater determinants)

R. Feng et al. / Journal of Electron Spectroscopy and Related Phenomena 123 (2002) 199–209

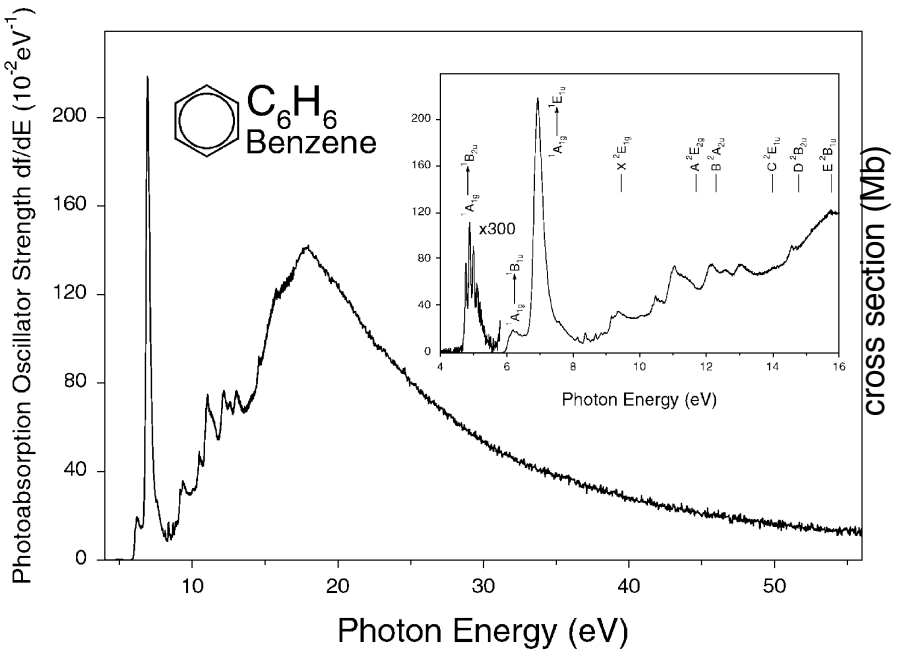

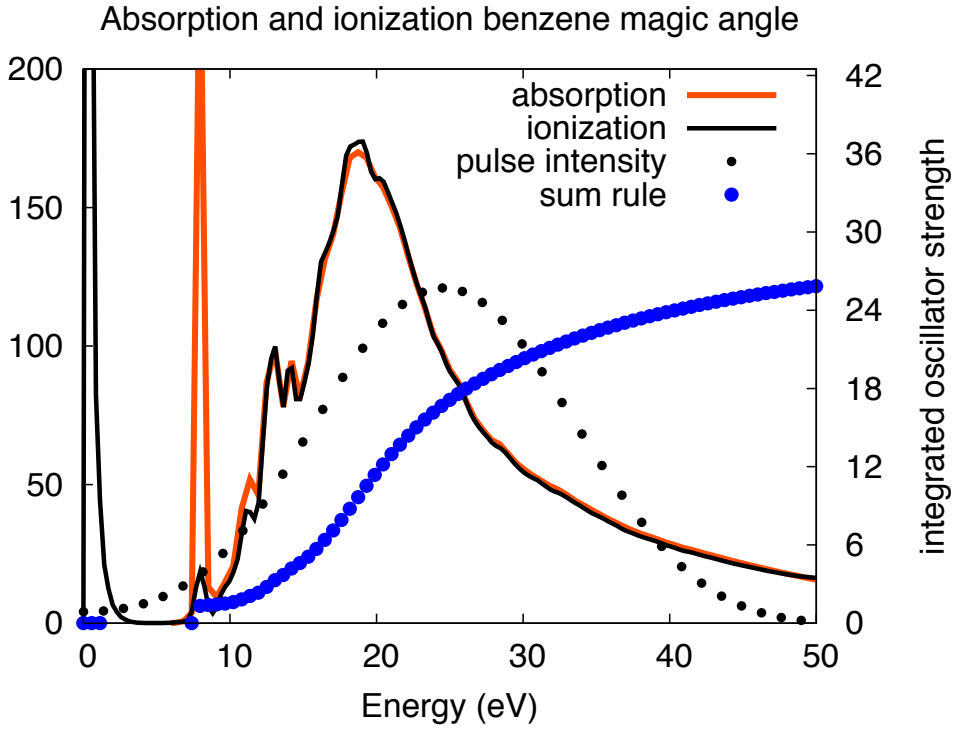

Algorithmic improvements for the medium-range future

1) Psi-prime method (calculate only the change in the wave function) : not numerically robust enough yet, but I have ideas

2) Kvaal's Lindblad evolution equation extension of MCTDHF for discriminating multiple ionization channels and multiple ionization in general (Peder Sather collaboration)

3) Fully nonadiabatic polyatomic quantum nuclear dynamics (small vibrations only, original intent of DOE Early Career project)

"Psi-prime" treatment is better but not numerically stable. Accurate results with fewer orbitals.

Solve only for the change in the wave function due to the pulse.

$$\Psi(t) = e^{-iE_0 t}\Psi(0) + \Psi'(t)$$

$$i\frac{\partial}{\partial t}\Psi'(t) = H(t)\Psi'(t) + V(t)e^{-iE_0 t}\Psi(0)$$

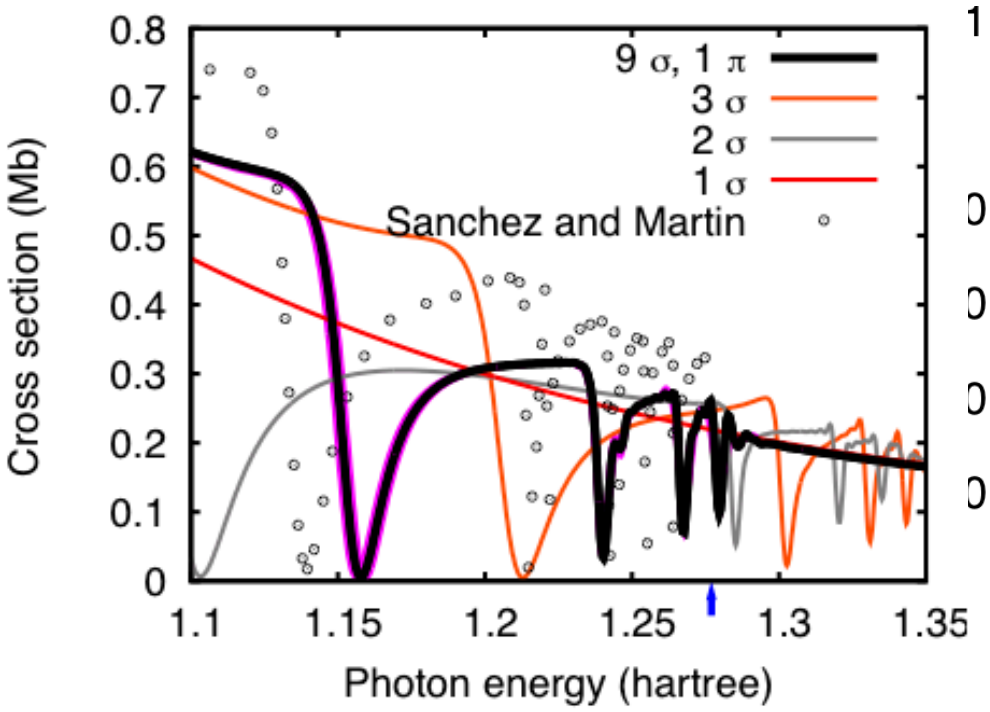

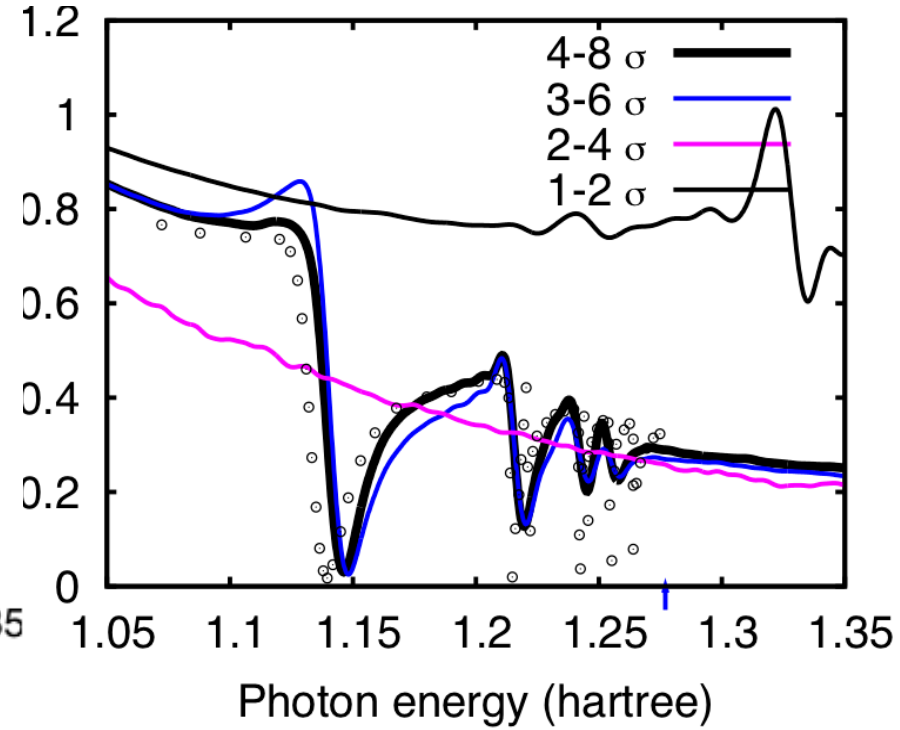

What LBNL-AMO-MCTDHF CAN'T do:

Only calculates N electron wave function!

. . . Will not follow cation after ionization.

E.g. if observed absorption is partially due to absorption by free cation, dication, etc. we cannot easily calculate this (without a big grid), and multiple ionization channels are not discriminated

. . . . SOLUTION: LINDBLAD EQUATION EXTENSION OF MCTDHF.

PHYSICAL REVIEW A **84**, 022512 (2011)

Multiconfigurational time-dependent Hartree method to describe particle loss due to absorbing boundary conditions

Simen Kvaal[1,2,*]

[1]*Mathematisches Institut, Universität Tübingen, Auf der Morgenstelle 10, D-72076 Tübingen, Germany*

[2]*Centre of Mathematics for Applications, University of Oslo, N-0316 Oslo, Norway*

(Received 7 March 2011; published 29 August 2011)

RESTRICTED CONFIGURATION SPACES

(PRUNING THE N-ELECTRON BASIS)

PHYSICAL REVIEW A **91**, 012509 (2015)

Two methods for restricted configuration spaces within the multiconfiguration time-dependent Hartree-Fock method

Daniel J. Haxton[1] and C. William McCurdy[1,2]

[1]*Lawrence Berkeley National Laboratory, Chemical Sciences, Berkeley, California 94720, USA*

[2]*Department of Chemistry, University of California, Davis, California 95616, USA*

(Received 1 October 2014; revised manuscript received 11 December 2014; published 20 January 2015)

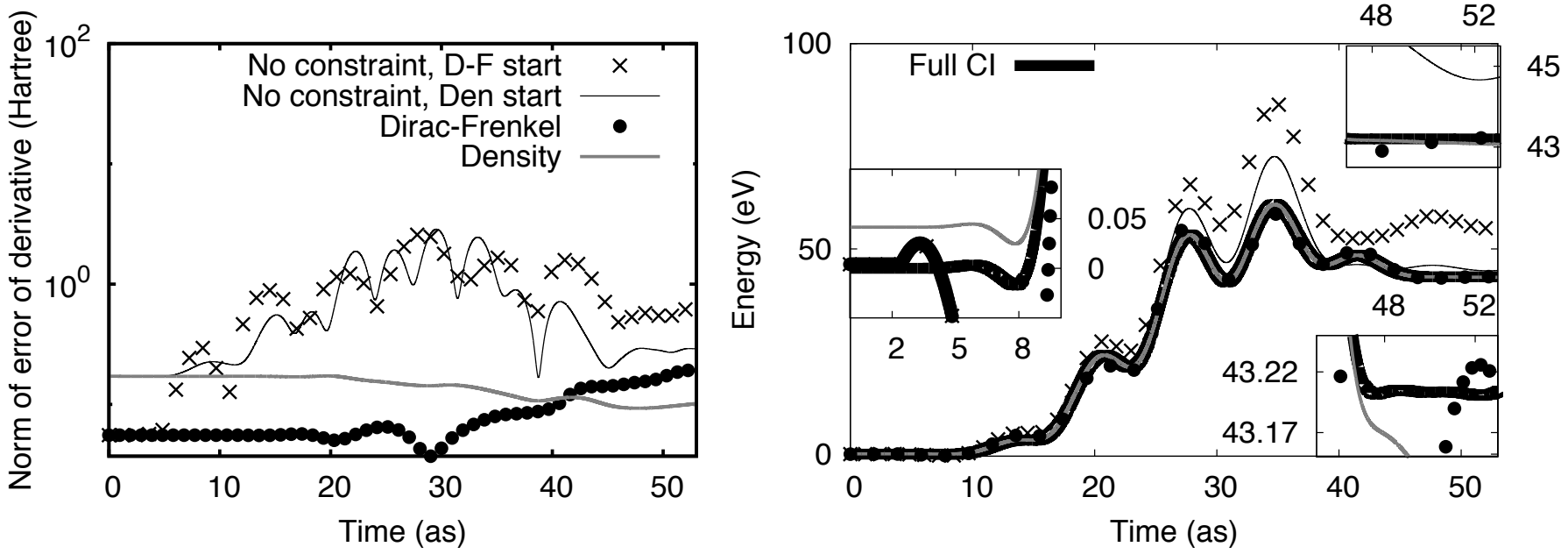

Explicit MCTDHF working equations implemented for McLachlan and Lagrangian (Dirac-Frenkel) stationary principles. Alternate density matrix method (enforce block diagonal density matrix, generalization of natural orbital constraint) works well too.

With restricted configuration spaces – in other words, without full configuration interaction – orbitals may be inequivalent. Two orbitals are equivalent if the Slater determinant space is invariant with respect to any rotation of the two orbitals into one another.

If orbitals are inequivalent, then they must rotate into one another in order to satisfy the chosen variational principle.

TO COMPLETE THE MCTDHF equations of motion, for any ansatz Slater determinant space, need to determine the rates and phases of rotation of inequivalent orbitals into one another. The rates and phases of rotation are given by the matrix *g*,

$$g_{\alpha\beta} = \left\langle \phi_\alpha \middle| i\frac{\partial}{\partial t}\phi_j \right\rangle$$

$$i\frac{\partial}{\partial t}\vec{\phi} = \left[(1-P)\left(\rho^{-1}\mathbf{W} + h_0\right) + g\right]\vec{\phi}$$

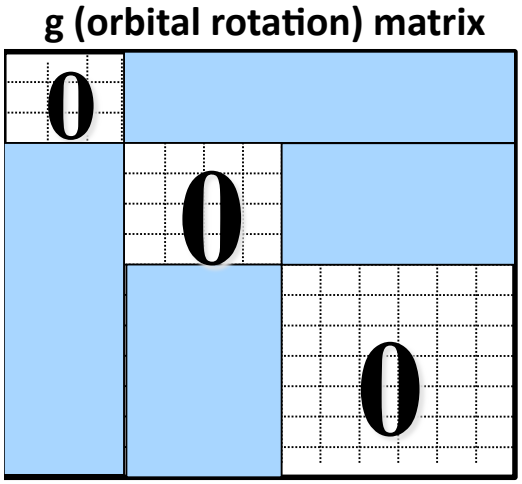

To obtain *g* matrix for MCTDHF equations of motion consider variations of orbitals within the space they span

$$\frac{\delta}{\delta\alpha\beta}|\vec{n}_a\rangle = a_\beta^\dagger a_\alpha |\vec{n}_a\rangle,$$

For Restricted Active Space, the expression for *g* is obtained from the Dirac-Frenkel variational principle,

Dirac-Frenkel:

$$\forall_{\alpha\beta} \quad \left\langle \frac{\delta}{\delta\alpha\beta}\Psi \middle| H - i\frac{\partial}{\partial t} \middle| \Psi \right\rangle \quad = 0$$

Lagrangian versus MacLachlan

For arbitrary Slater determinant spaces one must distinguish between Lagrangian and MacLachlan variational principles. Consider only variations of orbitals consistent with orthogonality constraint:

Dirac-Frenkel implies satisfaction of both MacLachlan and Lagrangian simultaneously which is not always possible

$$\begin{aligned}\left|\frac{\delta}{\delta(\alpha\beta)_r}\Psi\right\rangle &\equiv \left|\frac{\delta}{\delta\alpha\beta}\Psi\right\rangle - \left|\frac{\delta}{\delta\beta\alpha}\Psi\right\rangle \\ &= (a_\alpha^\dagger a_\beta - a_\beta^\dagger a_\alpha)|\Psi\rangle, \\ \left|\frac{\delta}{\delta(\alpha\beta)_i}\Psi\right\rangle &\equiv i\left|\frac{\delta}{\delta\alpha\beta}\Psi\right\rangle + i\left|\frac{\delta}{\delta\beta\alpha}\Psi\right\rangle \\ &= i(a_\alpha^\dagger a_\beta + a_\beta^\dagger a_\alpha)|\Psi\rangle,\end{aligned} \tag{41}$$

the statement of the Lagrangian, "time-dependent," or energy-conserving variational principles is thus

Machlachlan takes the imaginary part.

$$\begin{aligned}\forall_{\alpha<\beta} \quad \mathrm{Re}\left\langle\frac{\delta}{\delta(\alpha\beta)_r}\Psi\middle|H - i\frac{\partial}{\partial t}\middle|\Psi\right\rangle = 0, \\ \forall_{\alpha<\beta} \quad \mathrm{Re}\left\langle\frac{\delta}{\delta(\alpha\beta)_i}\Psi\middle|H - i\frac{\partial}{\partial t}\middle|\Psi\right\rangle = 0\end{aligned} \tag{42}$$

Lagrangian variational principle produces best agreement with full configuration interaction in terms of work done by the pulse

Calculation	Start	Finish	Change
Be Full CI	-14.30475	-12.71702	1.58773
Be Dirac-Frenkel	-14.30460	-12.71675	1.58785
Be Density matrix	-14.30322	-12.72322	1.58000
Be Denmat FCI	-14.30322	-12.72320	1.58002
Be None, DF start	-14.30460	-12.27275	2.03185
Be None, Den start	-14.30322	-12.65978	1.64345
BC^{2+} Full CI	-61.275139	-60.611515	0.663624
BC^{2+} Lagrangian	-61.275135	-60.611508	0.663627
BC^{2+} McLachlan	-61.275135	-60.611208	0.663927
BC^{2+} Combination	-61.275135	-60.611330	0.663805
BC^{2+} None	-61.275135	-60.645813	0.629322

SIGNIFICANT PROBLEM WITH DIRAC-FRENKEL / MCLACHLAN / LAGRANGIAN PRINCIPLES: SYMMETRY BREAKING IN 3D.

NO_2 in XY plane, c2 axis is Y.
Linear polarization in (X,Y,Z)=(0,1,1) B_1 irrep. transforms as X

SPURIOUS POPULATION IN B_1 STATE! SYMMETRY SEVERELY BROKEN.

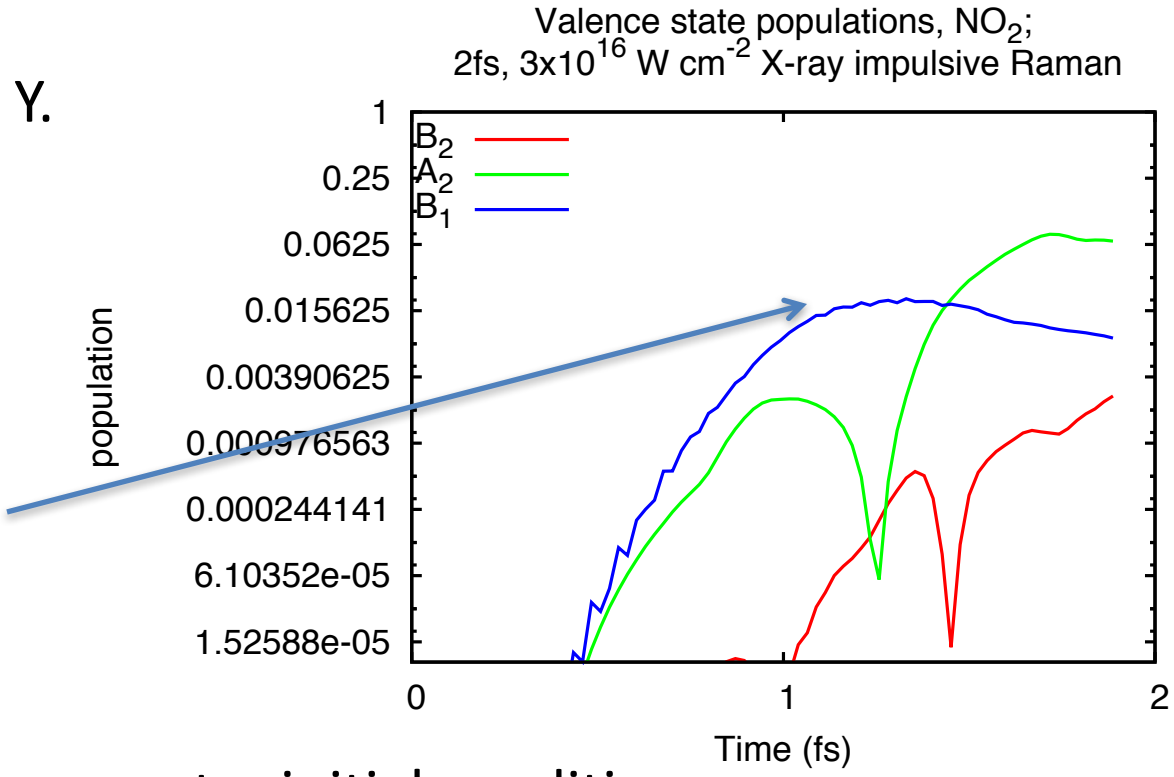

NO_2 Ground state broken symmetry initial condition

	x-dipole moment	y-dipole	x-reflection	energy
Full CI	0.00000	0.15627	1.00000	-185.868
Denmat	0.00000	0.15201	1.00000	-185.629
Dirac-Frenkel	0.00104	0.15598	0.99792	-185.858

X-ray and XUV Raman transitions

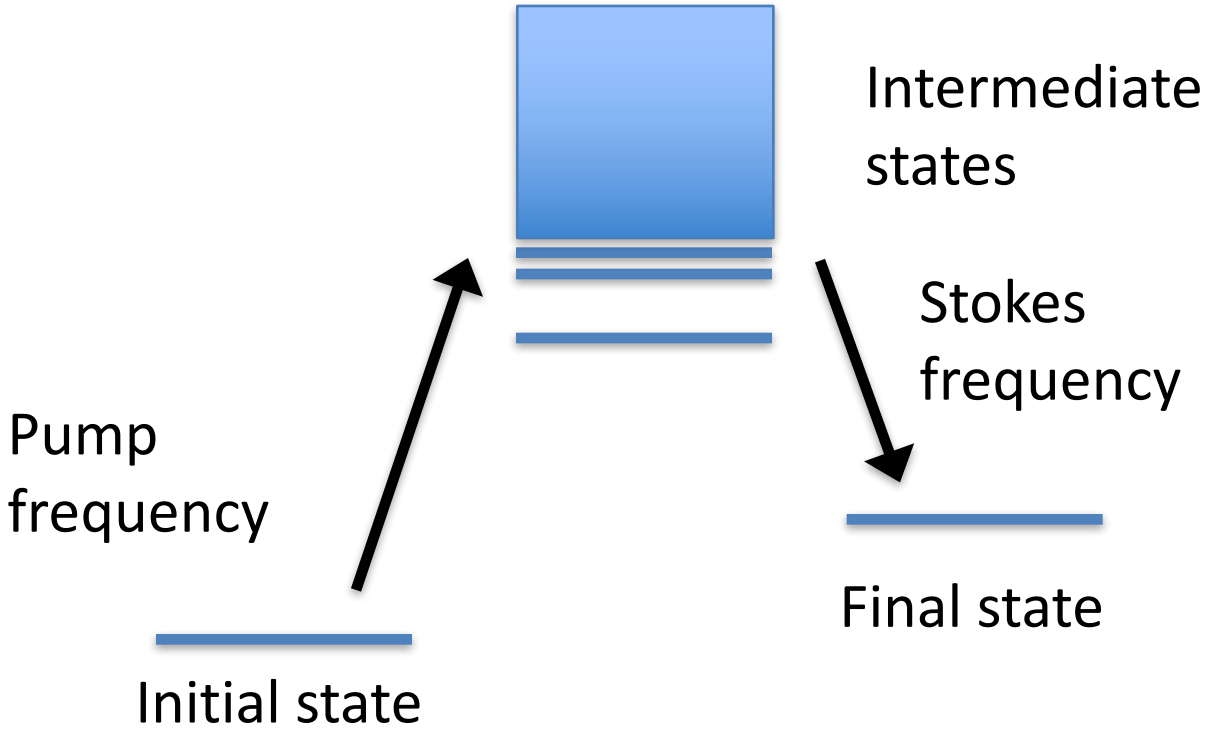

ONE BIG GOAL:

Develop ultrafast multidimensional spectroscopies

Papers on population transfer in Λ-type systems

- X. Li, C. W. McCurdy, and D. J. Haxton. **Population transfer between valence states via autoionizing states using two-color ultrafast π pulses in XUV and the limitations of adiabatic passage.** *Phys. Rev. A* **89**, 031404(R) (2014)
- D. J. Haxton and C. W. McCurdy. **Ultrafast population transfer to excited valence levels of a molecule driven by x-ray pulses.** *Phys. Rev. A* **90**, 053426 (2014).
- L. Greenman, K. B. Whaley, D. J. Haxton, and C. W. McCurdy. **Optimized pulses for Raman excitation through the continuum: verification using multi-configurational time-dependent Hartree- Fock.** Submitted to *Phys. Rev. A*; see http://arxiv.org/abs/1609.04505
- M. R. Ware, P. H. Bucksbaum, J. P. Cryan, and D. J. Haxton. **The attosecond regime of impulsive stimulated Raman excitation.** Submitted to *Phys. Rev. Lett.*; see http://arxiv.org/abs/1610.01190
- J. P. Cryan, M. R. Ware, and D. J. Haxton. **Optimizing impulsive X-ray Raman scattering for population transfer in atomic systems.** To be submitted to *Phys. Rev. A*; see http://arxiv.org/abs/1609.04175
- D. J. Haxton. **Impulsive X-ray Raman excitation of NO_2.** Submitted to *Phys. Rev. A*; see https://arxiv.org/abs/1609.04220

Would like to examine time delays in streaking experiments, e.g. Neon. . . If XUV pulse is much shorter than period of streaking field then formula should be ok

Stimulated Raman in nitric oxide NO

PHYSICAL REVIEW A **90**, 053426 (2014)

Ultrafast population transfer to excited valence levels of a molecule driven by x-ray pulses

D. J. Haxton[1] and C. W. McCurdy[2,3]
[1]*Chemical Sciences, Lawrence Berkeley National Laboratory, Berkeley, California 94720, USA*
[2]*Chemical Sciences and Ultrafast X-ray Science Laboratory, Lawrence Berkeley National Laboratory, Berkeley, California 94720, USA*
[3]*Department of Chemistry, University of California, Davis, California 95616, USA*
(Received 17 September 2013; published 21 November 2014)

Two colors, concurrent

Two-color stimulated X-ray Raman in NO

Phys. Rev. A **90**, 053426 (2014)

Aiming for $(1s)^2\ \pi_g^1 \rightarrow 1s^1\ \pi_g^2$

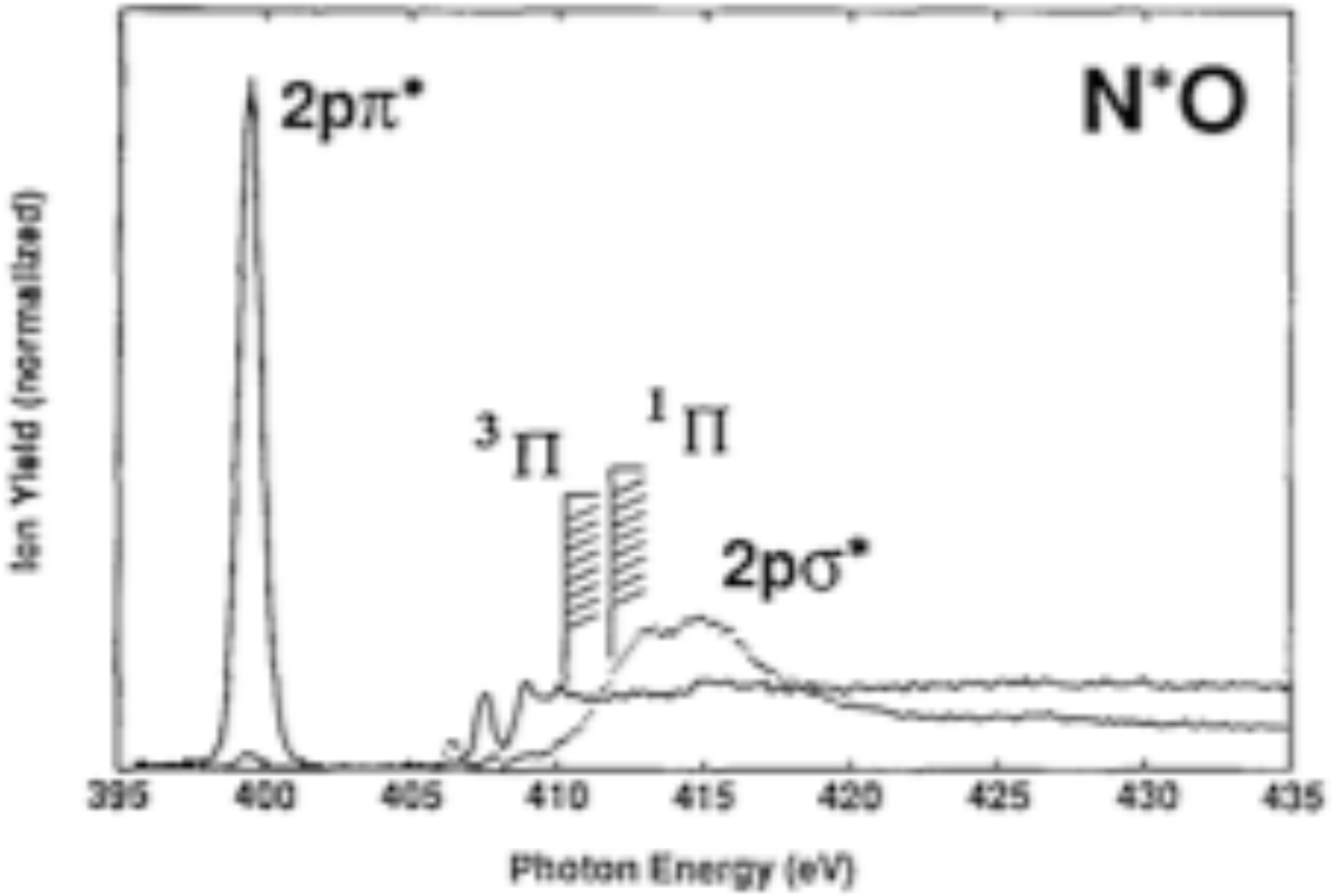

Parameters of pulse used

Sin^2 envelope FWHM 0.66fs, duration 1.32fs

H-bar Omega = 402.6, 393.3eV

Intensity=5 x 10^{16}, 3 x 10^{17} W cm^{-2}

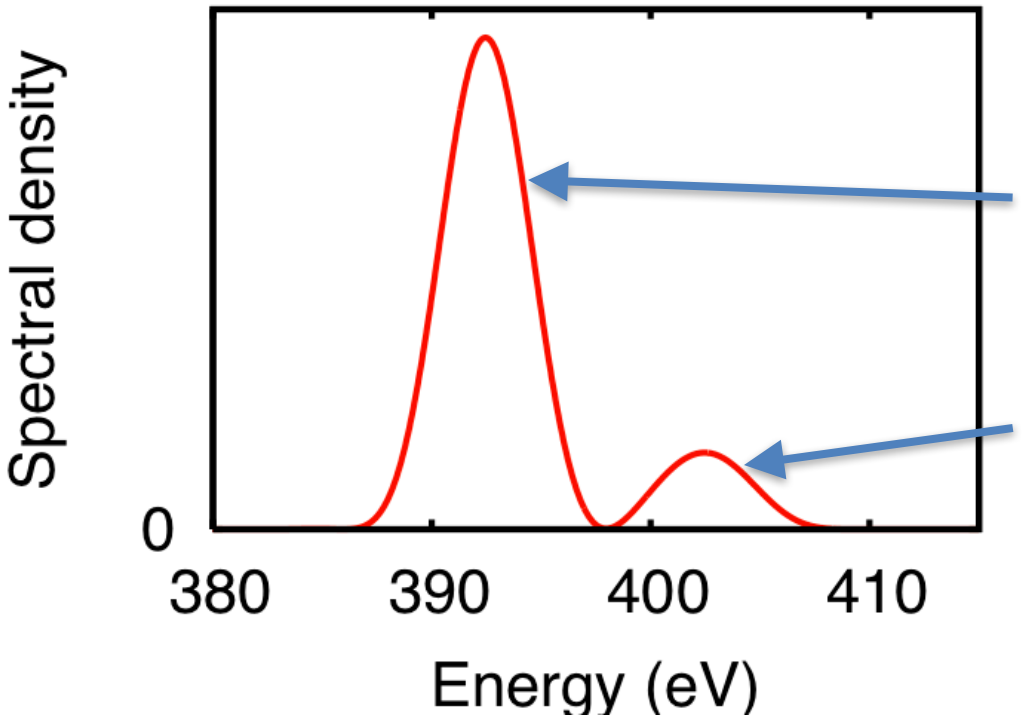

Fixed-nuclei calculation

Stokes: perpendicular polarization

Pump: parallel polarization

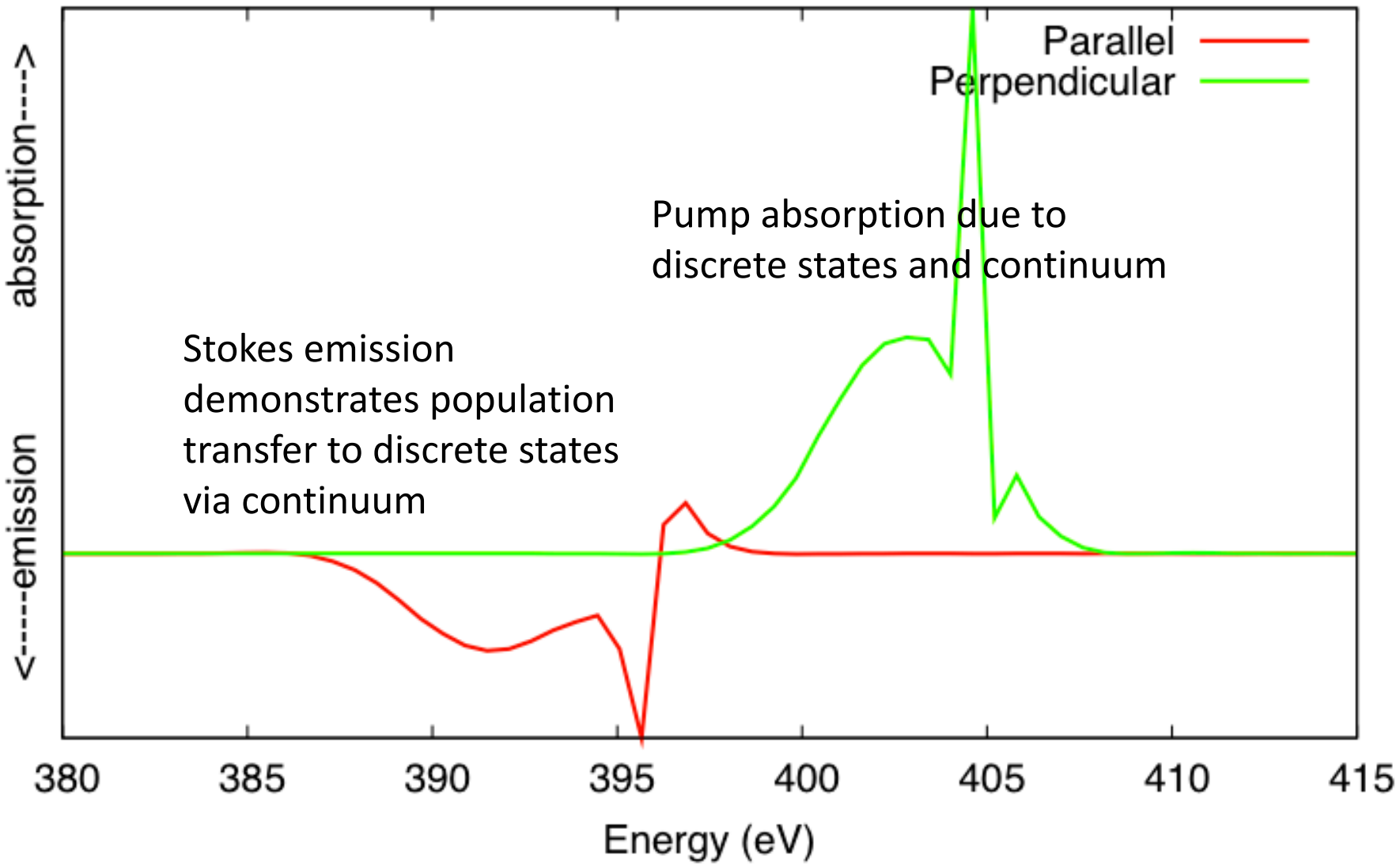
Parallel
Perpendicular
absorption--->
<-----emission
Pump absorption due to
discrete states and continuum
Stokes emission
demonstrates population
transfer to discrete states
via continuum
380
385
390
395
400
405
410
415
Energy (eV)

IMPULSIVE RAMAN

(One Color)

For attosecond pulses, continuum oscillator strength dominates!

arxiv 1609.04175, 1610.01190

SODIUM ATOM 10 ORBITALS 2p EDGE

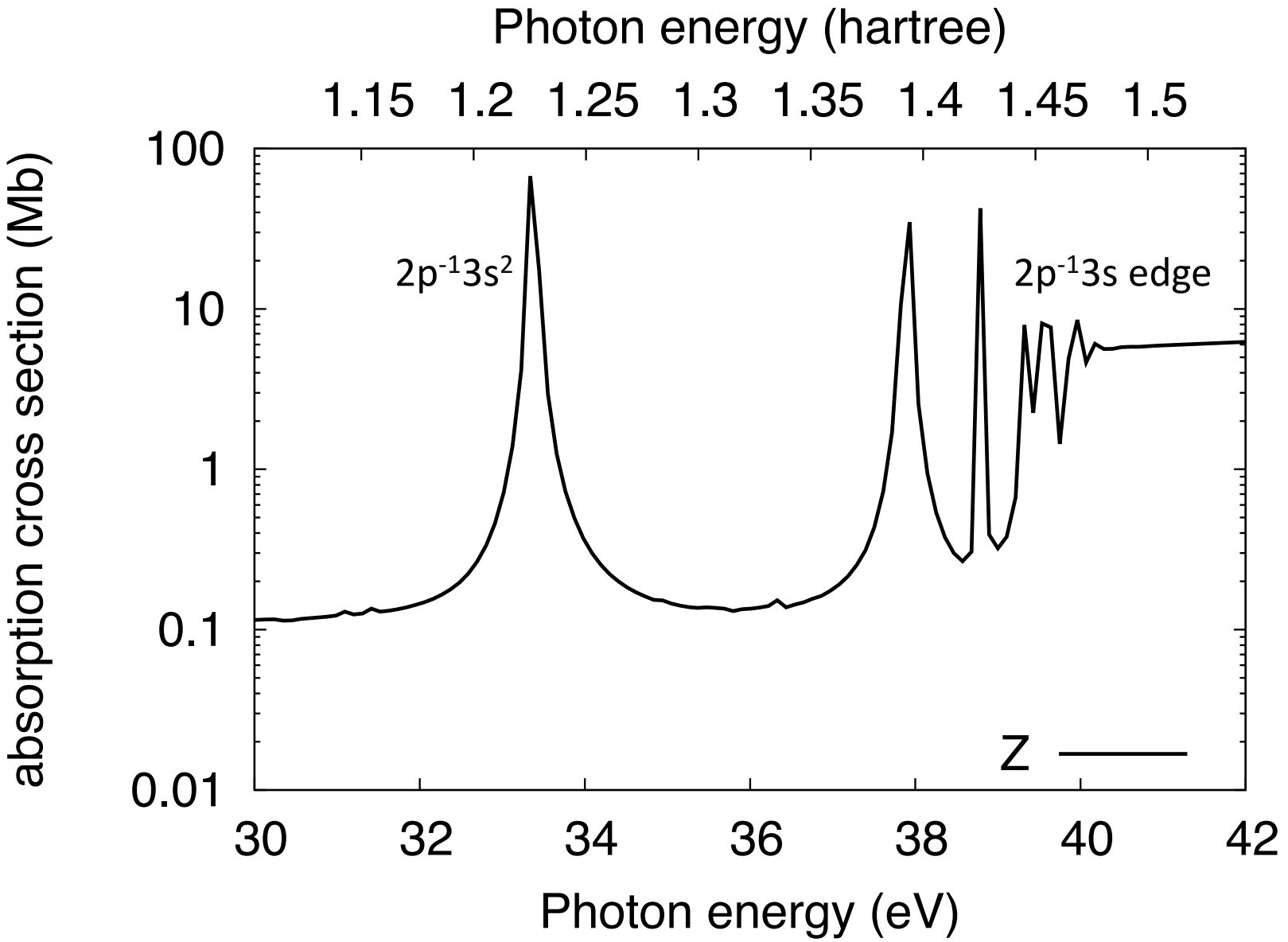

NIST: $2p^{-1}3s^2$ at 30.77eV; $2p^{-1}3s$ edge at 37.99eV

SODIUM ATOM 10 ORBITALS 2p EDGE

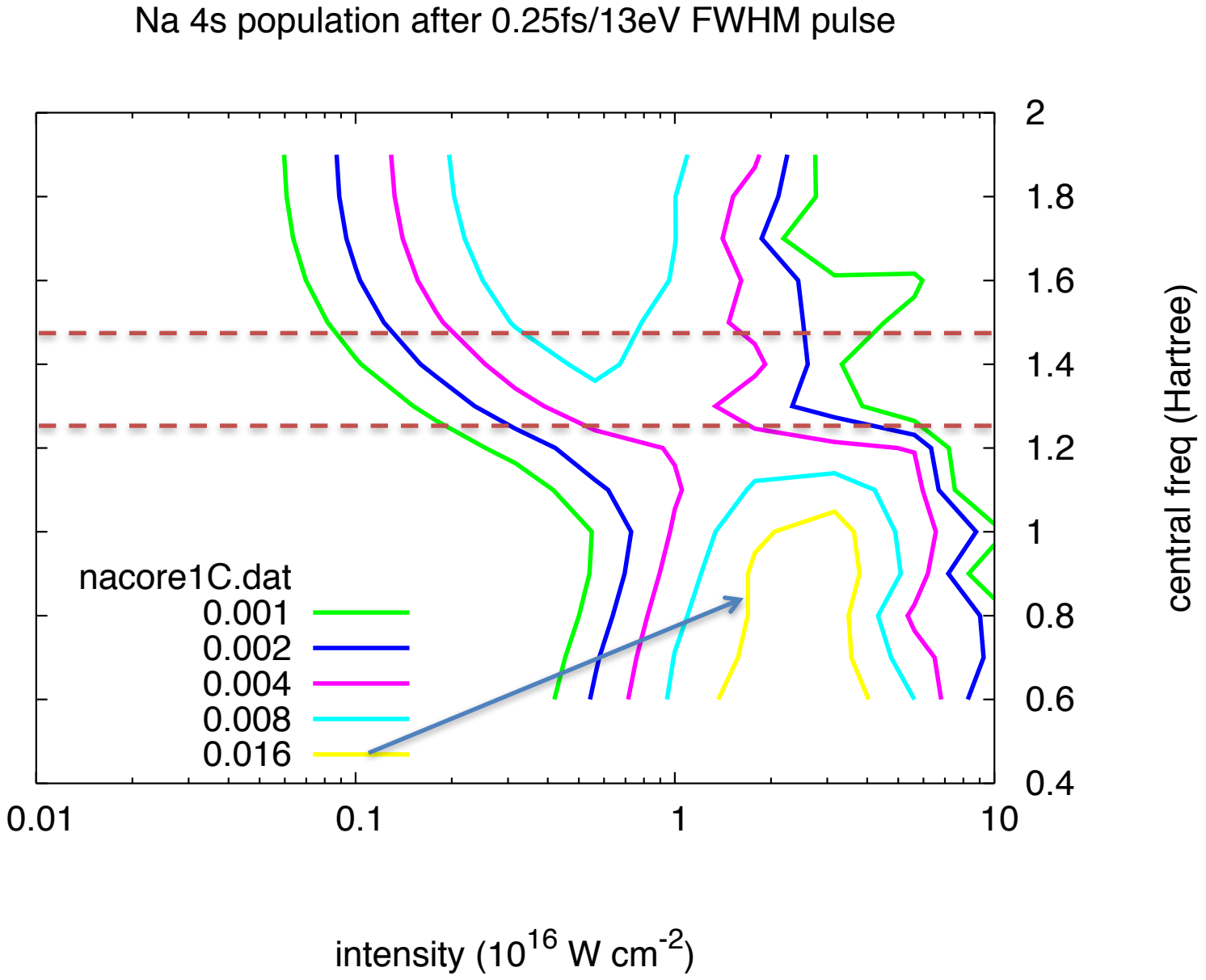

SODIUM ATOM 10 ORBITALS 2p EDGE

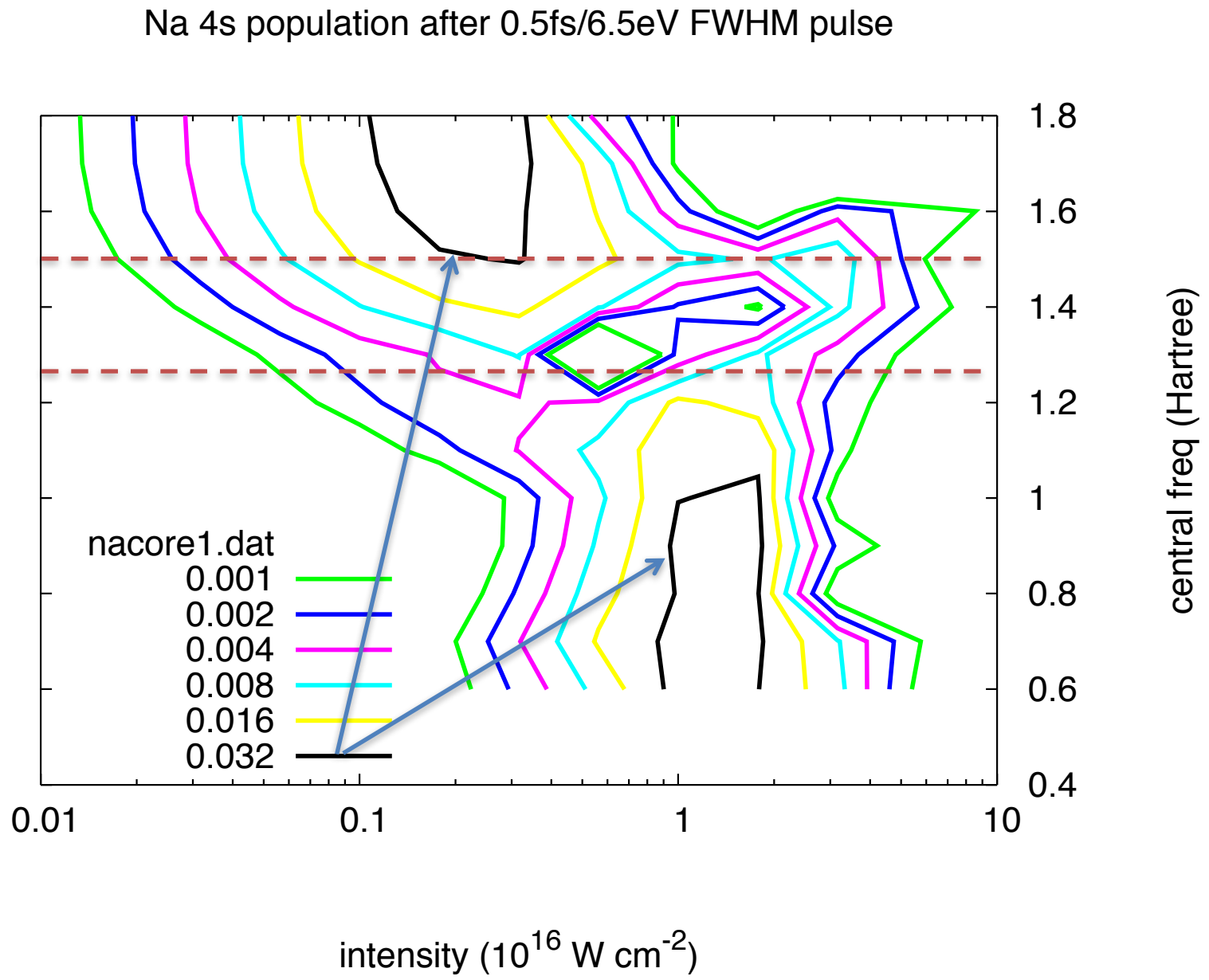

SODIUM ATOM 10 ORBITALS 2p EDGE

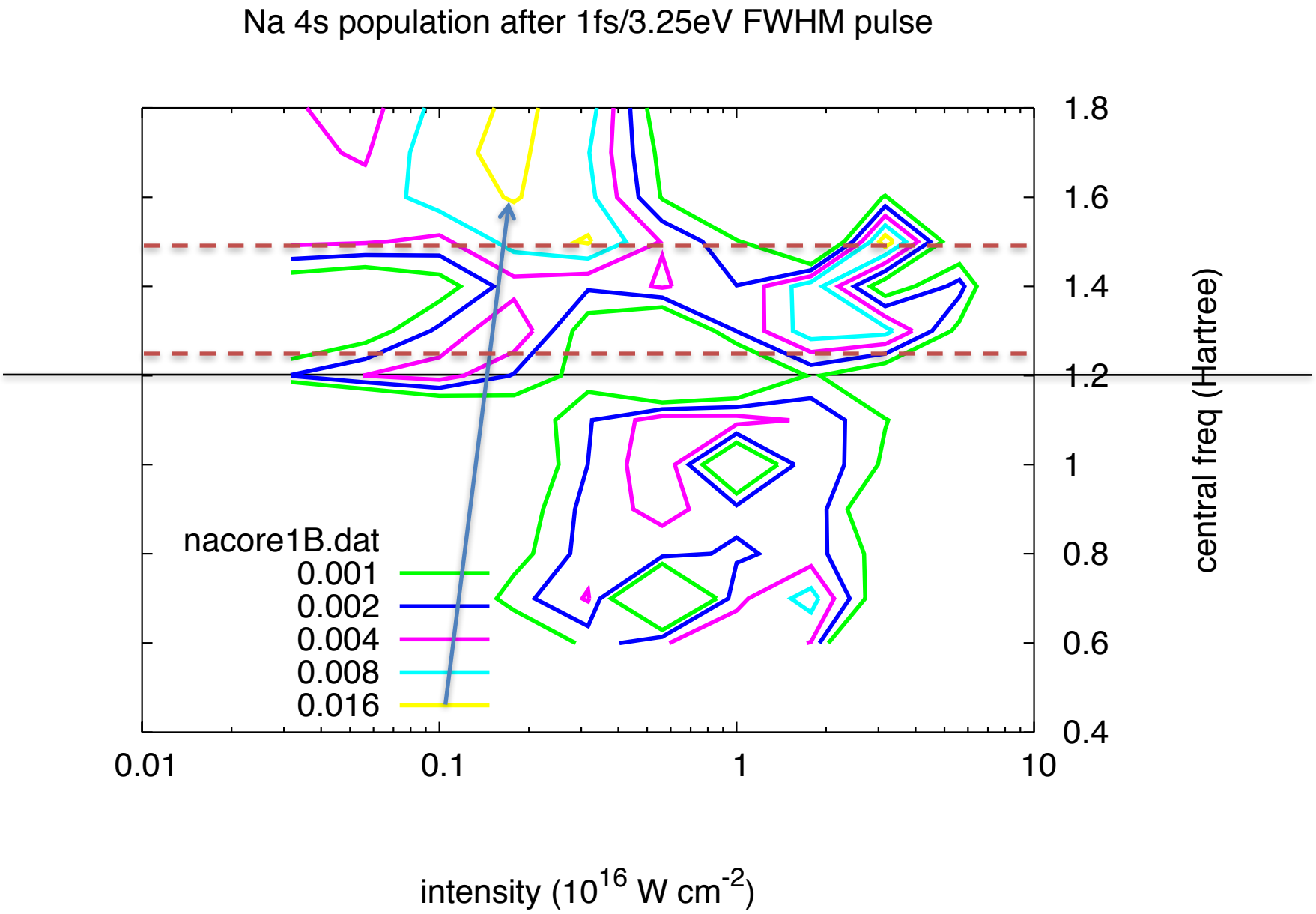

Transient Impulsive Electronic Raman Redistribution

S. Miyabe[1,2,*] and P. Bucksbaum[1,3]

Model result 35eV 1fs/3.25eV FWHM

In the previous plot I showed that optimum population transfer occurs not around 35eV but above 38 and below 27.

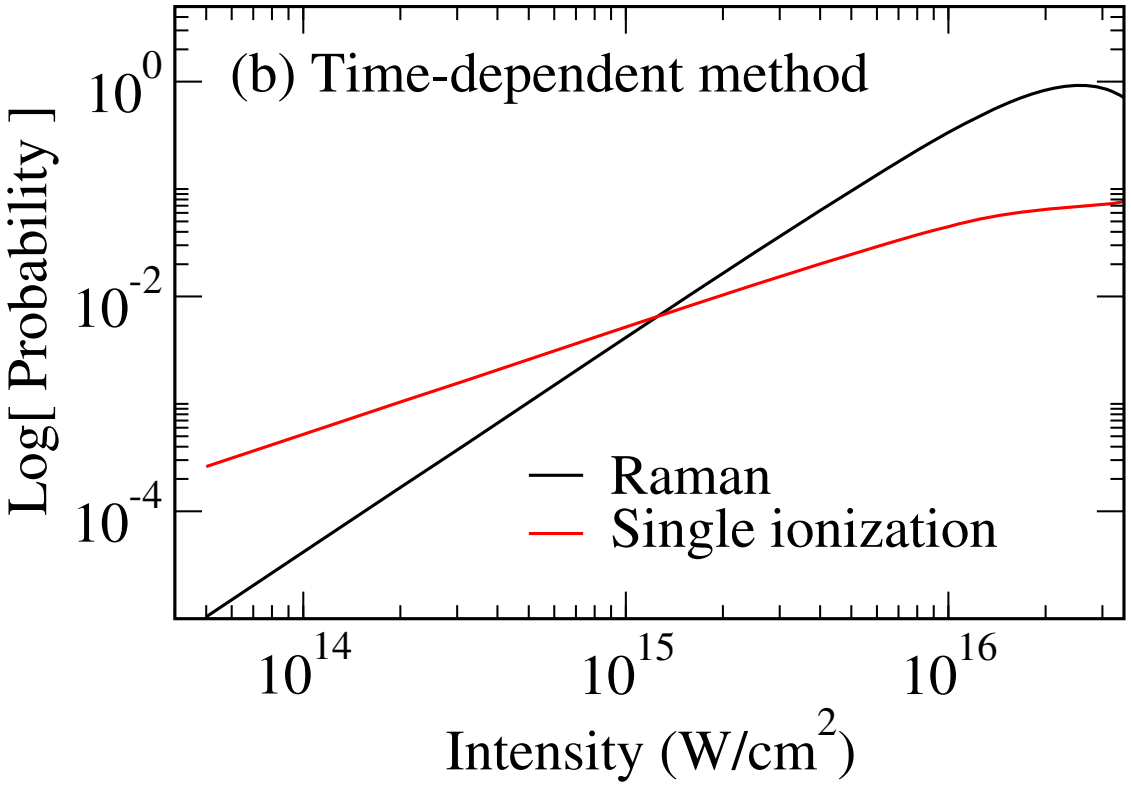

But considering my result at 1.2 Hartree (about 35eV) in the previous graph, we agree at 10^{15} (about half a percent population transfer) but then my result ***maxes out at about 1 x 10^{15} not 2 x 10^{16}***. arxiv 1610.01190

SODIUM ATOM 10 ORBITALS 1s K-EDGE

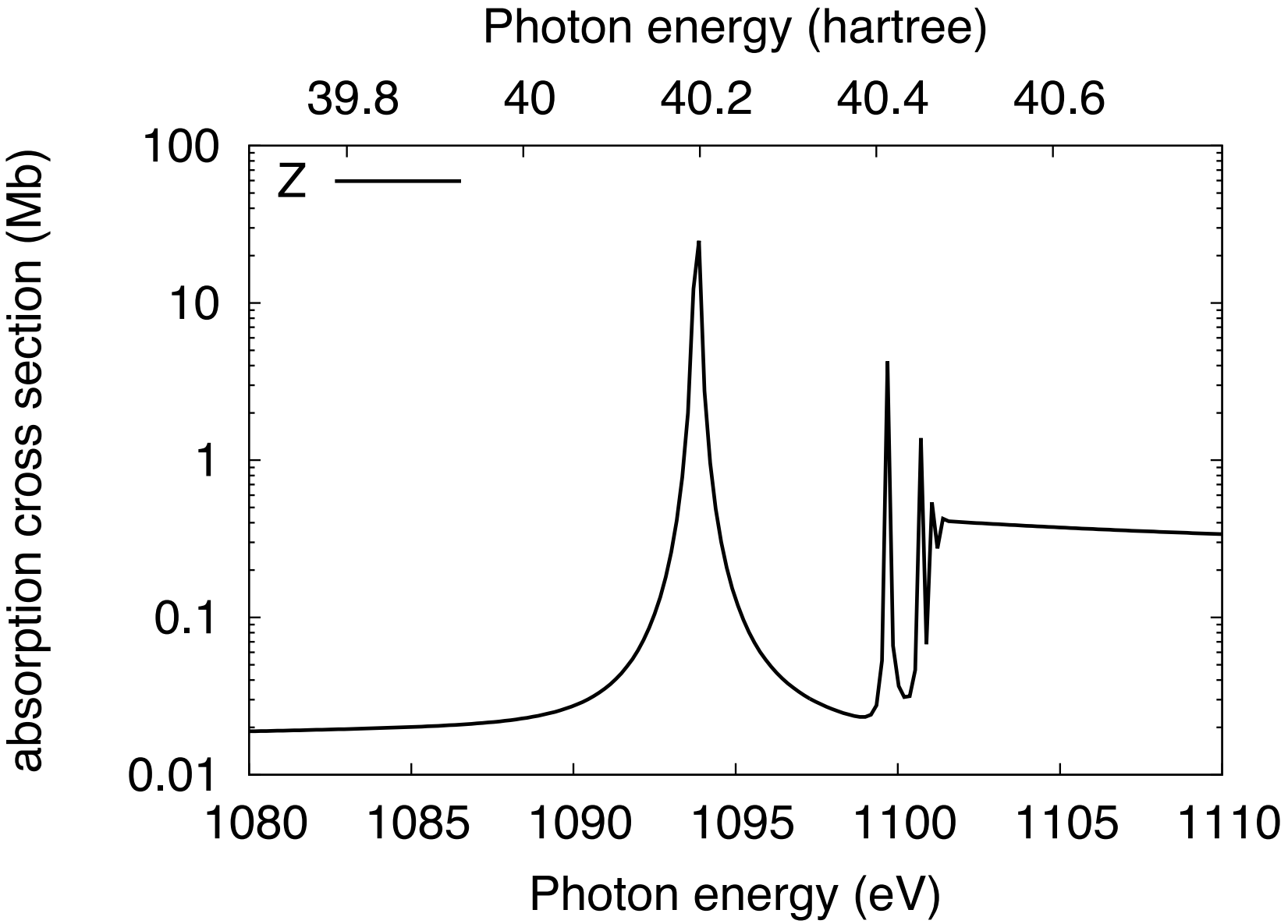

SODIUM ATOM 10 ORBITALS 1s K-EDGE

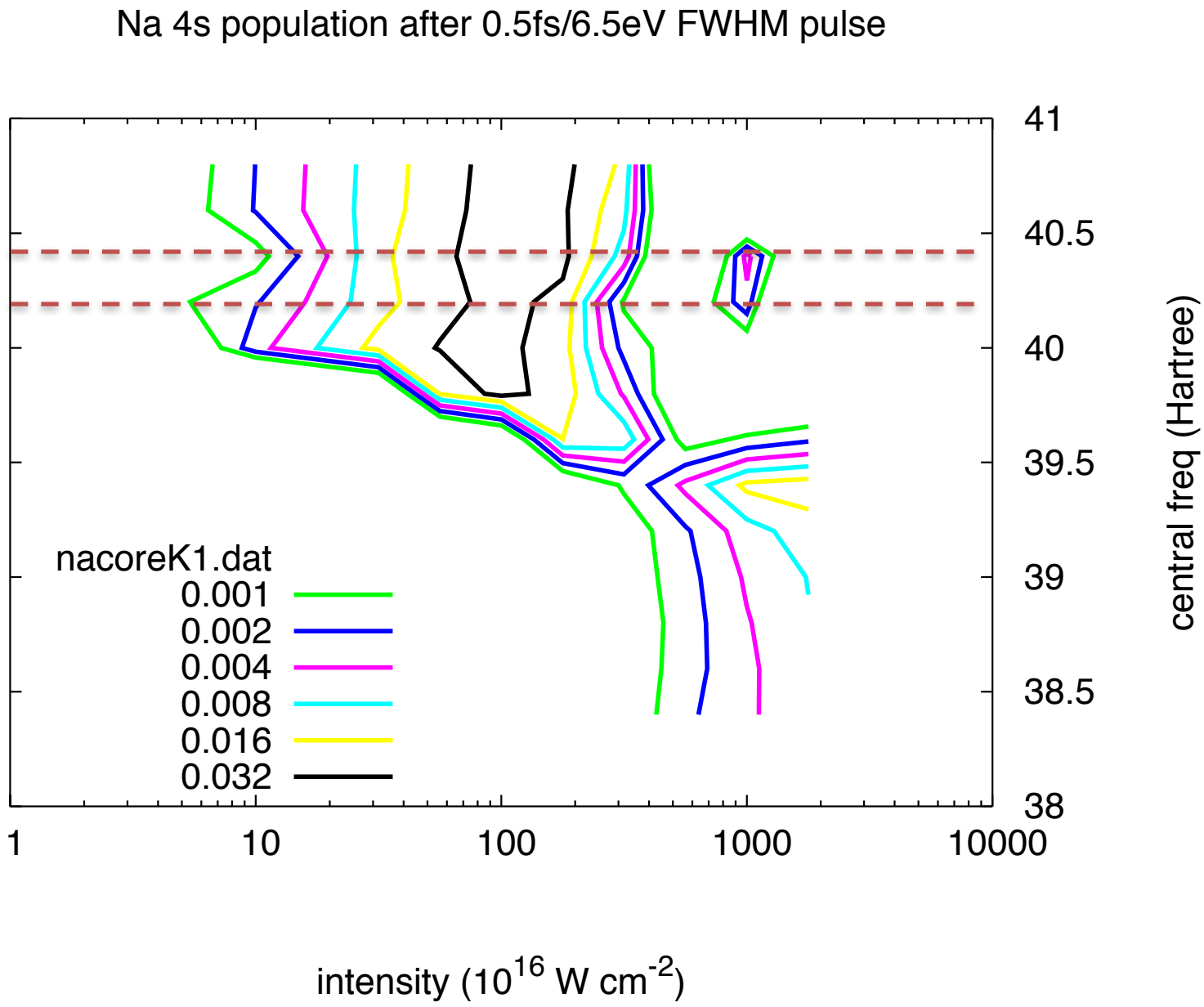

SODIUM ATOM 10 ORBITALS 1s K-EDGE

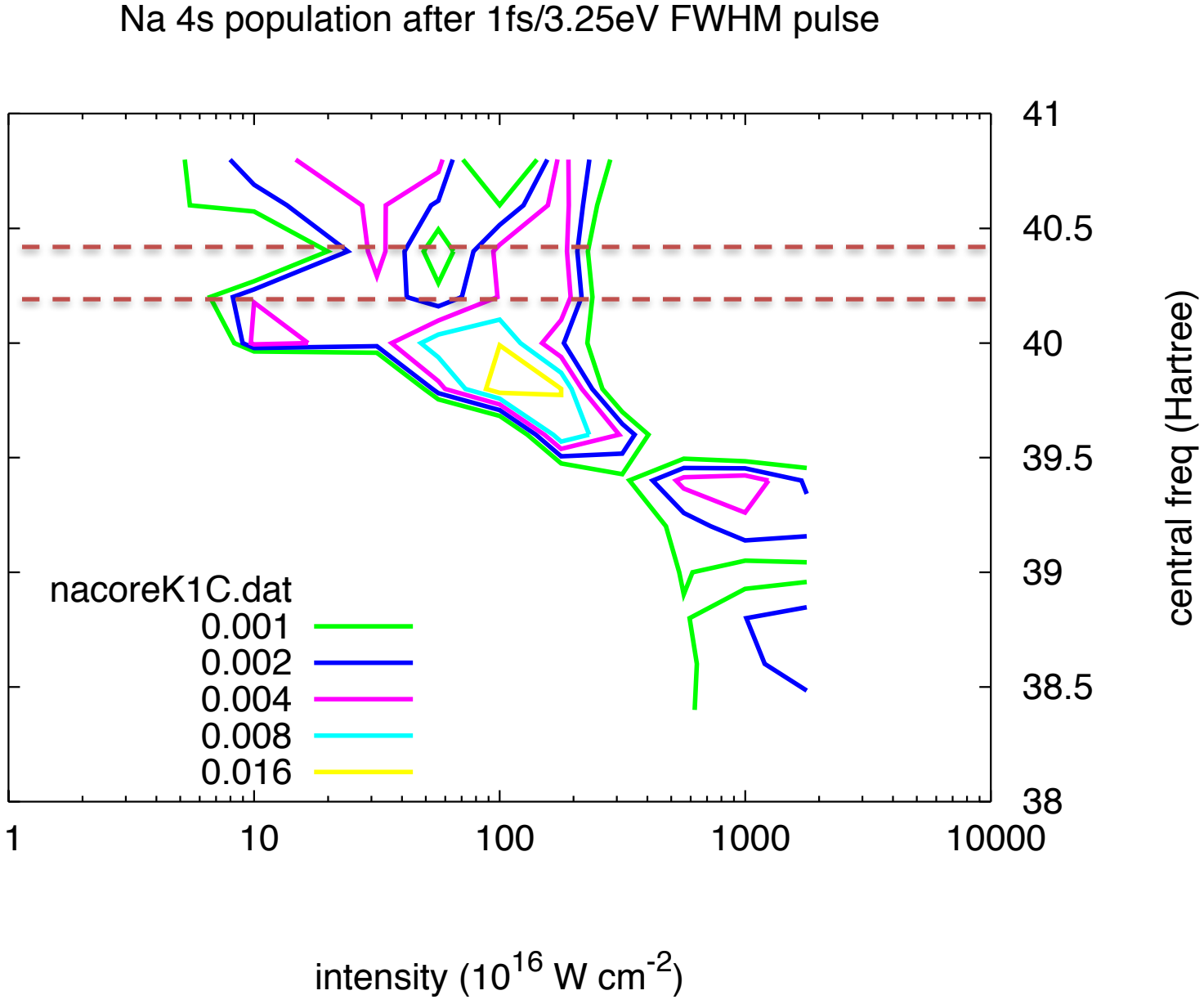

Hypothesis – red detuned is sometimes better than the conventional-wisdom sweet spot for impulsive Raman transitions

arxiv 1609.04175

Conventional-wisdom sweet spot is
red detuned pump, blue detuned Stokes

NEON ATOM 14 ORBITALS 1s K-EDGE

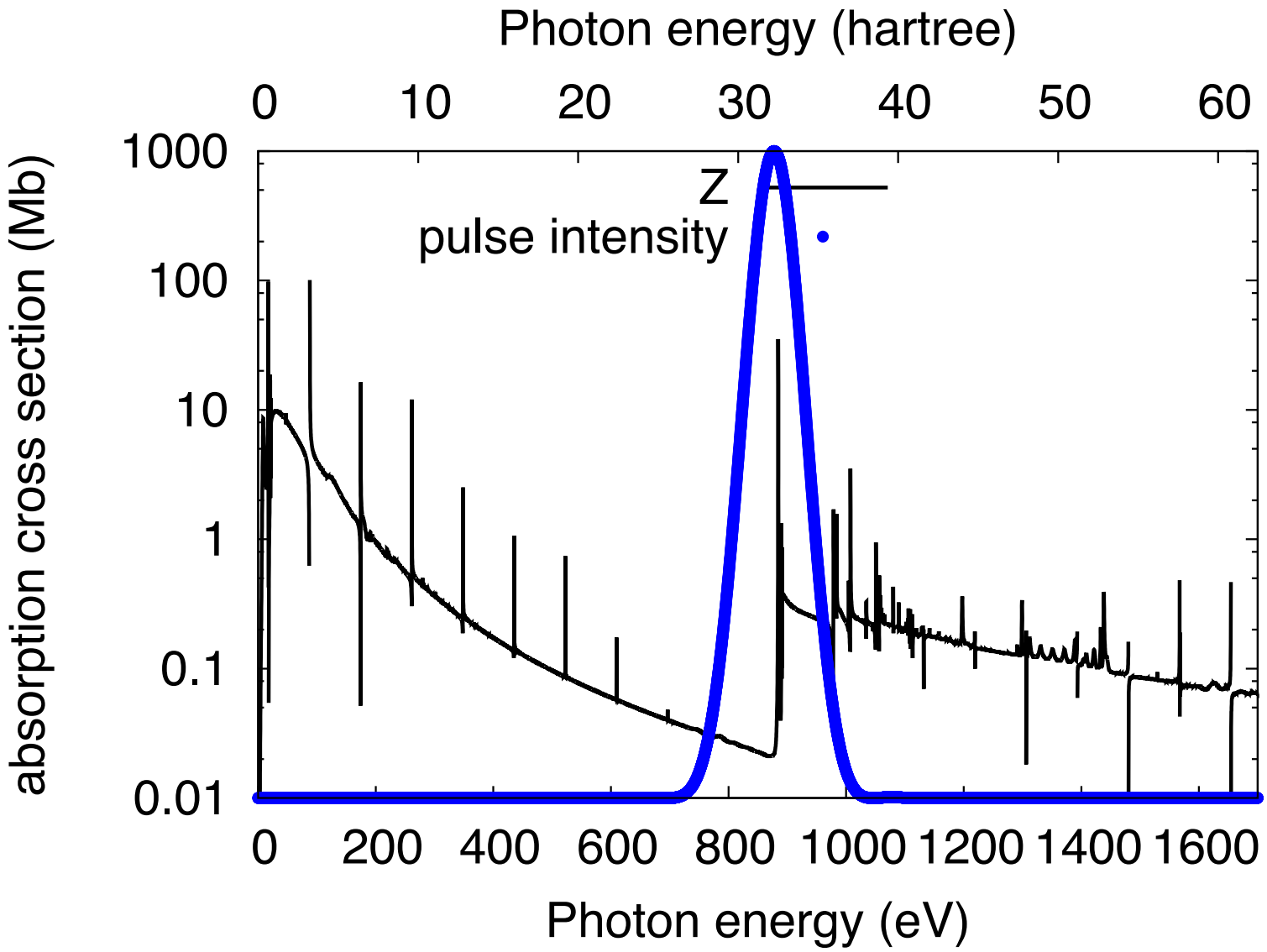

F.T. of pulse (pulse intensity) is zero at certain energies, giving spurious evenly-spaced peaks

NEON ATOM 14 ORBITALS 1s K-EDGE

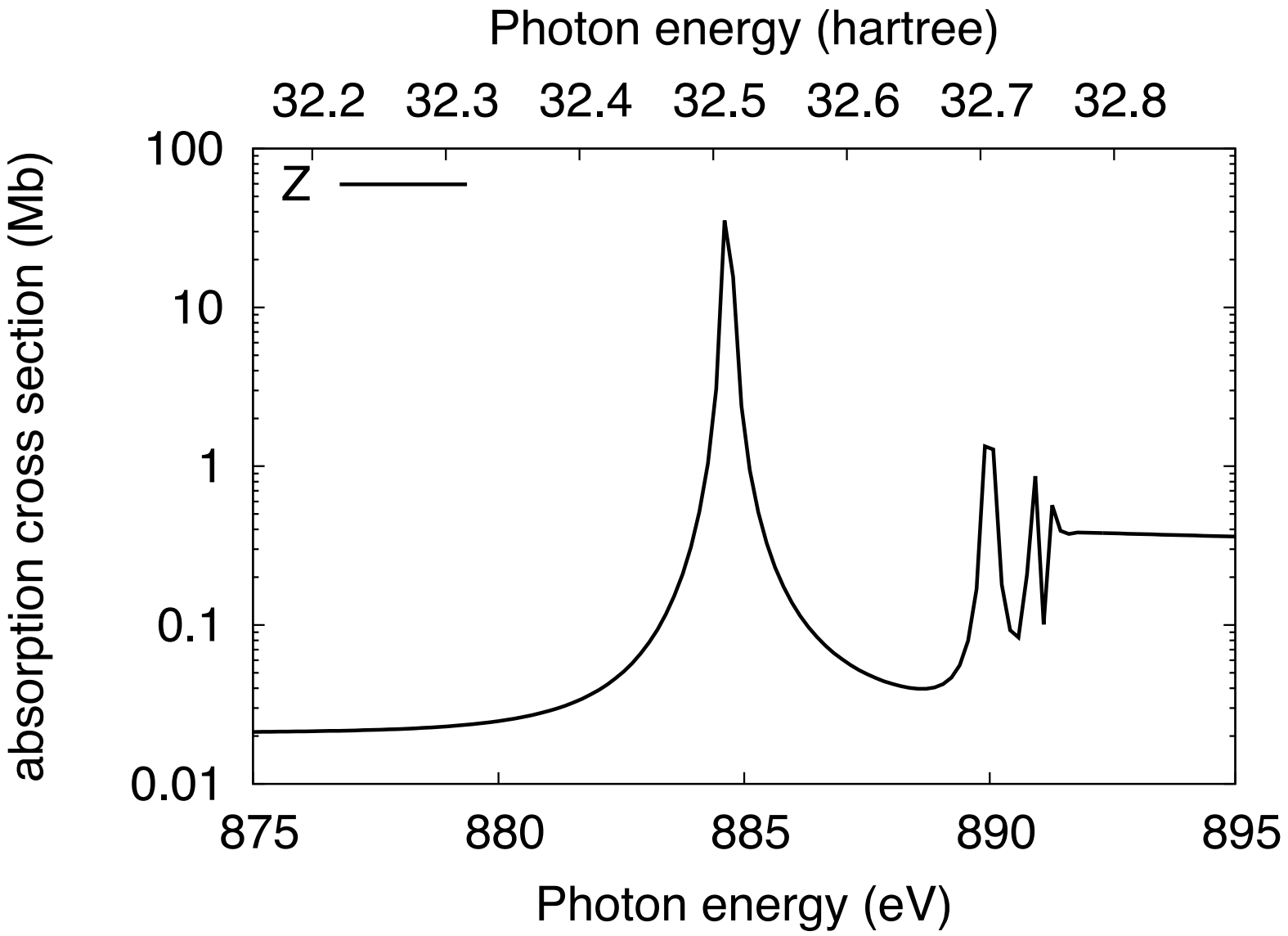

NEON ATOM 14 ORBITALS 1s K-EDGE

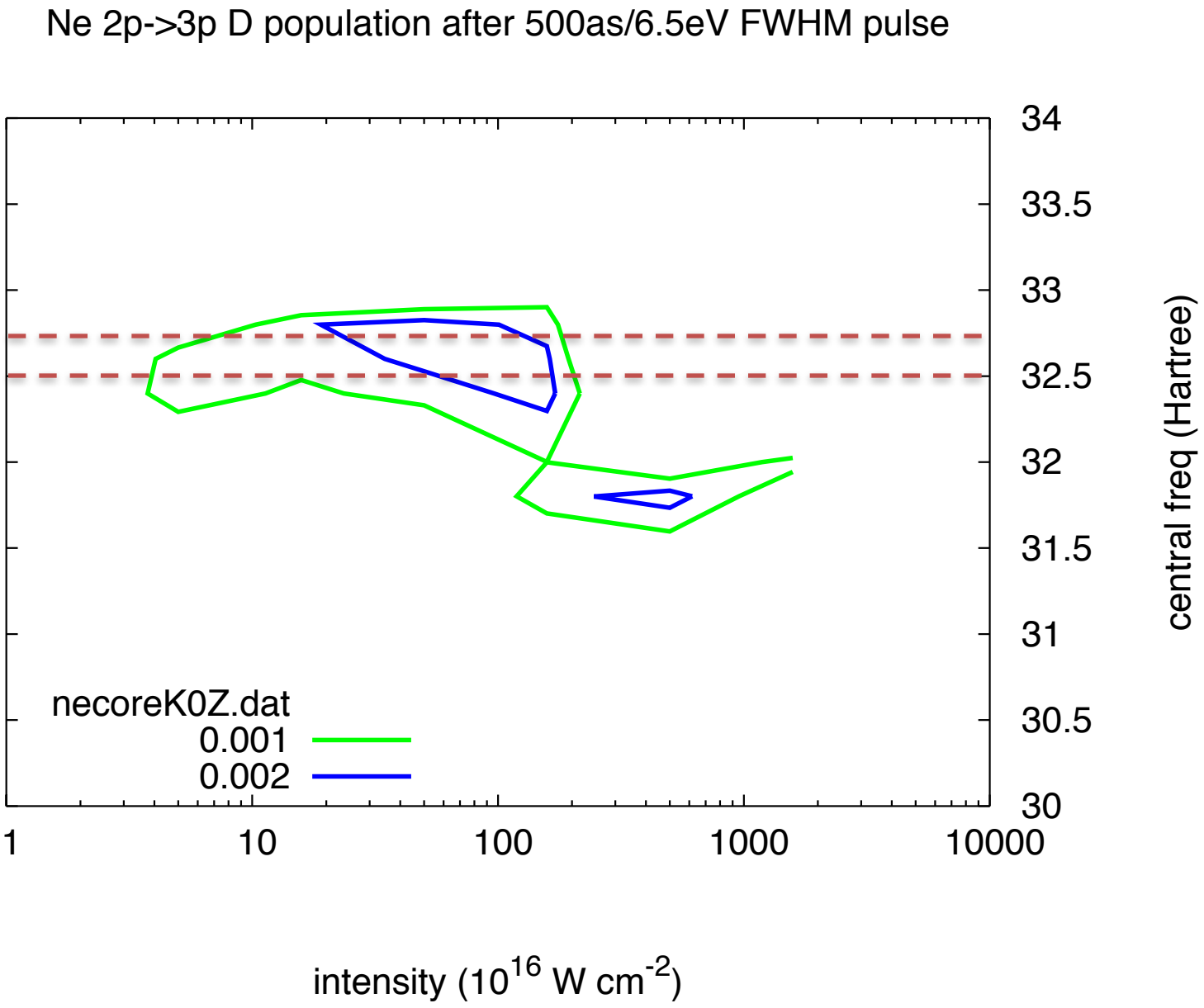

NEON ATOM 14 ORBITALS 1s K-EDGE

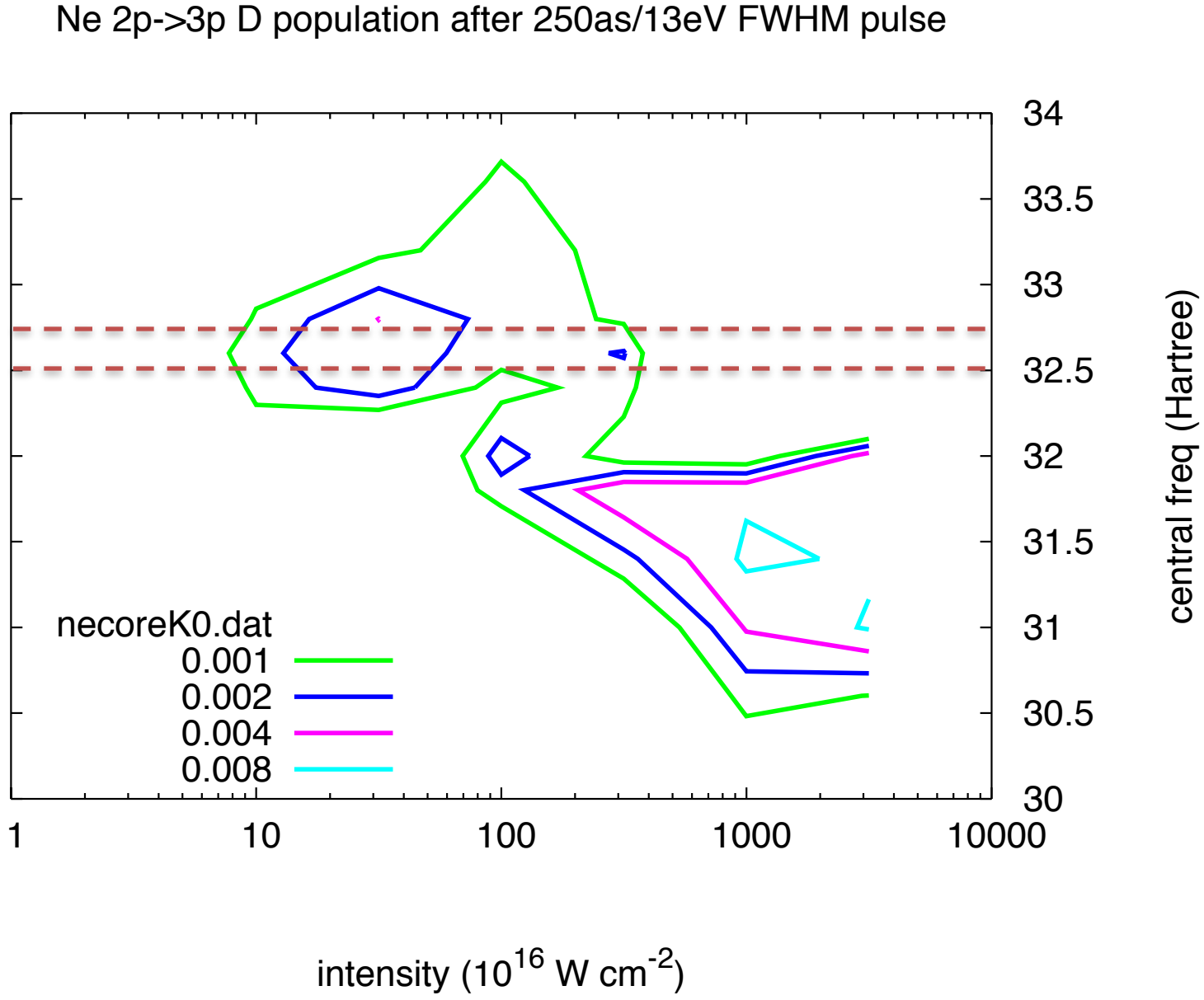

NEON ATOM 14 ORBITALS 1s K-EDGE

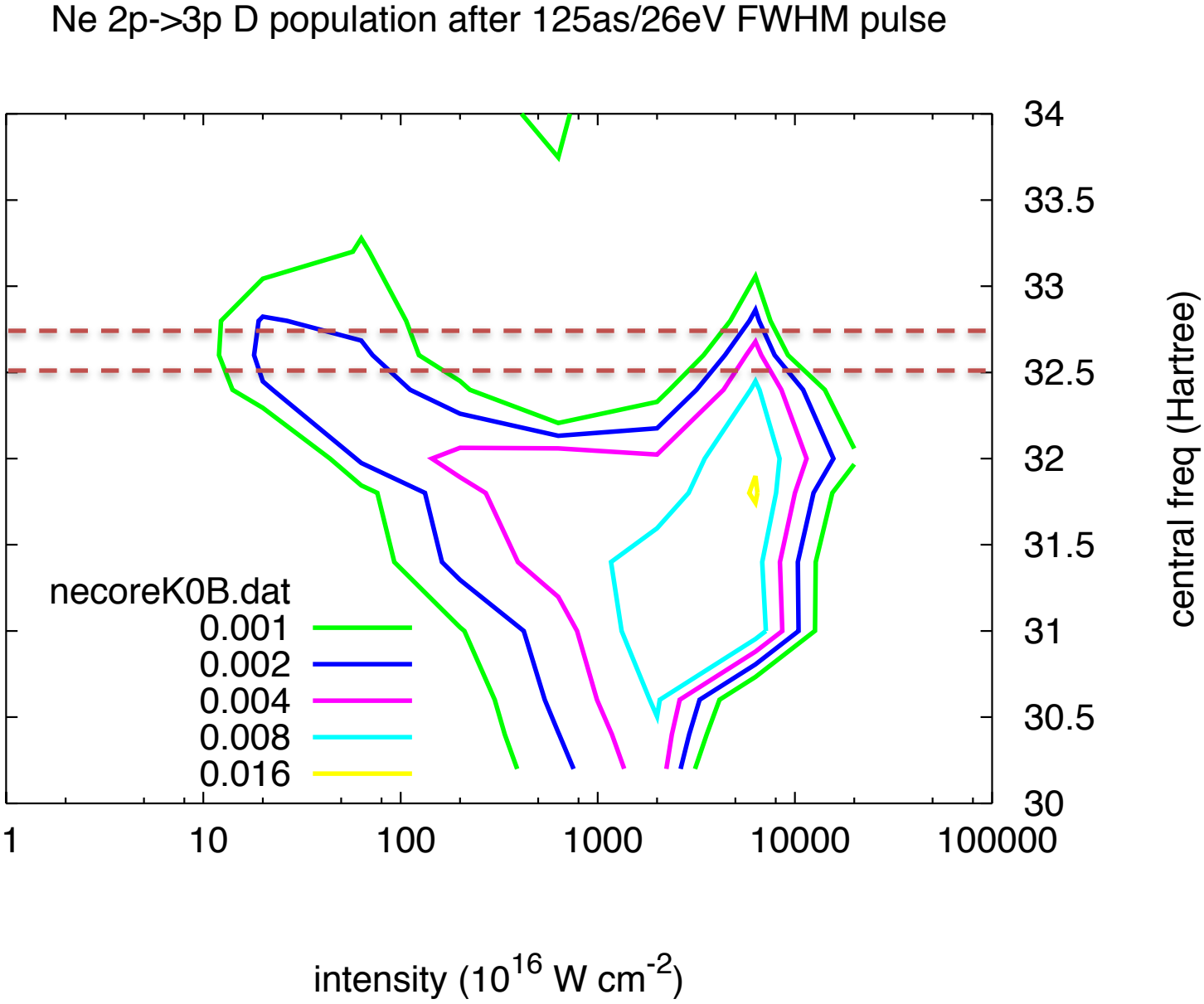

NEON ATOM 14 ORBITALS 1s K-EDGE

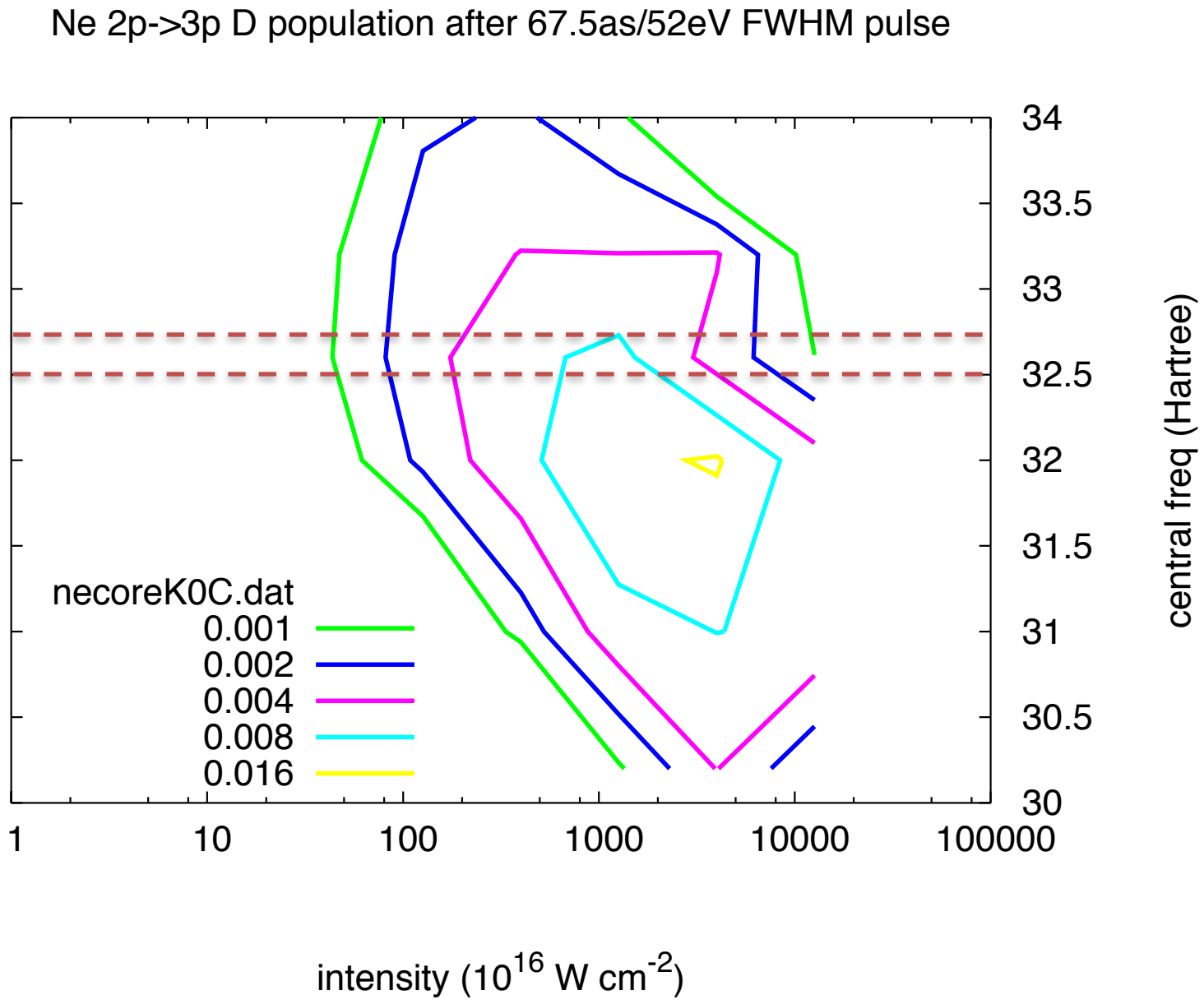

X-Ray Driven Impulsive Electronic State Redistribution in NO_2

James P. Cryan, Nora Berrah, Christoph Bostedt, Ryan Coffee, Raimund Feifel, Daniel Haxton, Jonathan Marangos, Agostino Marinelli, Shungo Miyabe, Shaul Mukamel Adi Natan, Nina Rohringer, Matthew Ware and Philip H. Bucksbaum

Abstract: Charge motion is the fundamental process that drives all chemistry. Multidimensional X-Ray spectroscopy has been proposed as a method that can create and track charge (or electron) motion in molecules. Even the simplest multidimensional x-ray spectroscopy has yet to be demonstrated, but recent experiments at the LCLS have taken the first step by observing stimulated x-ray Raman scattering (SXRS). SXRS and multidimensional spectroscopy are examples of non-linear spectroscopies, which play a vital role in the science goals of LCLS-II. Using x-rays to produce coherent electronic excitations, as we propose here, will prepare the way for LCLS-II science. Our proposal intends to use a previously untapped property of LCLS, its large coherent bandwidth when operating in "V-slotted-foil" mode, to create spatially localized coherent electronic disturbances at specific atomic locations in molecules. We will then follow the migration of these excited electrons by means of Auger electron spectroscopy probed by a second time-delayed x-ray pulse, produced using the "twin bunches + V-slotted-foil" method that has recently become available at LCLS.

NO_2 calculations: grid 55 x 55 x 55
(10^{97} primitive Slater determinants),
spacing 0.29 bohr, full CI 23 electrons in 15 orbitals
(621075 Slater determinants in MCTDHF)

arxiv.org 1609.04220

NO_2

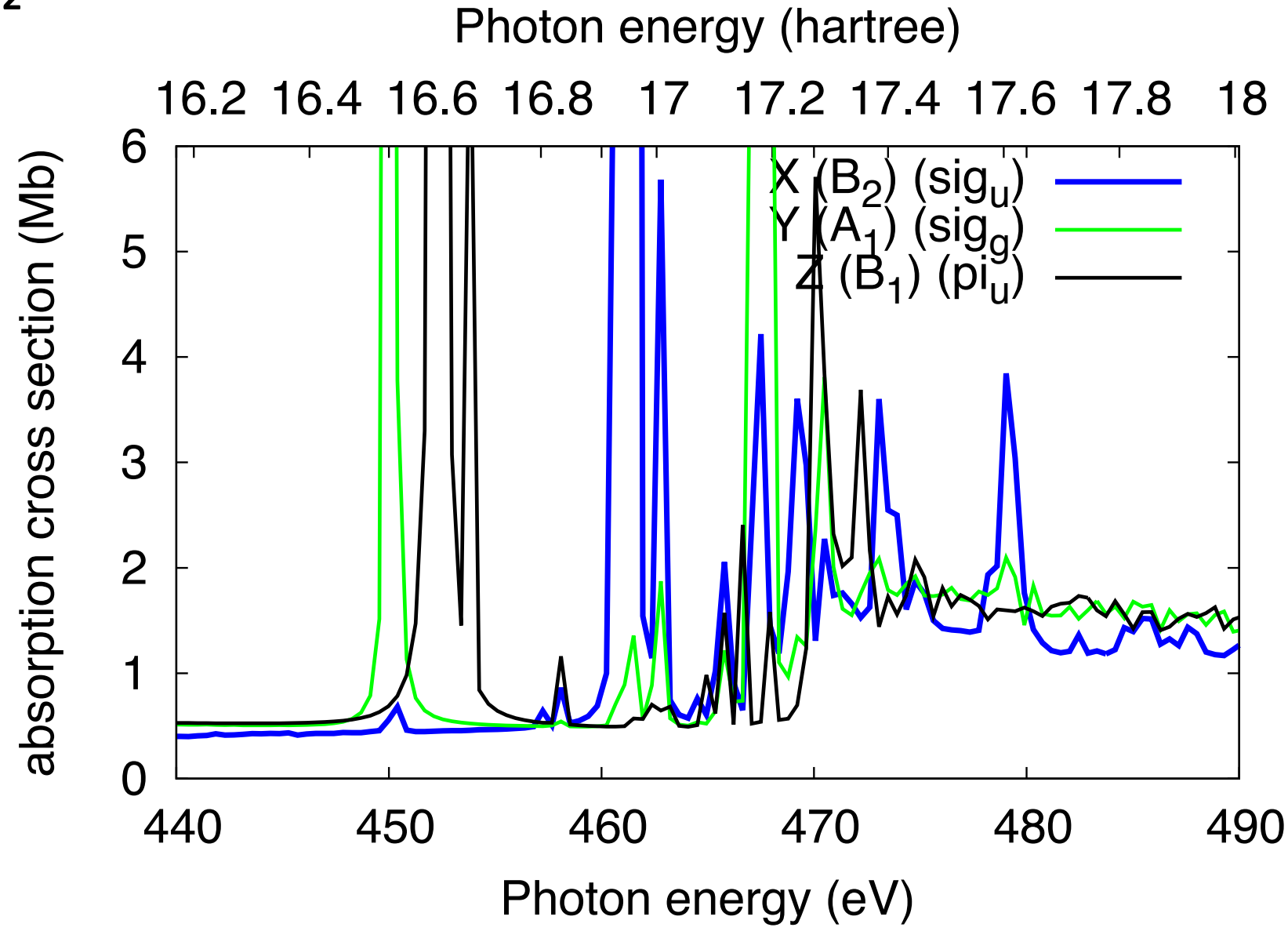
Photon energy (hartree)
16.2
16.4
16.6
16.8
17
17.2
17.4
17.6
17.8
18
absorption cross section (Mb)
0
1
2
3
4
5
6
X (B_2) (sig_u)
Y (A_1) (sig_g)
Z (B_1) (pi_u)
440
450
460
470
480
490
Photon energy (eV)

NO_2

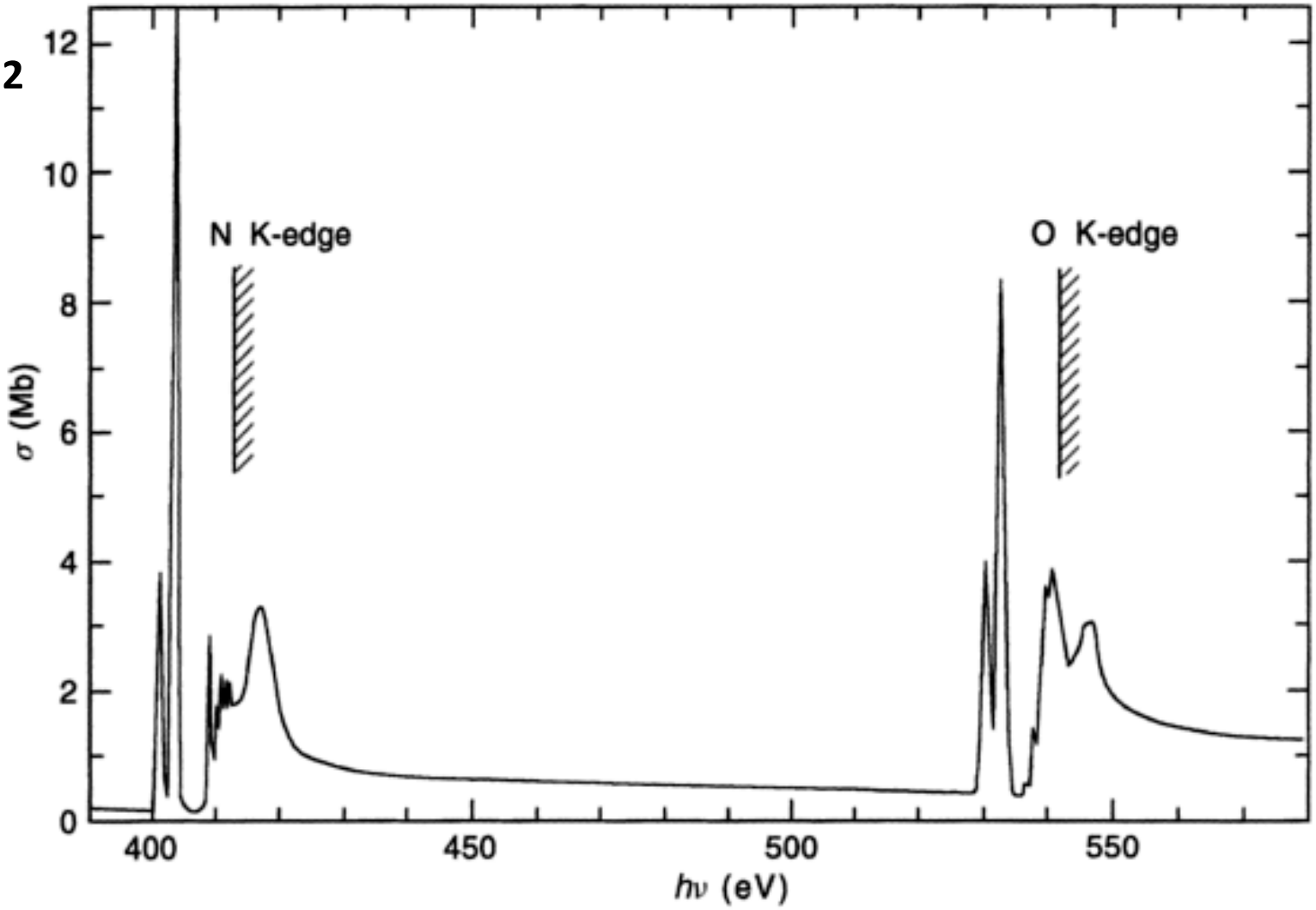

Fig. 5.10 Absolute photoabsorption spectrum of NO_2, K-edge regions. Based on Zhang *et al*. (1990), with corrections described in text

Berkowitz, "Atomic and Molecular Photoabsorption: Absolute cross sections"

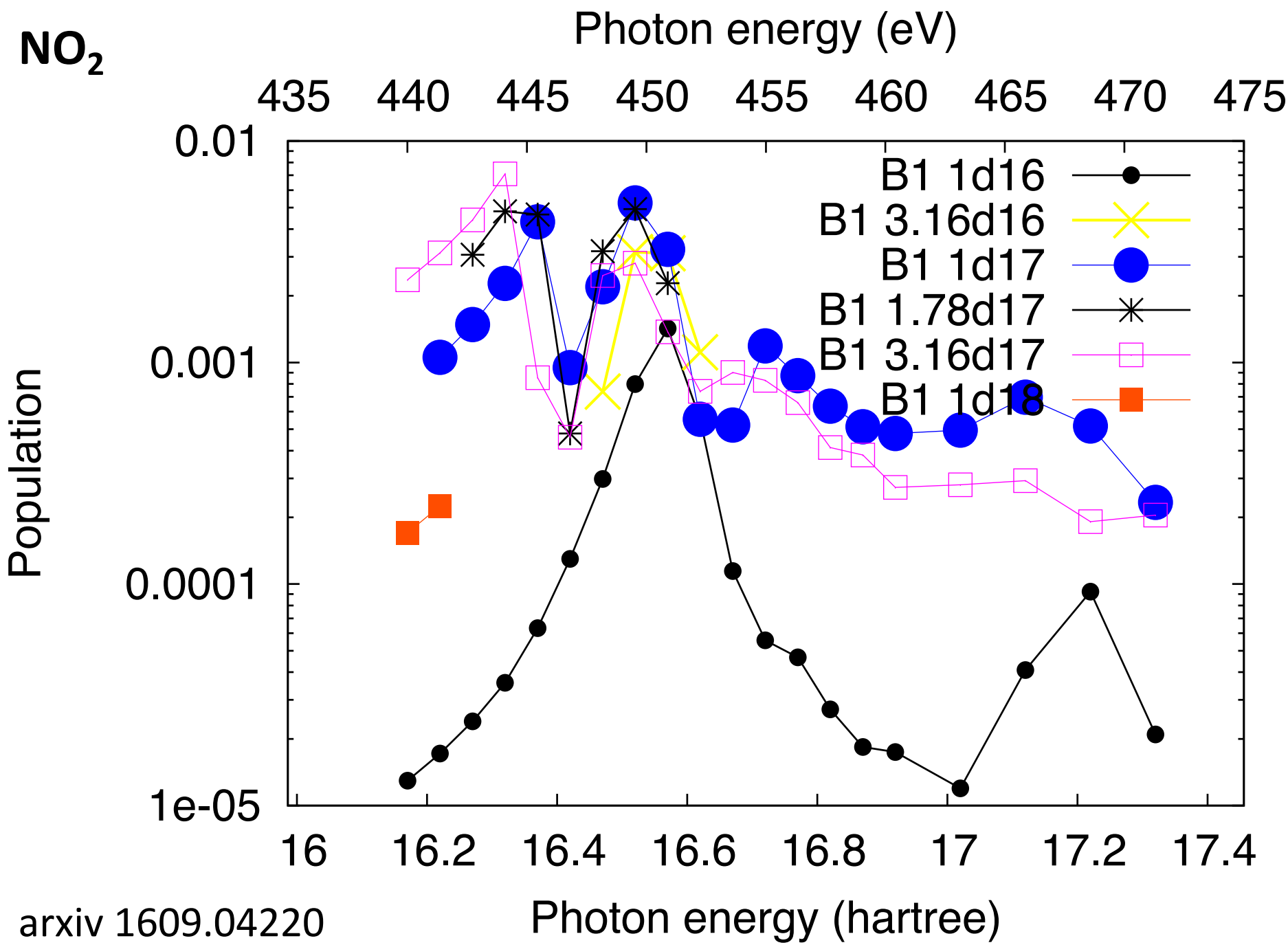
NO2
Photon energy (eV)
435
440
445
450
455
460
465
470
475
0.01
0.001
0.0001
1e-05
Population
B1 1d16
B1 3.16d16
B1 1d17
B1 1.78d17
B1 3.16d17
B1 1d18
16
16.2
16.4
16.6
16.8
17
17.2
17.4
Photon energy (hartree)
arxiv 1609.04220

LBNL-AMO-MCTDHF code is available for download, version 1.32

https://github.com/LBNL-AMO-MCTDHF
https://commons.lbl.gov/display/csd/LBNL-AMO-MCTDHF
http://danhax.us/Research/LBNL-AMO-MCTDHF.html

http://danhax.us/ITAMP2016.pdf

END

http://danhax.us/ITAMP2016.pdf

Brant Abeln

Thorsten Kurth,
Nuclear Science Division
LBL

Khaled Ibrahim, Sam Willams, Sherry (Xiaoye) L,
Computing Sciences Division LBL

(DOE SCIDAC COLLABORATION)

U.S. DEPARTMENT OF ENERGY

All results here were calculated on LBL's Lawrencium supercluster.

scs.lbl.gov

Obtain complete basis limit easily with this grid method.

Wave function represented entirely in complex plane

	R_0	N_η	n_ξ	ξ elements	Energy
H_2	1.4	9	14	3.0, 10.0, 10.0	-1.13362957146
	same with $\theta = 15°$			$1.1\times10^{-9}\ i$	-1.133629573
	same with $\theta = 30°$			$1.2\times10^{-9}\ i$	-1.133629572
				HF limit	-1.1336295715 [55]
Li_2	5.051	25	20	0.75, 3× 4.0	-14.8715620178
				eliptic basis HF	-14.8715619 [56]
LiH	3.015	21	19	1.0, 3× 5.0	-7.987352237
				numerical HF	-7.987352237 [57]
CO	2.132	21	19	1.5, 7.5, 7.5	-112.79090718
	same with $\theta = 15°$			$1.1\times10^{-8}\ i$	-112.79090714
	same with $\theta = 30°$			$8\times10^{-8}\ i$	-112.79090714
				numerical HF	-112.790907 [57]
N_2	2.068	21	19	1.5, 7.5, 7.5	-108.99382563
				numerical HF	-108.9938257 [57]
N_2	same basis, (14/10) CAS-SCF				-109.14184793(5)
	(14/10) Columbus ccpvtz				-109.132509251
	(14/10) Columbus ccpvqz				-109.140039408

Haxton, Lawler, McCurdy
PRA 83, 063416 (2011)

ELECTRONIC REPRESENTATION FOR POLYATOMICS

Polyatomic grid method using sinc basis functions

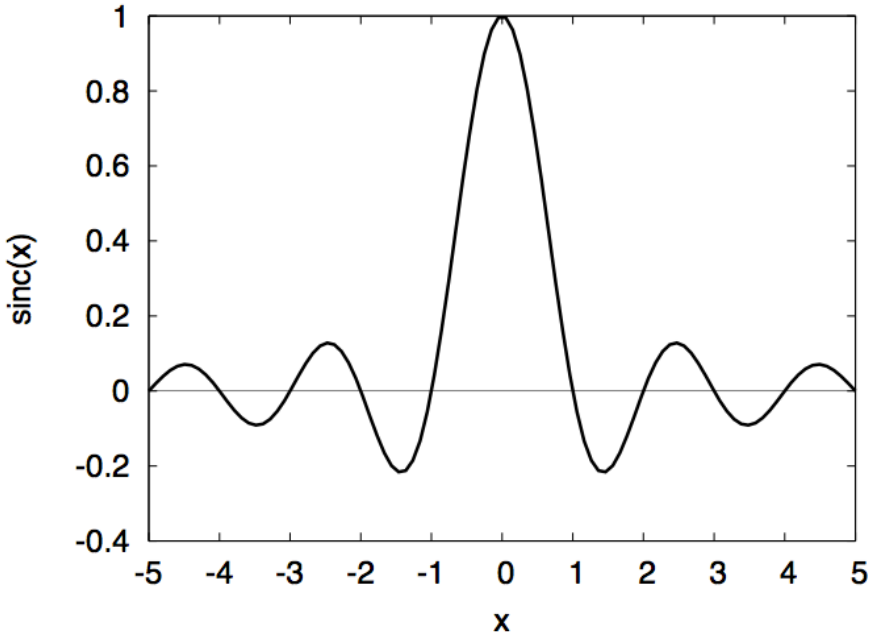

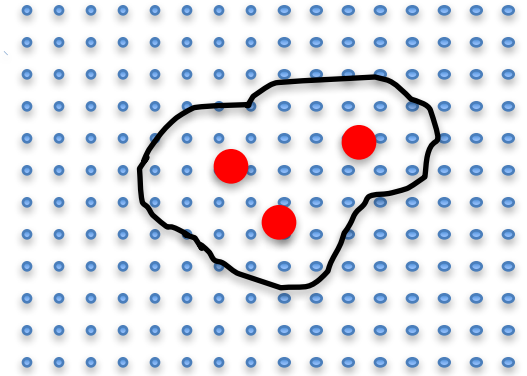

$$\mathrm{sinc}(x) \equiv \frac{\sin(\pi x)}{\pi x}$$

$$\phi_{i_1 i_2 i_3}(x, y, z) = \mathrm{sinc}(x/\Delta - i_1)\mathrm{sinc}(y/\Delta - i_2)\mathrm{sinc}(z/\Delta - i_3)$$

Polyatomic grid method using sinc basis functions

A) Use Poisson's equation to obtain sparse representation of $1/r_{12}$ via kinetic energy

$$\langle \vec{i}\vec{j}| \frac{1}{r_{12}} |\vec{k}\vec{l}\rangle \approx \delta^3_{\vec{i}\vec{k}} \delta^3_{\vec{j}\vec{l}} \, 2\pi \Delta^{-3} (T^{-1})_{\vec{i}\vec{j}}$$

Limit of matrix inverse as size of matrix goes to infinity

An ideal resolution-of-the-identity approximation in which the auxilliary basis, the basis in which the density is expanded, is the same as the basis used in the calculation.

Following McCurdy, Baertschy, and Rescigno, J. Phys. B, 37, R137 (2004)
See http://arxiv.org/abs/1507.03324, to appear in Mol. Phys.

Polyatomic grid method using sinc basis functions

B) Basis functions are all the same, just translated

$$\langle \vec{i}\vec{j}|\frac{1}{r_{12}}|\vec{k}\vec{l}\rangle = \langle (\vec{i}-\vec{a})(\vec{j}-\vec{a})|\frac{1}{r_{12}}|(\vec{k}-\vec{a})(\vec{l}-\vec{a})\rangle$$

$$\langle \vec{i}|T|\vec{j}\rangle = \langle (\vec{i}-\vec{a})|T|(\vec{j}-\vec{a})\rangle$$

→ Matrix elements of any translationally invariant operator in this Cartesian product sinc basis, having a translational automorphism are **TRIPLE TOEPLITZ** (3-level Toeplitz)

$$T_{\vec{i}\vec{j}} = t_{\vec{i}-\vec{j}} \quad 2\pi\Delta^{-3}(T^{-1})_{\vec{i}\vec{j}} = v_{\vec{i}-\vec{j}}$$

Triple Toeplitz matrix-vector multiplication (Triple Toeplitz Matvec)

Reduced potential due to a transition density is obtained via triple Toeplitz matrix-vector multiplication

$$v^{\alpha\beta}_{i1,i2,i3} = \sum_{j1,j2,j3} \phi^{\alpha}_{j1,j2,j3} \phi^{\beta}_{j1,j2,j3} v_{i1-j1,i2-j2,i3-j3}$$

A two-electron matrix element is the contraction of the reduced potential with another transition density

$$[\alpha\beta||\gamma\delta] = \sum_{i1,i2,i3} \phi^{\gamma}_{i1,i2,i3} \phi^{\delta}_{i1,i2,i3} v^{\alpha\beta}_{i1,i2,i3}$$

Toeplitz matrices

$$M_{ij} = m_{i-j} \qquad \text{e.g } M = \begin{matrix} A & B & C & D \\ Z & A & B & C \\ Y & Z & A & B \\ X & Y & Z & A \end{matrix}$$

A rank-n Toeplitz matrix may be embedded in a rank-m circulant matrix, m=2n

$$C_{ij} = c_{mod(i-j,\, m)} \qquad \text{e.g } C = \begin{matrix} 0 & X & Y & Z & A & B & C & D \\ D & 0 & X & Y & Z & A & B & C \\ C & D & 0 & X & Y & Z & A & B \\ B & C & D & 0 & X & Y & Z & A \\ A & B & C & D & 0 & X & Y & Z \\ Z & A & B & C & D & 0 & X & Y \\ Y & Z & A & B & C & D & 0 & X \\ X & Y & Z & A & B & C & D & 0 \end{matrix}$$

Toeplitz matrix-vector multiplication may be accomplished in O(n log n) multiplication operations using Fast Fourier Transform

Triple Toeplitz matrices

A rank-N (e.g. $N=n^3$) triple Toeplitz matrix
may be embedded in a rank-8N triple circulant matrix

$$M_{i_1 i_2 i_3, j_1 j_2 j_3} = m_{(i_1 - j_1)(i_2 - j_2)(i_3 - j_3)}$$

Triple Toeplitz mat-vec using O(N log N) multiplication operations via 3D Fast Fourier Transform

This was a key insight of mine, something not known in my science community, but very useful generally.
Can be found in this reference:

Jie Chen and Tom Li. Parallelizing the conjugate gradient algorithm for multilevel Toeplitz systems. Procedia Computer Science 18, 571 (2013)

Triple Toeplitz mat-vec

Implemented 3 algorithms for 3-dimensional Fast Fourier Transform (3D FFT) using distributed memory (MPI) for triple Toeplitz matvec.

Used libraries for local FFTs, then built MPI parts myself.

Although MPI FFTs are available (e.g. Intel), building my own MPI FFT allows maximum portability and makes optimization easy.

MPI FFT Algorithms

(1) All-to-all / some-to-some, transposing indices
(2) Some-to-some, without transposing indices, MPI Cooley-Tukey on each index
(3) MPI Cooley-Tukey with MPI recursion

(1) Is common knowledge; (2) and (3) seem less well known

PARALLELIZATION OF MCTDHF METHOD

Parallelization of MCTDHF method

Three aspects:

1) Slater determinants
2) Different orbitals, different processors atom & diatomic
3) Every orbital divided among all processors polyatomics

$$i\frac{\partial}{\partial t}\vec{A} = (H - \tau)\vec{A}$$

$$i\frac{\partial}{\partial t}\vec{\phi} = \left[(1 - P)\left(\rho^{-1}\mathbf{W} + h_0\right) + g\right]\vec{\phi}$$

Parallelization of MCTDHF method

Three aspects:

1) Slater determinants

The Slater determinant list is kept completely arbitrary; each determinant is given a different index, and the sparse structure of matrices is tabulated before the calculation starts. Then two modes are available: (A) sparse matrices can be explicitly constructed in-between each mean field time step, or (B) direct CI in which sparse matrices are never constructed, loops over orbitals

2) Different orbitals, different processors atom & diatomic
3) Every orbital divided among all processors polyatomics

Parallelization of MCTDHF method

Three aspects:

1) Slater determinants
2) Different orbitals, different processors atom & diatomic

Among blocks of nblock processors (e.g. 20 processors, nspf=10 orbitals → 2 blocks, nblock=10), only **nspf^4/nblock** two-electron matrix elements, **nspf^2/nblock** elements of W, w are stored
Some-to-some operation required for reduced operator W

$$\mathbf{W}_{\alpha\beta} = \sum_{\gamma\delta} \Gamma^{\gamma\delta}_{\alpha\beta} \mathbf{w}_{\gamma\delta}$$

$$i\frac{\partial}{\partial t}\vec{\phi} = \left[(1-P)\left(\rho^{-1}\mathbf{W} + h_0\right) + g\right]\vec{\phi}$$

3) Every orbital divided among all processors polyatomics

Parallelization of MCTDHF method

Three aspects:

1) Slater determinants
2) Different orbitals, different processors atom & diatomic
3) Every orbital divided among all processors polyatomics

Cubic grids nx=ny=nz are used and 1, 2, or 3 dimensions are divided among procesors.

E.g. 64x64x64, 32 processors, 64x64x2 each
135x135x135, 81 processors, 135x15x15 each

Densities are constructed locally, then parallel communication occurs during MPI 3D fast Fourier transform (different MPI 3D FFT methods implemented)

More NO

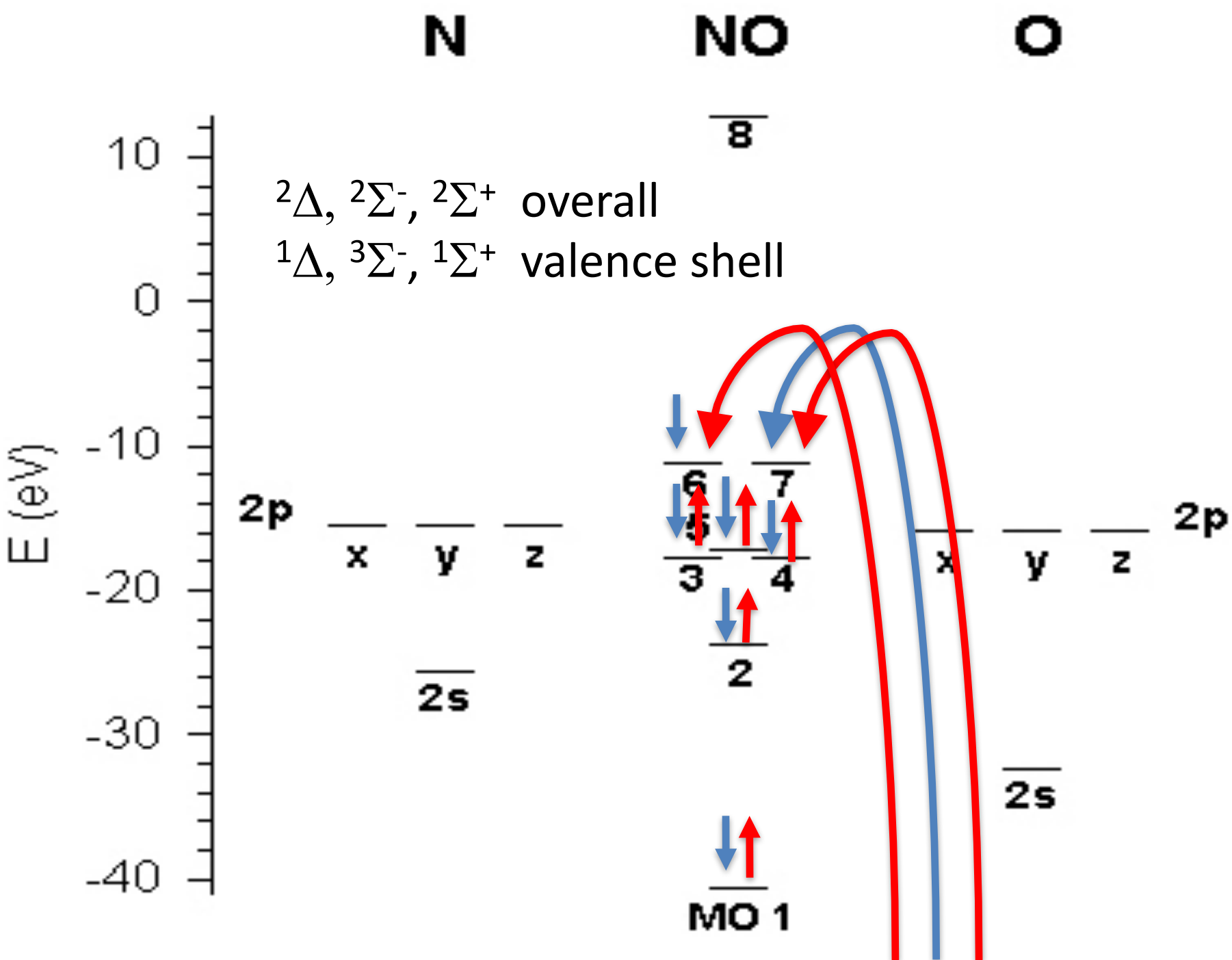
N
NO
O
$^2\Delta$, $^2\Sigma^-$, $^2\Sigma^+$ overall
$^1\Delta$, $^3\Sigma^-$, $^1\Sigma^+$ valence shell
E (eV)
10
0
-10
-20
-30
-40
2p
x
y
z
2s
8
6
7
5
3
4
2
MO 1
2p
x
y
z
2s

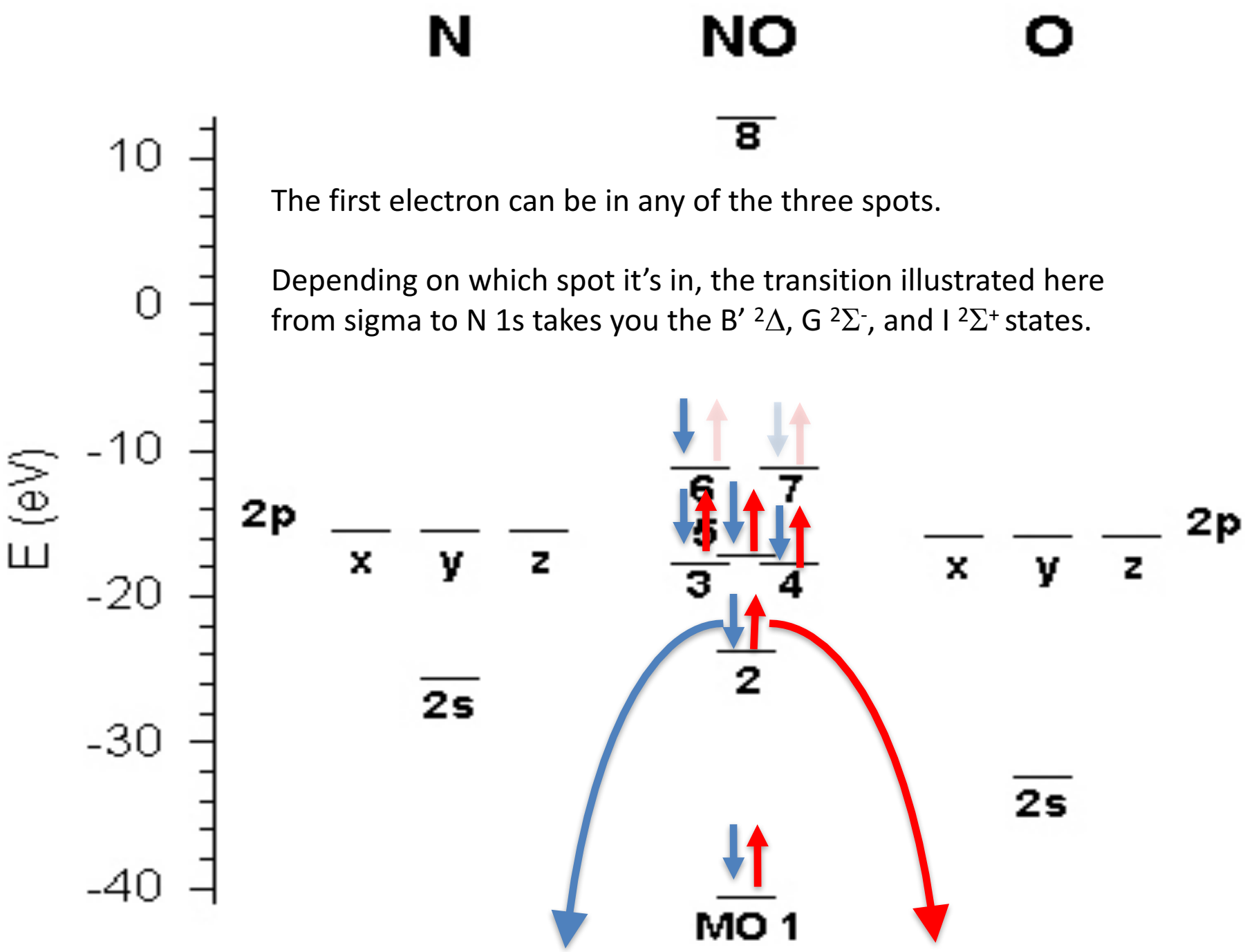

The first electron can be in any of the three spots.

Depending on which spot it's in, the transition illustrated here from sigma to N 1s takes you the B' $^2\Delta$, G $^2\Sigma^-$, and I $^2\Sigma^+$ states.

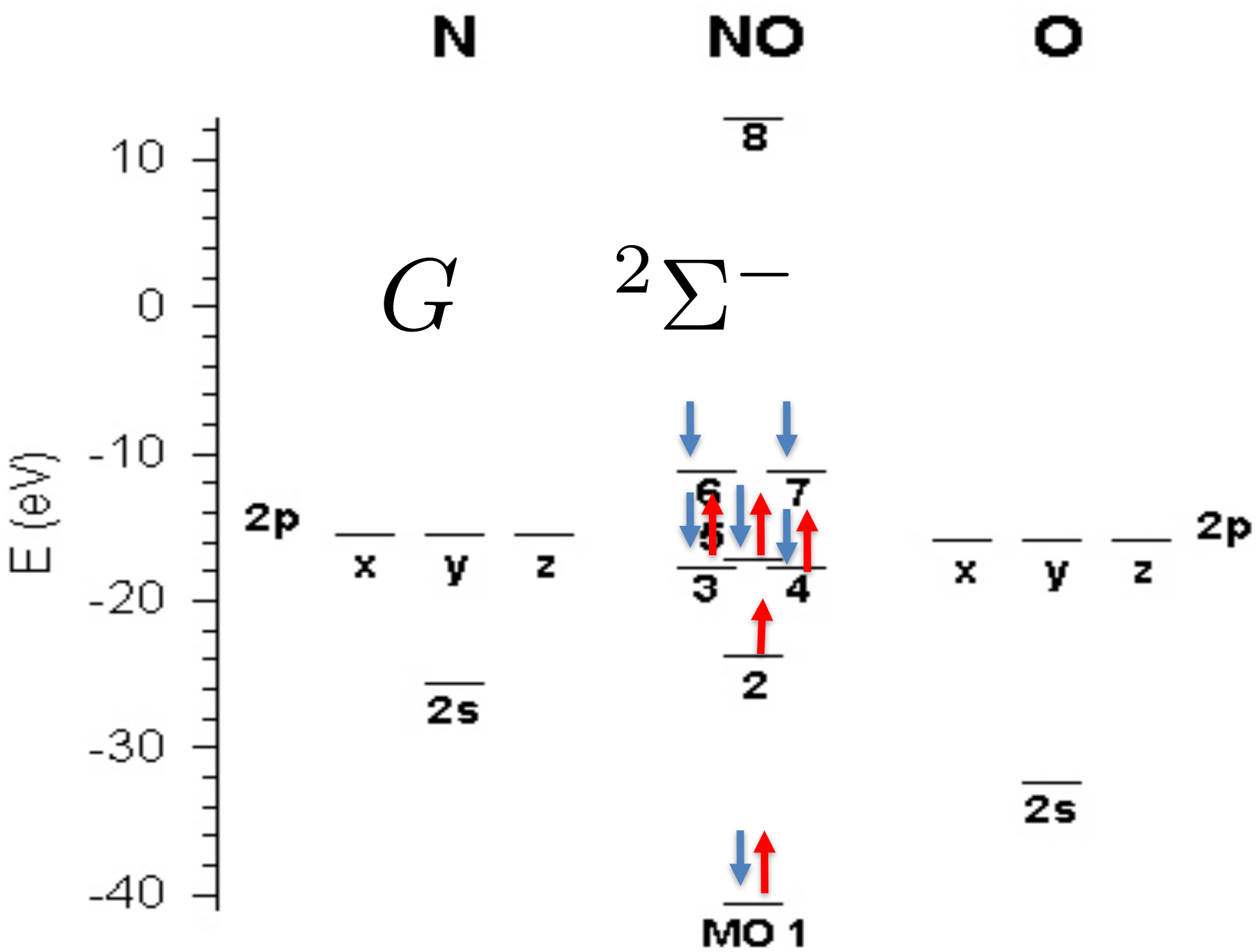
N
NO
O
$G \quad {}^2\Sigma^-$
E (eV)
10
0
-10
-20
-30
-40
2p
x
y
z
2s
8
6
7
5
3
4
2
MO 1
2p
x
y
z
2s

The Raman signal

Frequency dependent response function

$$\tilde{\mathbf{S}}(\omega) = 2\mathrm{Im}[\tilde{\mu}(\omega)\tilde{\mathcal{E}}(\omega)^*]$$

Emission/absorption of energy $\propto \omega\tilde{\mathbf{S}}(\omega)$

FT of $\langle\Psi(t)|\mu|\Psi(t)\rangle$

FT of field

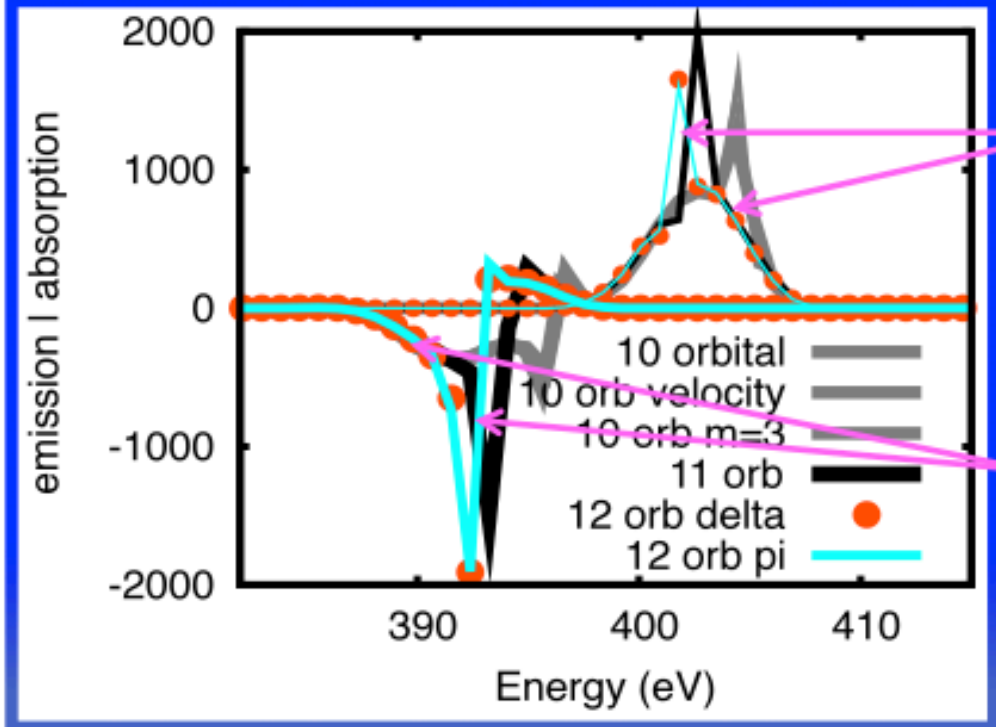

Absorption: peak near 400 eV and background with energy profile of pulse

Raman emission: peak near 393 eV and background with energy profile of pulse -- Raman via the continuum

Convergence with respect to orbitals – core states

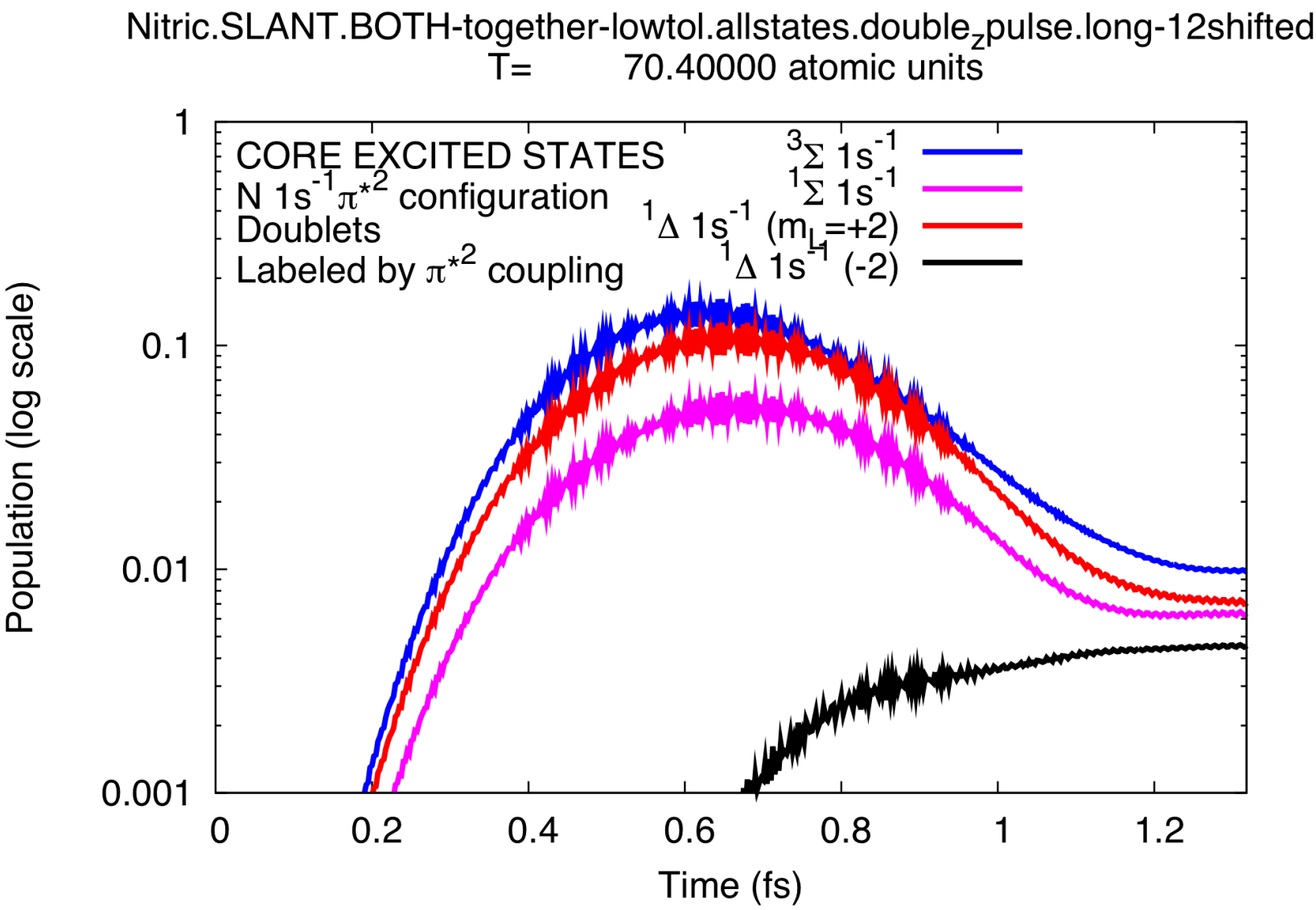

Convergence with respect to orbitals – core states

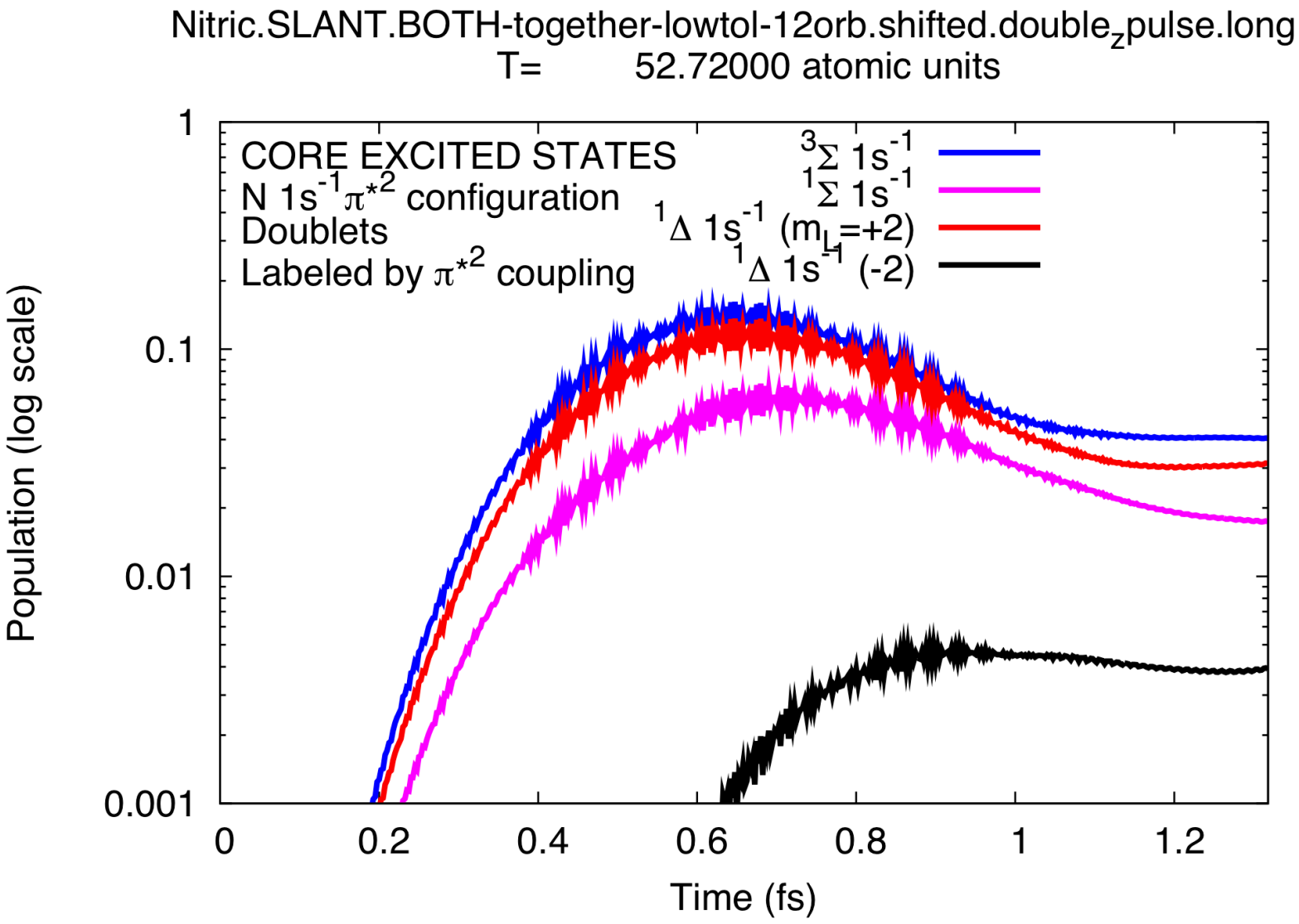

Convergence with respect to orbitals – valence states

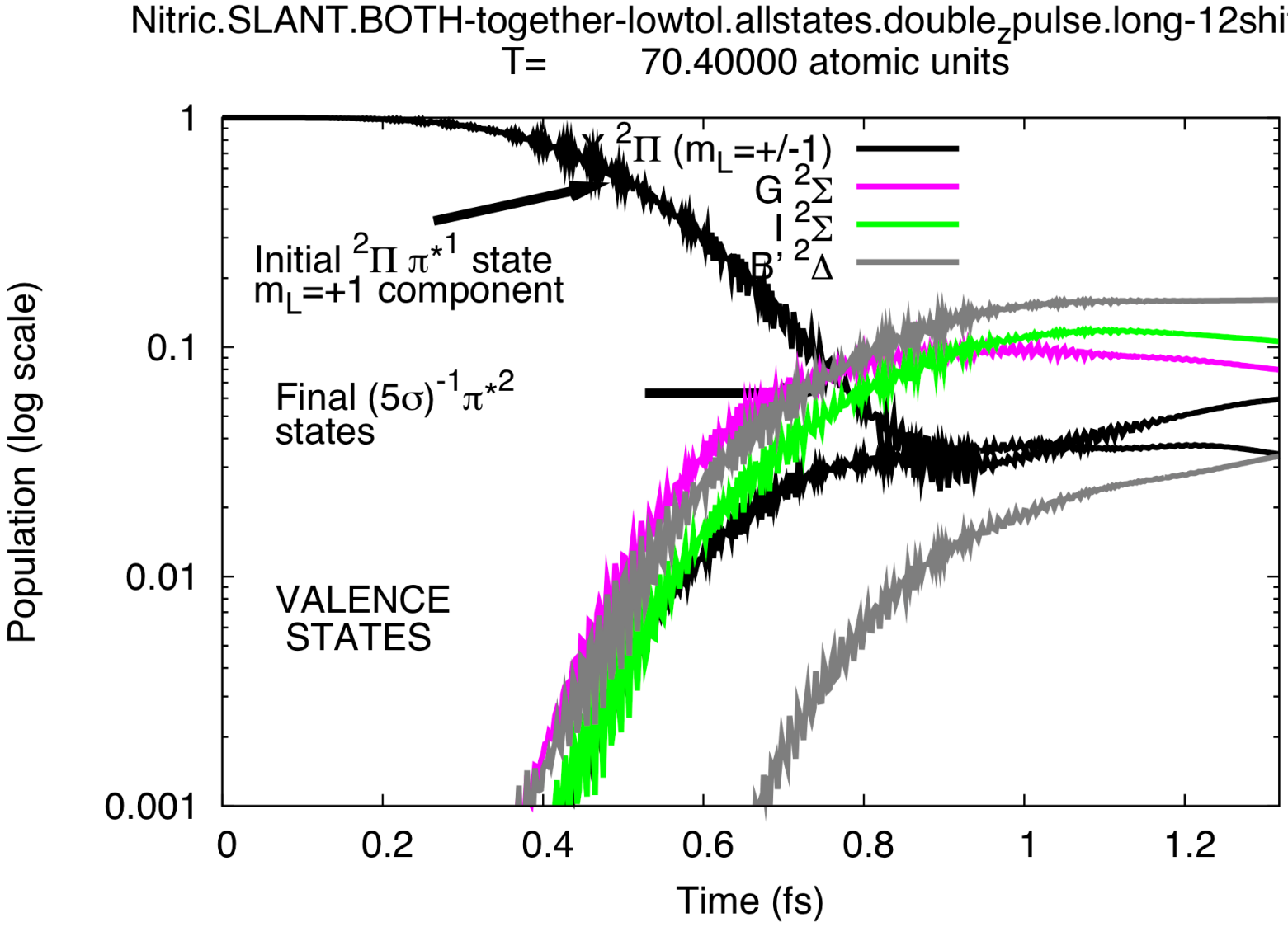

Convergence with respect to orbitals – valence states

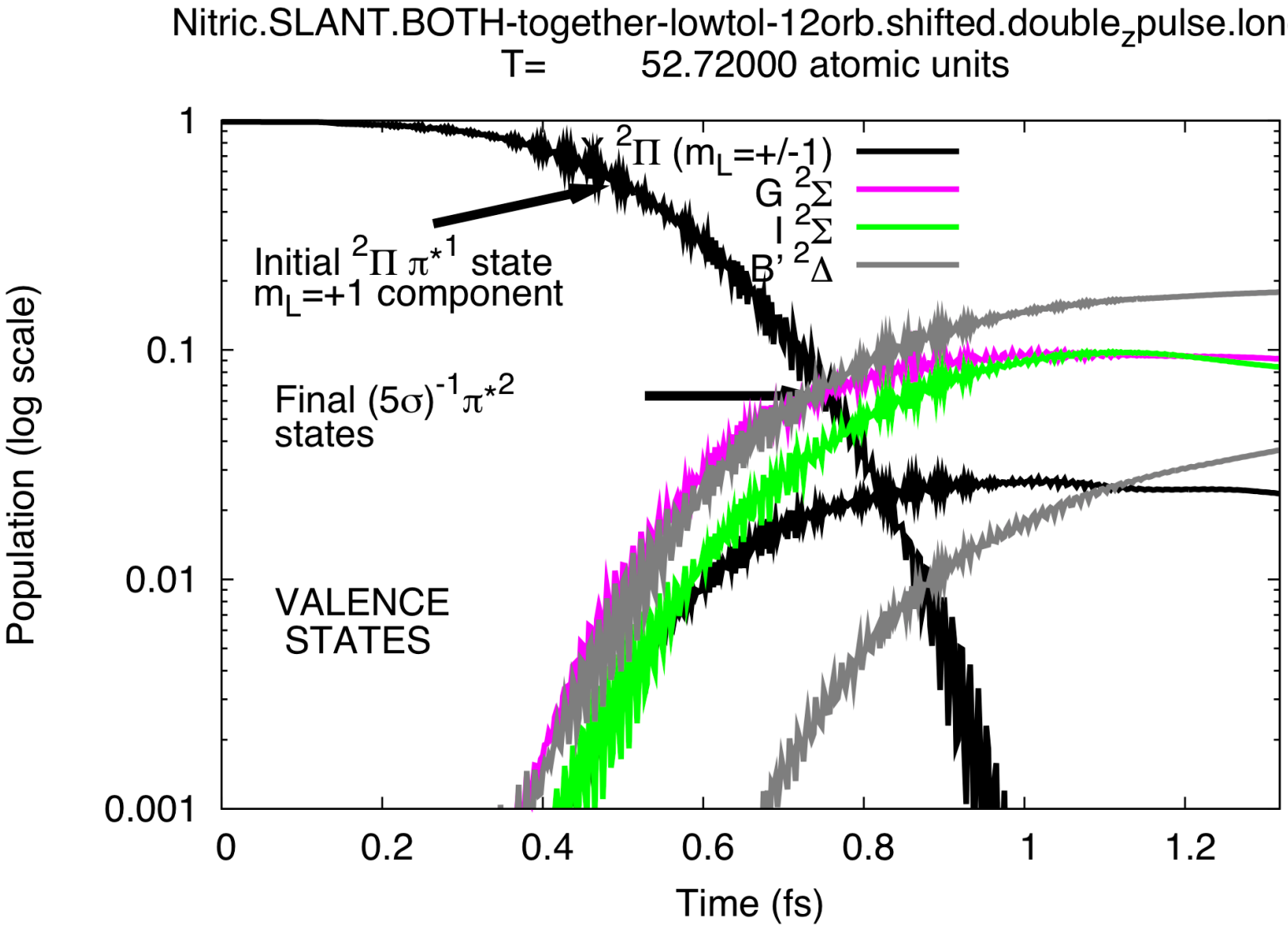

Photoionization

Photoionization

Apply few cycle perturbative pulse.

Analyze wave function after pulse (50fs):

$$\hat{F} = i[\hat{H}, \Theta]$$

Use a Fourier transform with flux operator
Also can project onto final cation states

Formally: flux operator F; Θ is 1 in ionization region, 0 elsewhere
→ math →

Antihermitian part of ECS hamiltonian

$$f(E) = \int_0^\infty dt \int_0^\infty dt' \, e^{iE(t-t')} \left\langle \Psi(t') \left| i(\hat{H} - \hat{H}^\dagger) \right| \Psi(t) \right\rangle$$

Formalism of Heidelberg group (they use complex absorbing potentials, inappropriate for electrons)

Photoionization

Need matrix elements between nonorthogonal slater determinants at t, t'

$$f(E) = \int_0^\infty dt \int_0^\infty dt'\, e^{iE(t-t')} \left\langle \Psi(t') \left| i(\hat{H} - \hat{H}^\dagger) \right| \Psi(t) \right\rangle$$

Overlap and Hamiltonian matrix elements are FULL. Intractable.
Solution: transform orbitals $\phi_\alpha(t)$, $\phi_\alpha(t')$ to biorthogonal basis

$\langle\phi_\alpha(t)|\phi_\beta(t')\rangle = s_{\alpha\beta}$ $\quad \varphi(t') = s^{-1}\,\phi(t')$ $\quad \langle\phi_\alpha(t)|\varphi_\beta(t')\rangle = \delta_{\alpha\beta}$

Must transform A-vector at time t' to leave wave fn unchanged

$$\Psi(t') = \sum_{\vec{n}} A_{\vec{n}} |\vec{n}\rangle = \sum_{\vec{m}} B_{\vec{m}} |\vec{m}\rangle \qquad \vec{A}(t') = \boldsymbol{S}(t')\vec{B}(t')$$

Full

$$\boldsymbol{S}_{\vec{n}\vec{m}} = \langle \vec{n}(t') | \vec{m}(t') \rangle \qquad \rightarrow \vec{B} = \mathbf{exp}\,(-\mathbf{ln}\,\boldsymbol{S})\vec{A}$$

!

Choose sparse branch

HF: Valence photoionization PRA 86, 013406

PARALLEL

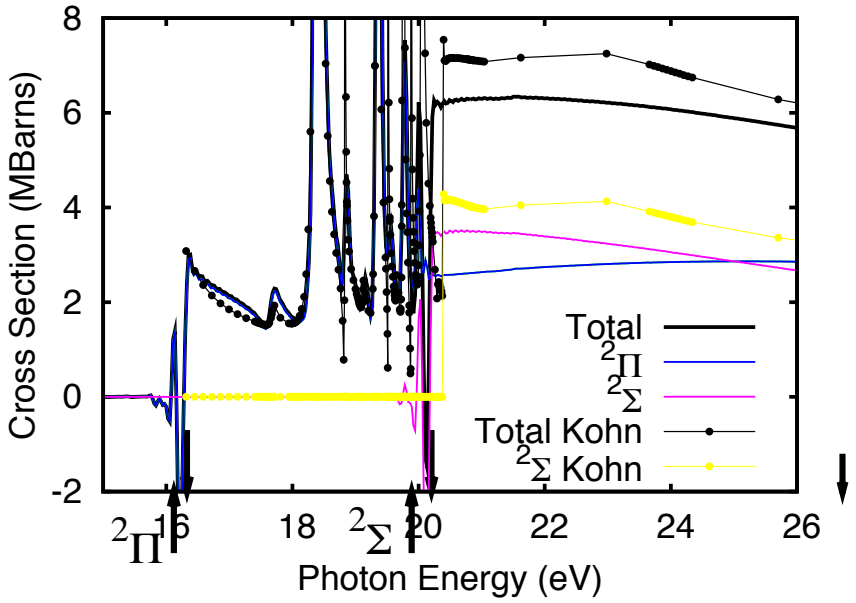

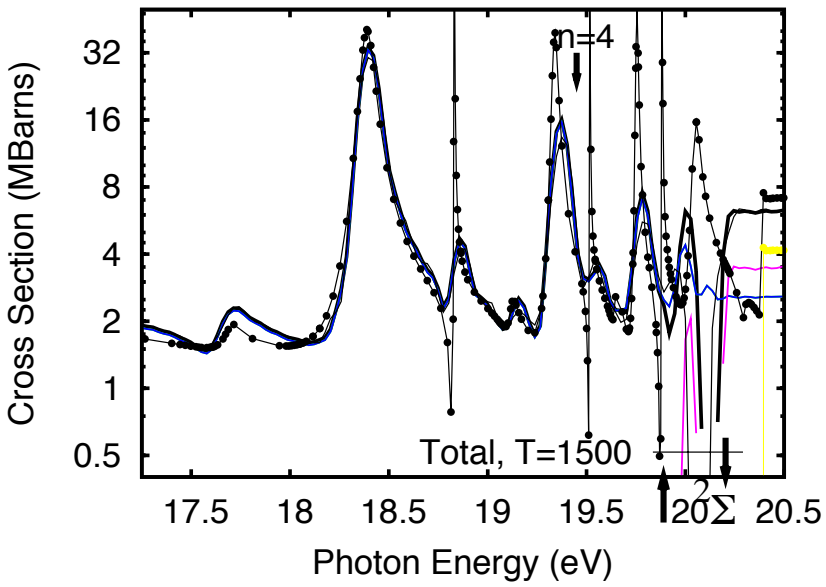

Favorable comparison between results calculated with time-dependent LBNL-AMO-MCTDHF code (lines) and time-independent complex Kohn scattering code of Rescigno and McCurdy (dotted lines)

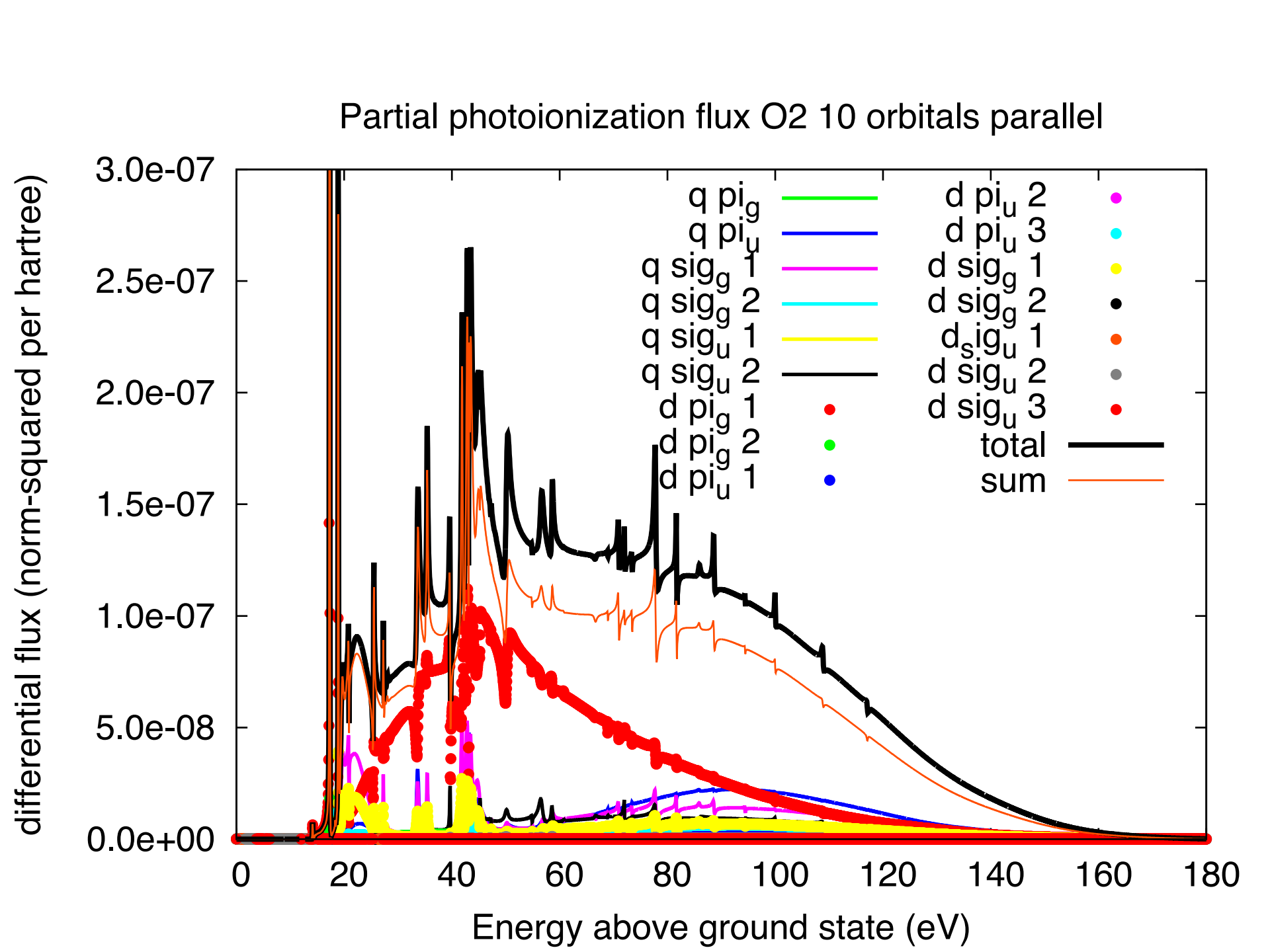
Partial photoionization flux O2 10 orbitals parallel
differential flux (norm-squared per hartree)
Energy above ground state (eV)
3.0e-07
2.5e-07
2.0e-07
1.5e-07
1.0e-07
5.0e-08
0.0e+00
0
20
40
60
80
100
120
140
160
180
q pi_g
q pi_u
q sig_g 1
q sig_g 2
q sig_u 1
q sig_u 2
d pi_g 1
d pi_g 2
d pi_u 1
d pi_u 2
d pi_u 3
d sig_g 1
d sig_g 2
d_s ig_u 1
d sig_u 2
d sig_u 3
total
sum

Partial photoionization flux O_2: integrals dt and dE agree

(Nontrivial, different formulas)

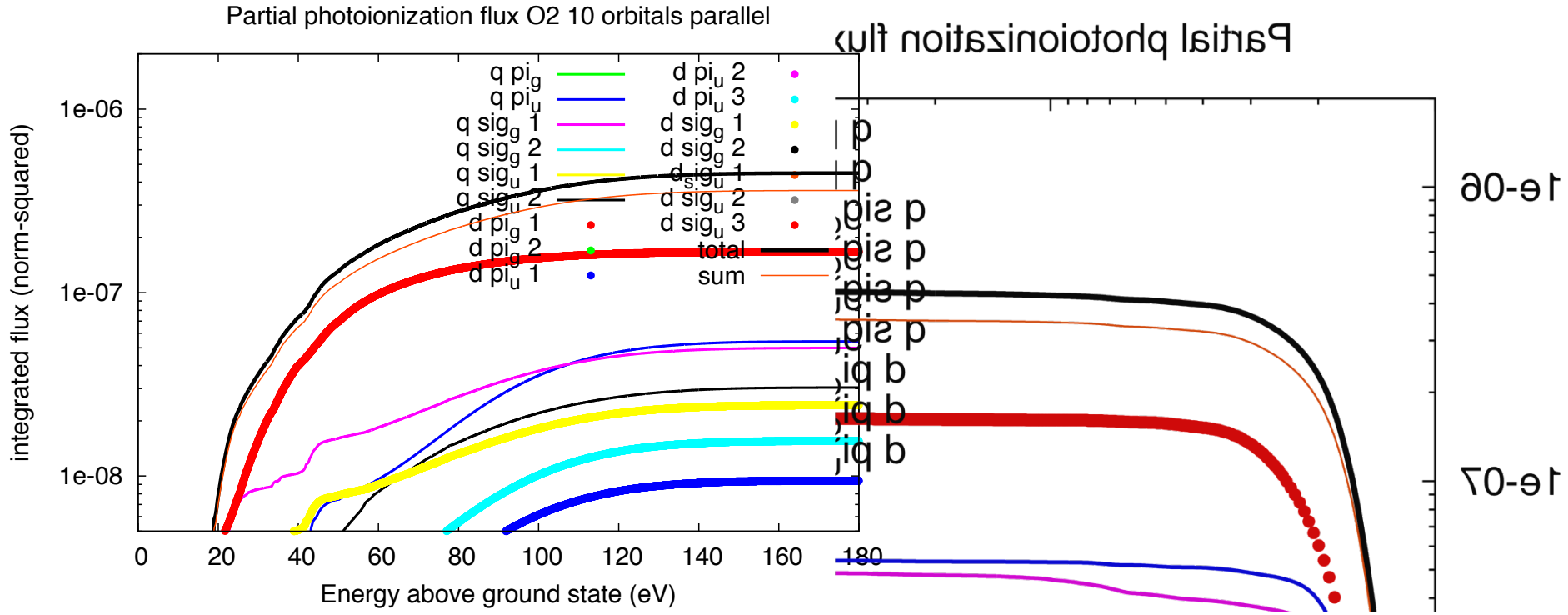

Flux integral dE

Flux integral dt

SCALING CARTESIAN

Complex coordinate scaling for molecules

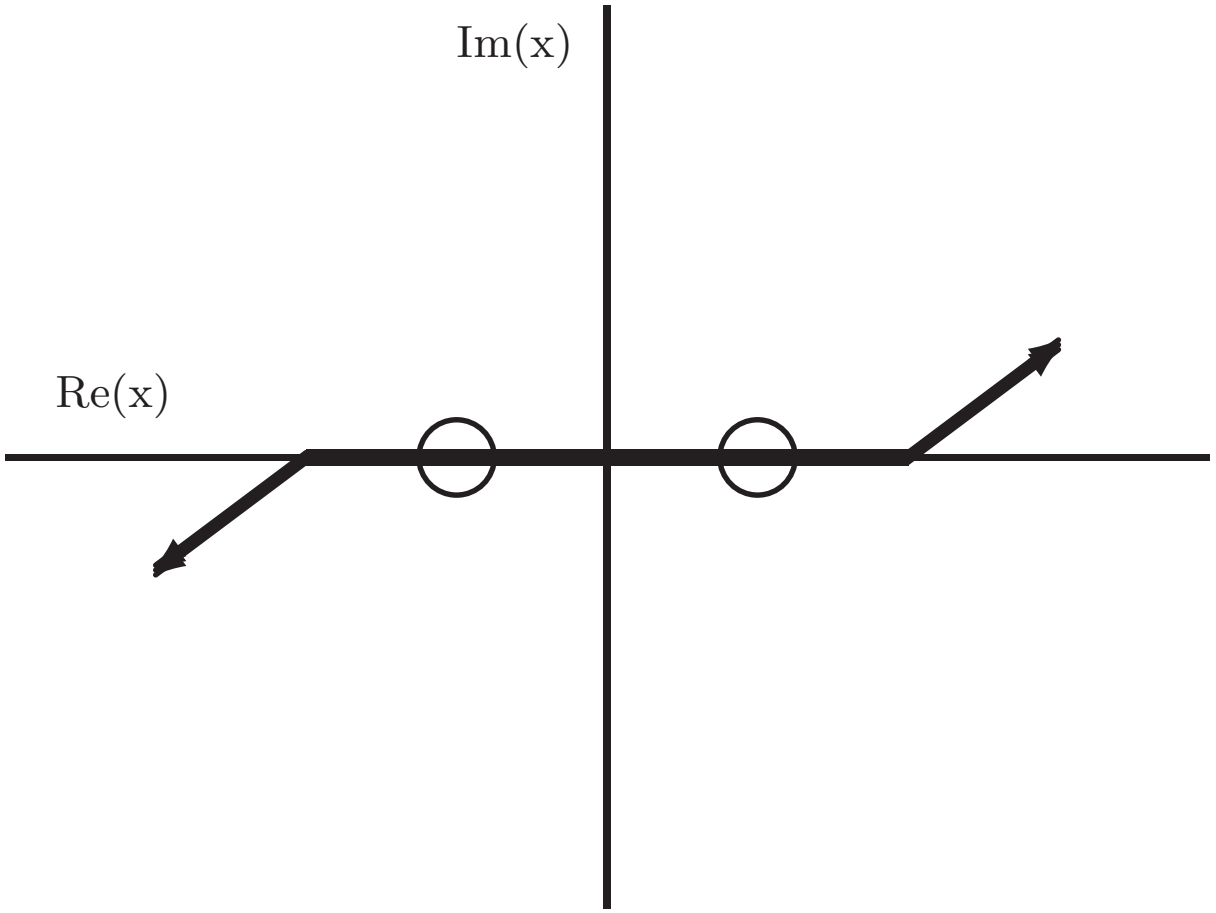

Exterior complex scaling so that the nuclei are on the grid

Complex coordinate scaling for molecules

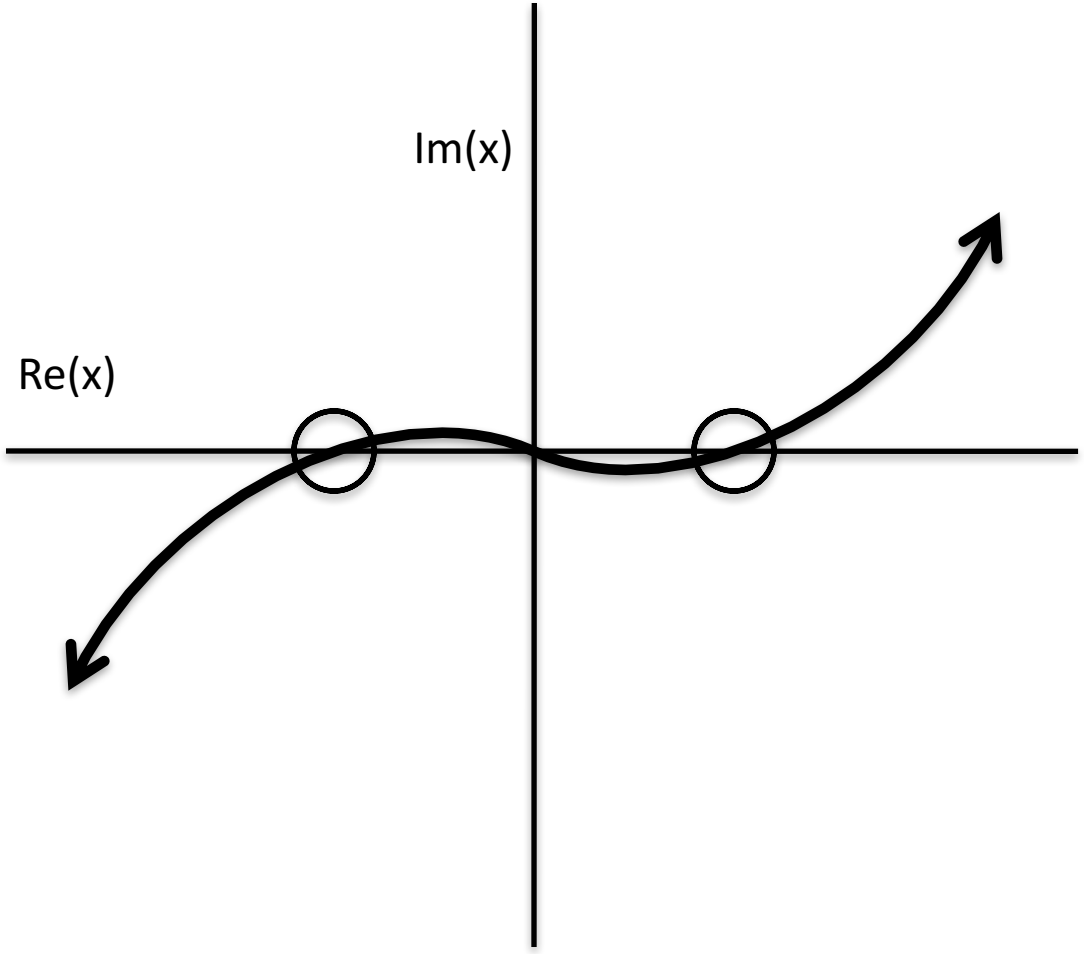

Everywhere complex scaling so that the nuclei are on the grid

Complex coordinate scaling for molecules

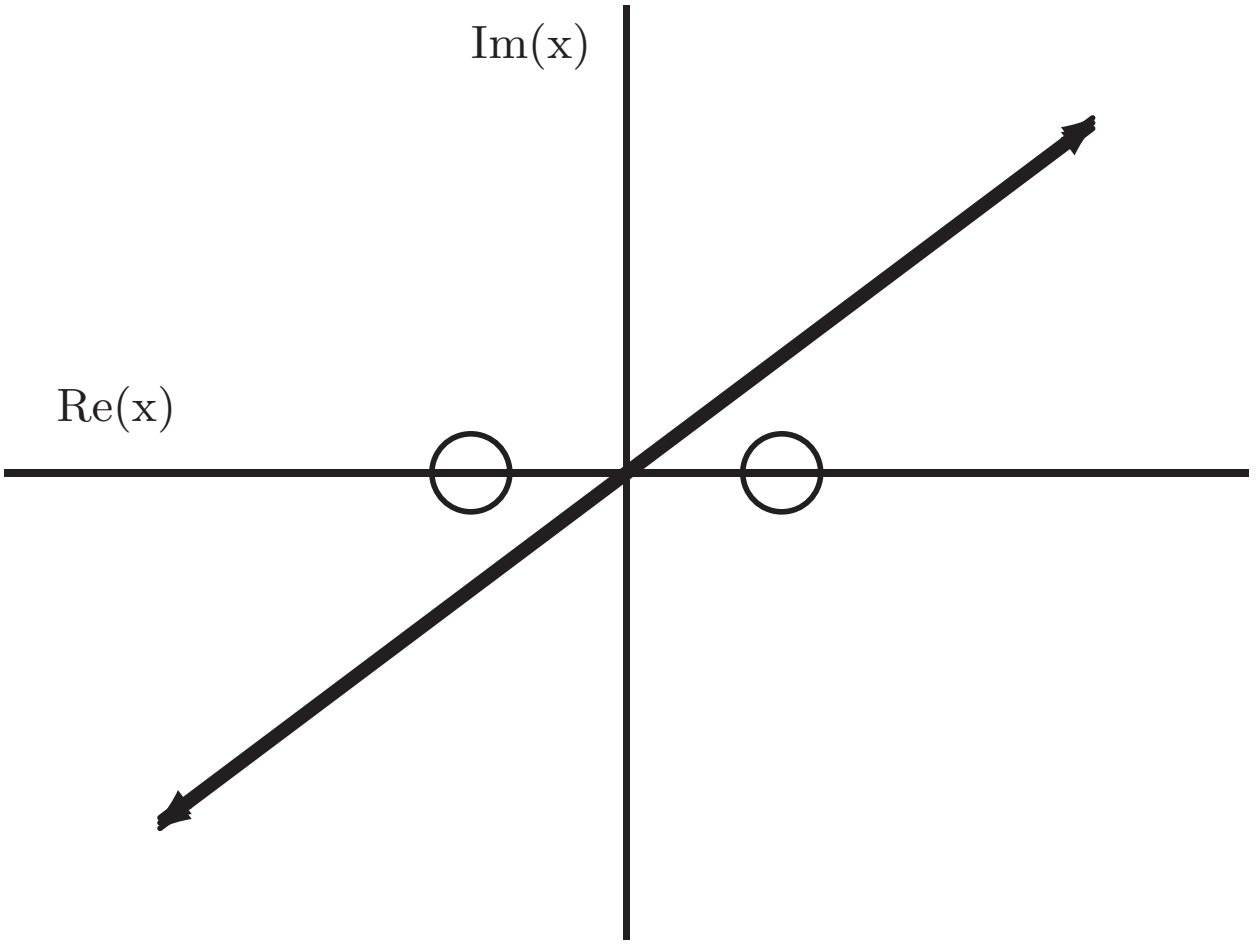

Is this possible? Straight scaling with nuclei not on the grid?

Straight complex scaling does not seem possible for molecules

$$X = xe^{i\theta}$$
$$Y = ye^{i\theta}$$
$$Z = ze^{i\theta}$$

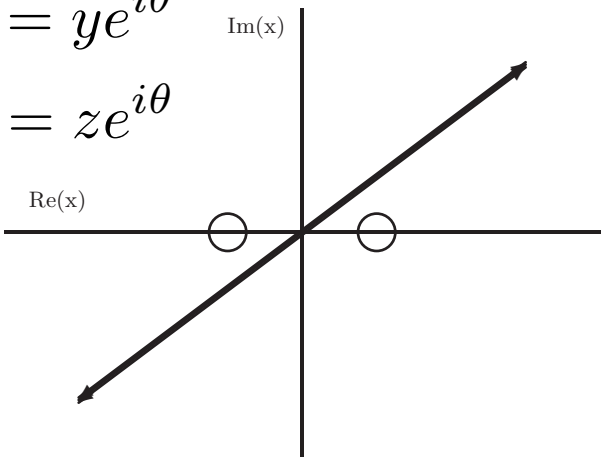

Consider nucleus at (0,0,1)

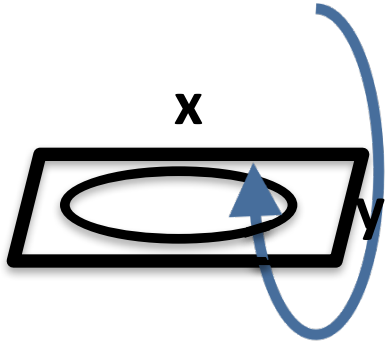

r = sqrt[$X^2 + Y^2 + (Z - 1)^2$]

$r^2 = 0$ at $x^2 + y^2 = \sin^2(\theta)$, $z = \cos(\theta)$

r is NOT SINGLE VALUED

(. . . . but . . . what if the scaling is done with quaternions? Complex scaled quantum mechanics with biquaternions?

$$X = e^{\hat{i}\theta}x \quad Y = e^{\hat{j}\theta}y \quad Z = e^{\hat{k}\theta}z$$

$$h\frac{\partial}{\partial t}\Psi = H\psi \qquad)$$

Complex coordinate scaling for sinc DVR

OUTSTANDING ISSUE:

Complex coordinate scaling destroys triple Toeplitz structure of kinetic energy matrix and therefore kinetic energy matrix inverse.

We DO NOT have a good way to complex scale the two-electron operator with a stretched/scaled basis.

We WANT a way to use triple Toeplitz trick with a stretched/scaled basis!

(But… we really should try quaternion straight scaling which would avoid this problem)

Complex coordinate scaling for sinc DVR

For now: smooth exterior complex scaling and stretching separately in x,y,z for everything EXCEPT FOR COULOMB OPERATORS.

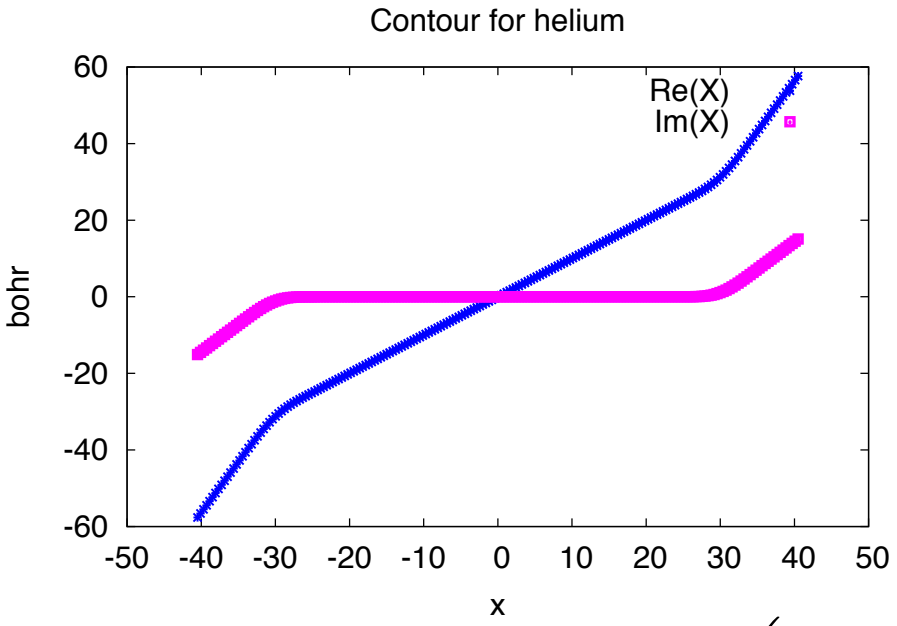

Smooth scaling over finite interval from $x_0=24a_0$ to $x_1=36a_0$.
Values of *a*, *b* and *c* in contour formula below are determined by scaling angle and stretching factor and by making the fourth derivative of X(x) continuous.

$$X(x) = x + a(x - x_0) + b\sin\left(\pi\frac{x - x_0}{x_1 - x_0}\right) + c\sin^3\left(\pi\frac{x - x_0}{x_1 - x_0}\right) \qquad x_0 < x < x_1$$

$$T_x = \left(-\frac{1}{2}\right)\frac{1}{X'(x)}\frac{\partial^2}{\partial x^2}\frac{1}{X'(x)} + \frac{3X''(x)^2 - 2X'''(x)X'(x)}{8X'(x)^4}$$

Complex coordinate scaling for sinc DVR

Model potential

$$V = 0.35(x^2 + y^2 + z^2)\exp\left(-0.13[x^2 + y^2 + (z-2)^2] - 0.13[x^2 + y^2 + (z+2)^2]\right)$$

Converged prolate spheroidal result

energy= 1.15898996 -0.0110861052 i CWM

spacing	points	energy	
0.10 bohr	256^3	1.158989961	-0.011086105 i
0.13 bohr	200^3	1.158989963	-0.011086085 i
0.13 bohr	240^3	1.158989963	-0.011086085 i
0.20 bohr	96^3	1.158951414	-0.011102016 i
0.20 bohr	128^3	1.158989937	-0.011086103 i
0.20 bohr	160^3	1.158989937	-0.011086103 i

Complex coordinate scaling for sinc DVR

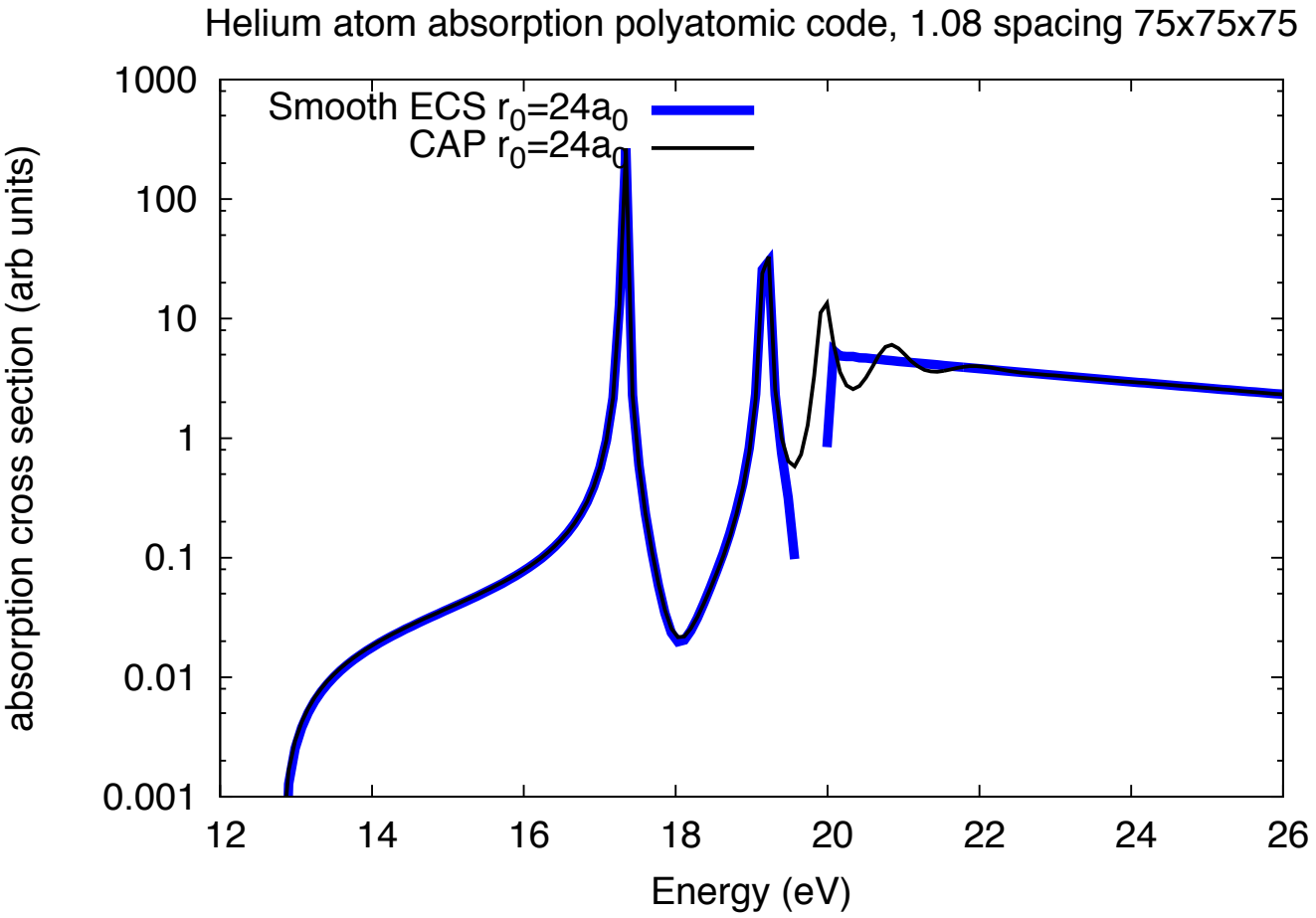

$$V_{CAP}(r) = 0.001 \max(0, r - 24)^2$$

with 1.08 a_0 spacing: E(He^+) = -1.822 E(He^+) = -2.578 → IP = 20.54eV not actual 24.54eV

WITH NUCLEAR MOTION

Prolate spheroidal coordinates for diatoms with nuclear motion

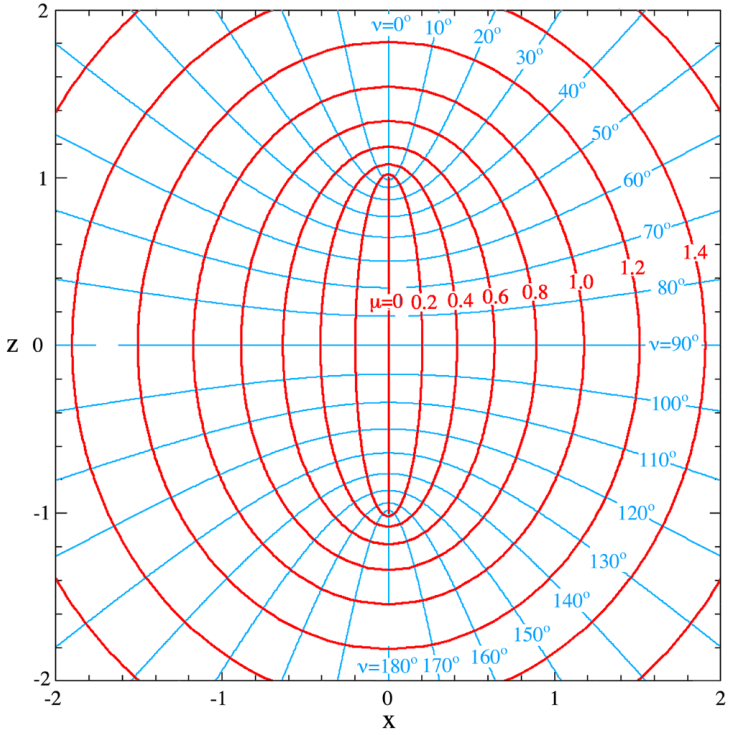

Prolate coordinates ξ, η, azimuthal angle ϕ

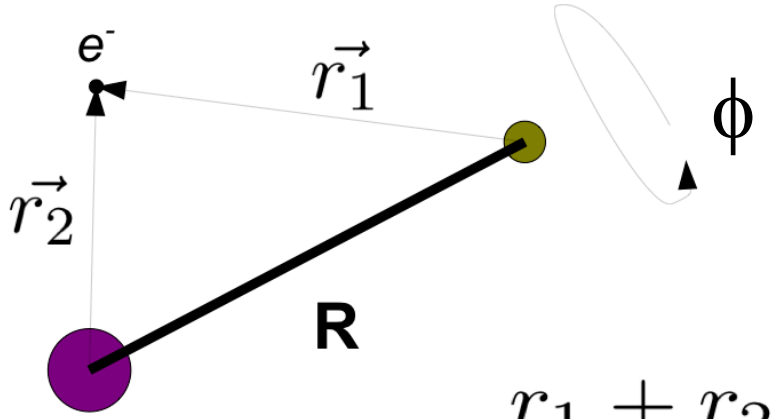

$$\xi = \frac{r_1 + r_2}{R}$$

$$\eta = \frac{r_1 - r_2}{R}$$

See Tao, Rescigno, McCurdy PRA 79, 012719, PRA 80, 013402 (2009); PRA 82, 023423 (2010)

Prolate spheroidal Hamiltonian: Esry & Sadeghpour, PRA 60, 3604 (1999)

One set of orbitals used for all nuclear geometries,
parameterized by nuclear geometry.

Cusps follow nuclei.

Vibrational transitions converge with respect to number of orbitals.

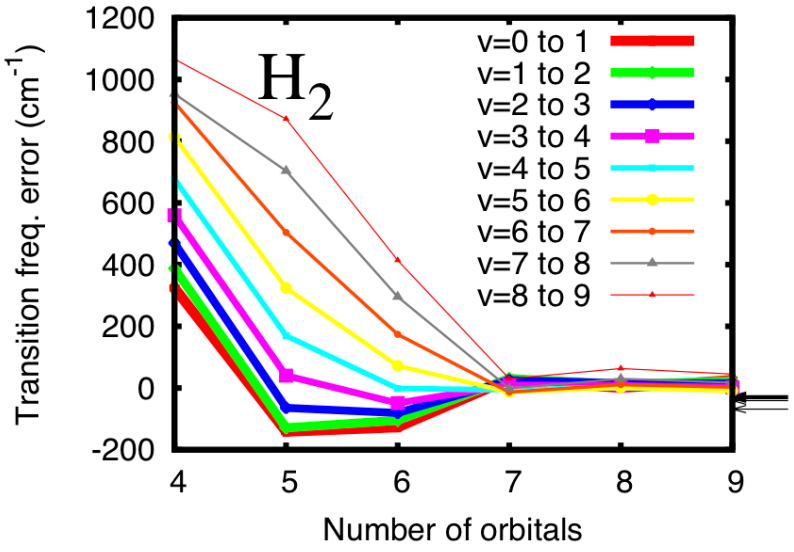

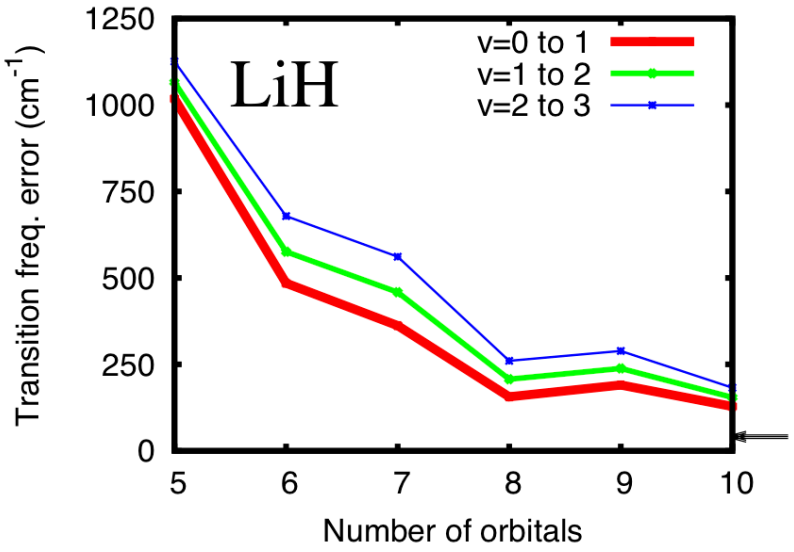

Natural orbital occupations
are close to those
of Born Oppenheimer wave
function –
Prolate coordinates are good

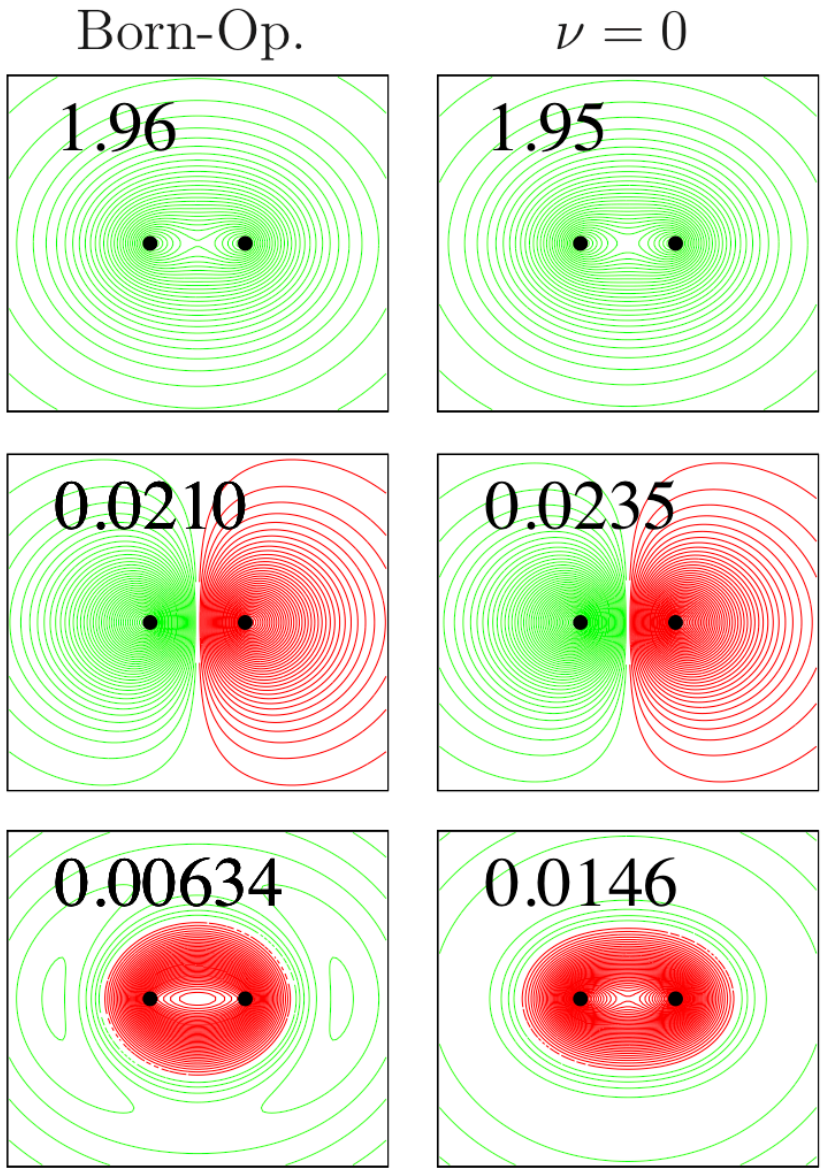

	ν	$< E >$	$\langle T \rangle$	$\langle V \rangle$	$\langle r_1 \rangle$	$\langle r_1^2 \rangle$	$\langle r_2 \rangle$	$\langle r_2^2 \rangle$	$\langle R \rangle$	$\langle R^2 \rangle$	D
5σ 1π H_2	0	-1.16008	1.16006	-2.32014	1.5834	3.1894	1.5834	3.1893	1.4553	2.1451	0.0000
8σ 1π H_2	0	-1.16088	1.16085	-2.32174	1.5784	3.1620	1.5784	3.1620	1.4527	2.1383	0.0000
Ref. [63][a], [64][b]	0	-1.16403[a,b]	1.16403[b]	2.32805[b]					1.4487[a]	2.1270[a]	
5σ 1π B.O.	0			-2.32242	1.5773	3.1557	1.5773	3.1557	1.4520	2.1367	0.0000
5σ 1π H_2	1	-1.14047	1.14040	-2.28087	1.6270	3.3691	1.6270	3.3691	1.5482	2.4787	0.0000
8σ 1π H_2	1	-1.14156	1.14167	-2.28324	1.6295	3.38286	1.6295	3.3826	1.5482	2.4817	0.0000
Ref. [63]	1	-1.14506							1.5453	2.4740	
5σ 1π HD	0	-1.16164	1.16158	-2.32322	1.57520	3.14928	1.57547	3.15029	1.44634	2.11511	-.0005391
Ref. [65]	0	-1.16547			1.57119	3.13009	1.57148	3.13120	1.44223	2.10432	
5σ 1π B.O.	0			-2.32506	1.5738	3.1409	1.5738	3.1409	1.4456	2.1142	0.0
6-σ 1π LiH	0	-8.03762	8.03765	-16.0753	2.5808	7.8354	1.9864	6.6936	3.0834	9.5398	2.3458
Ref.[66]	0	-8.06644			2.5651	7.74517	1.9719	6.5857	3.0610	9.4197	
6-σ 1π BO	0			-16.08629	2.6219	8.1238	2.0066	6.8593	3.1285	9.8404	2.3306

TABLE III: Properties of vibronic states. The H_2 calculation is from a state averaged calculation on the $\nu = 0$ and $\nu = 1$ states. Otherwise the energy of the ground vibrational state has been minimized. With six σ and one π orbital for LiH, fixed nuclei at 3.015, the dipole moment calculated was 2.2856 atomic units as may be compared with the prior result of 2.306 [67].

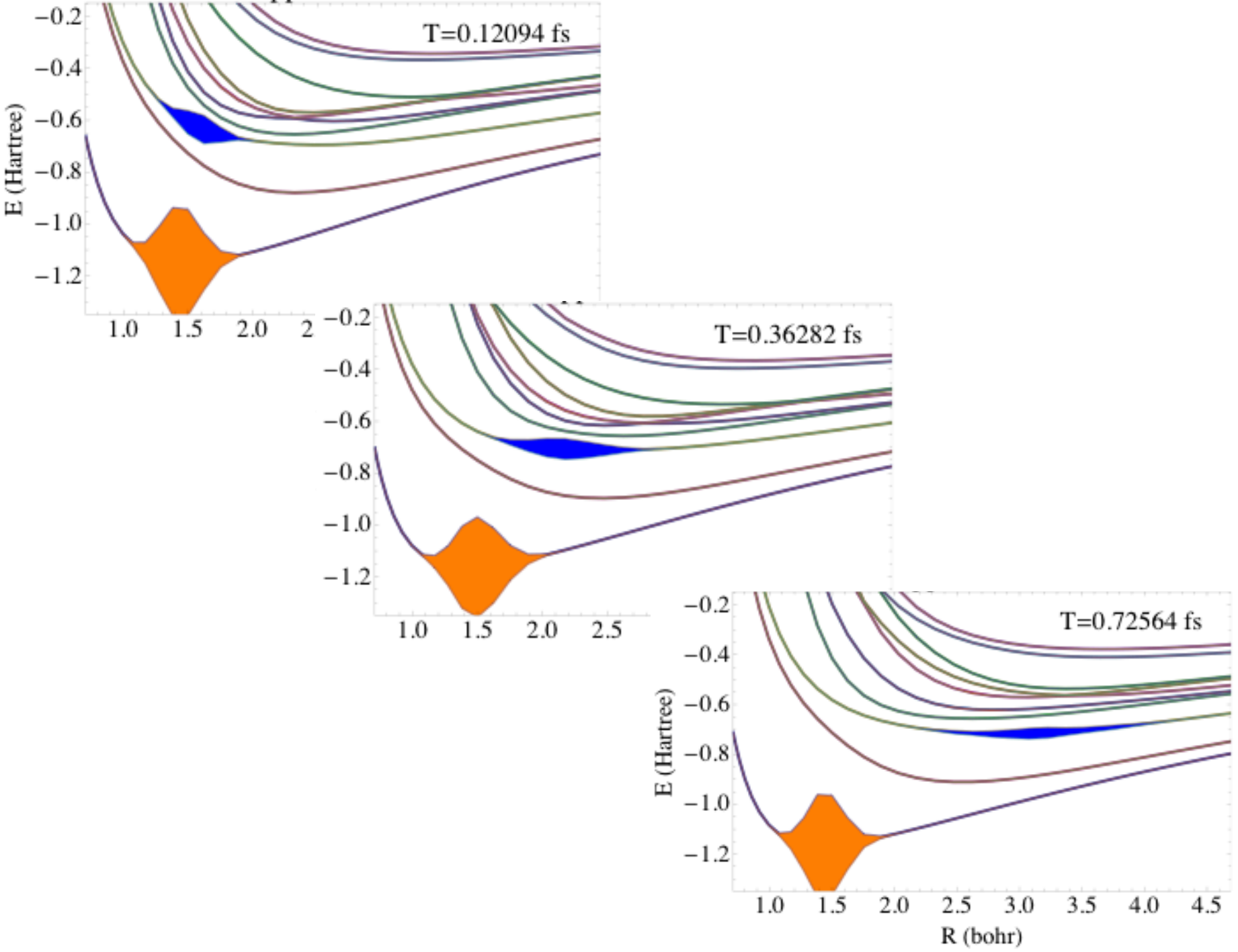
T=0.12094 fs
T=0.36282 fs
T=0.72564 fs
E (Hartree)
R (bohr)
−0.2
−0.4
−0.6
−0.8
−1.0
−1.2
1.0
1.5
2.0
2.5
3.0
3.5
4.0
4.5

Dissociative ionization of H_2^+ PRA 91, 062502

PARALLEL

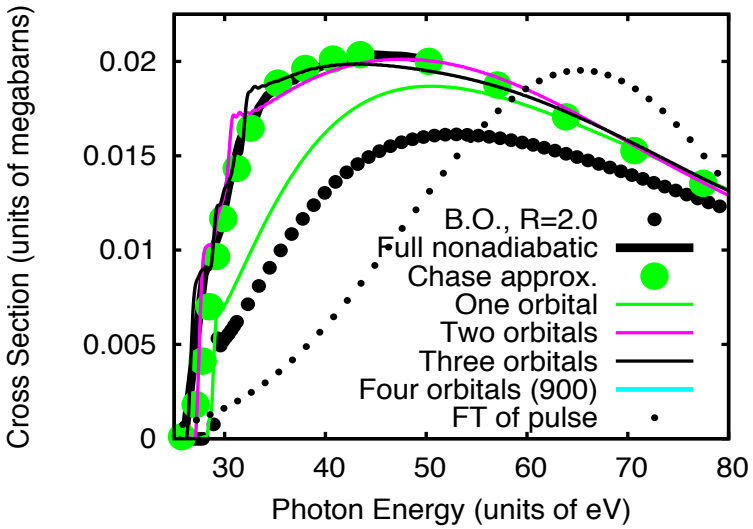

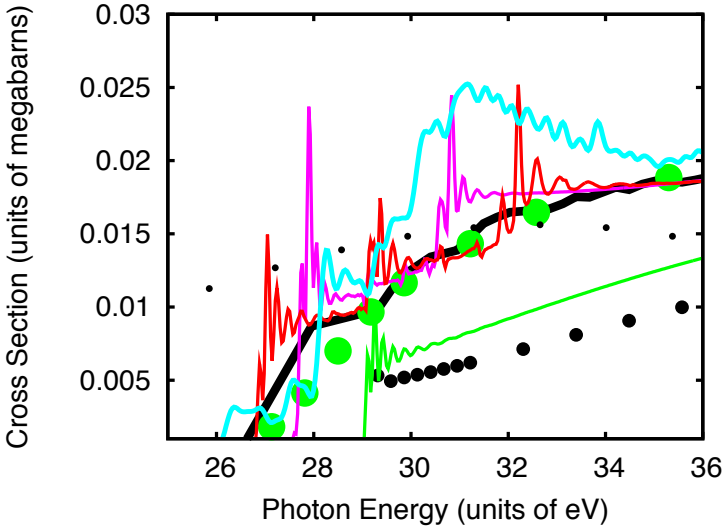

PERPENDICULAR

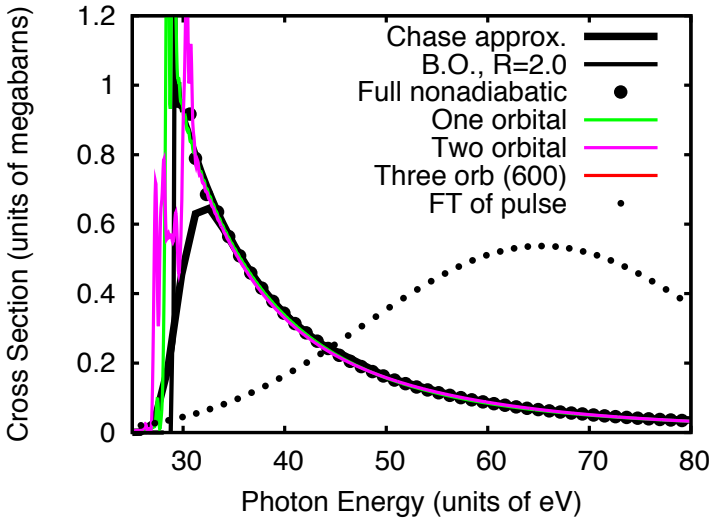

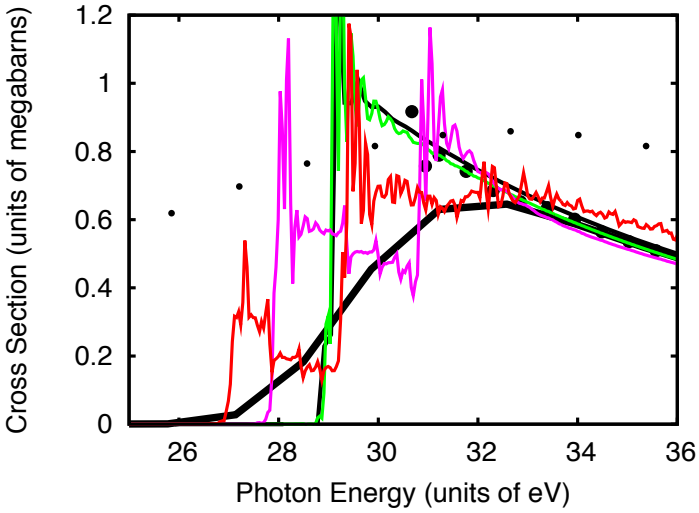

uxsl ultrafast x-ray science laboratory
uxsl ultrafast x-ray science laboratory

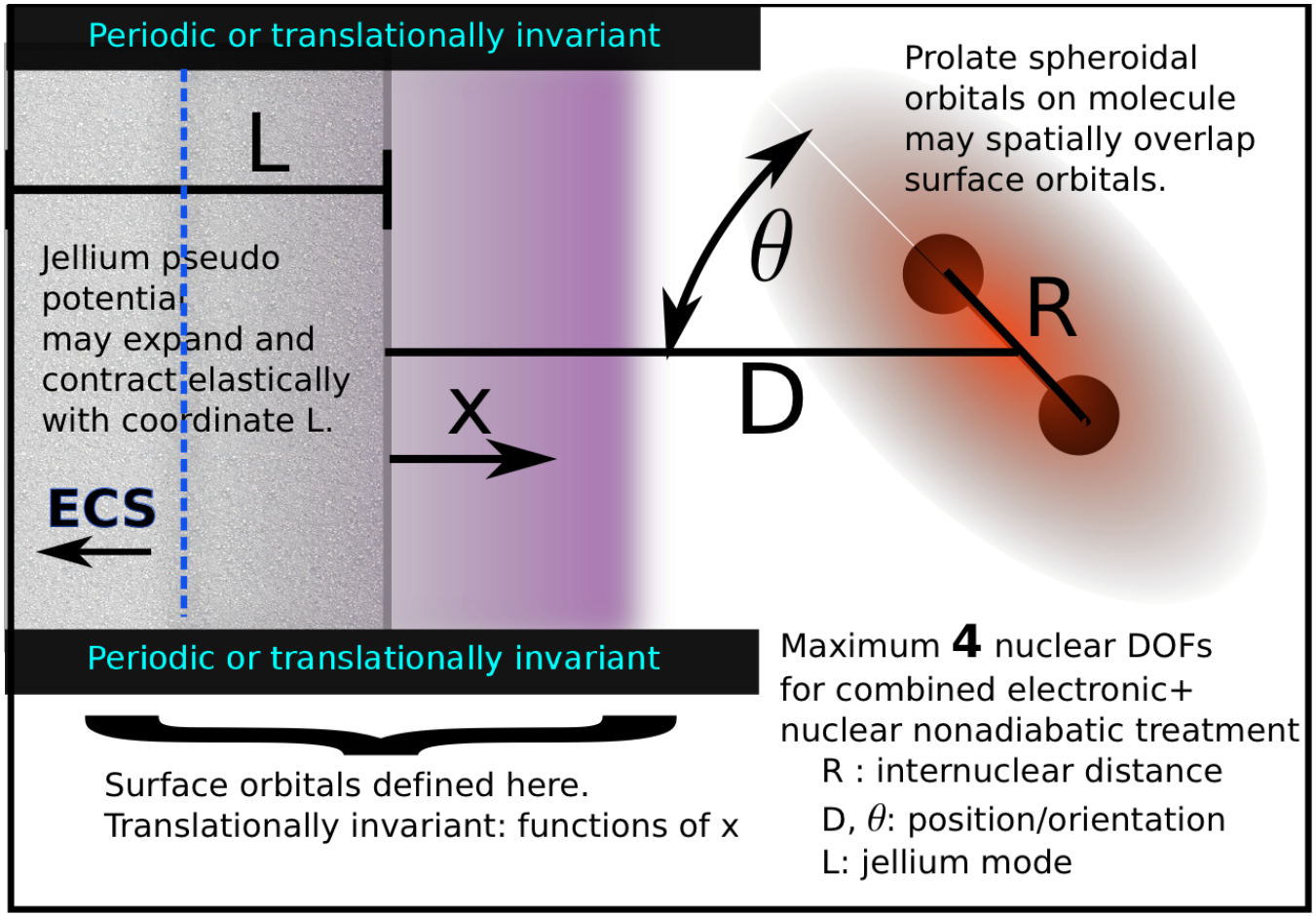

$$H(L, D, \theta, R, \vec{x}) \approx T + \frac{k}{2}(L - L_0)^2 + \frac{Z_1 Z_2}{R}$$
$$+ \sum_{i,a=1,2} \frac{-Z_a}{r_{ia}} + \sum_{i\langle j} \left[\frac{1}{r_{ij}} + H^{int}_{jellium}(x_i, x_j; L, D?, \theta?, E?) \right]$$

COMPLEX DOMCKE WAVE-MIXING

WE WANT TO DECOMPOSE THE SIGNAL FROM A NONLINEAR LASER EXPERIMENT INTO ITS CONTRIBUTIONS FROM DIFFERENT NUMBERS OF PHOTONS ABSORBED/EMITTED FROM EACH LASER USED IN THE EXPERIMENT.

Wavelength dependence of momentum-space images of low-energy electrons generated by short intense laser pulses at high intensities

C M Maharjan[1], A S Alnaser[1,2], I Litvinyuk[1], P Ranitovic[1] and C L Cocke[1]

J. Phys. B: At. Mol. Opt. Phys. 39, 1955 (2006)

We have measured momentum-space images of low-energy electrons generated by the interaction of short intense laser pulses with argon atoms at high intensities. We have done this over a wavelength range from 400 to 800 nm. The spectra show considerable structure in both the energy and angular distributions of the electrons. Some, but not all, energy features can be identified as multi-photon resonances. The angular structure shows a regularity which transcends the resonant structure and may be due instead to diffraction. The complexity of the results defies easy model-dependent interpretations and invites full solutions to Schrödinger's equation for these systems.

of momentum-space images of low-energy electrons

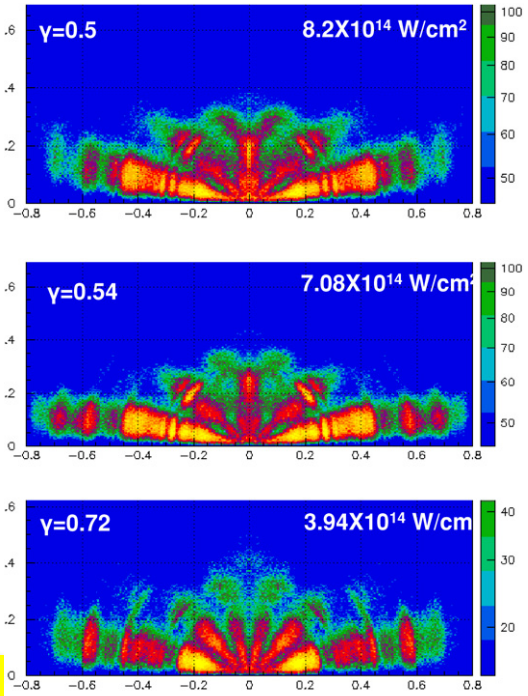

Transient XUV absorption in Helium + IR

This feature is He 1s2s + 1 IR photon

CHEN, WU, GAARDE, AND SCHAFER

Phys Rev A 87, 033408 (2013)

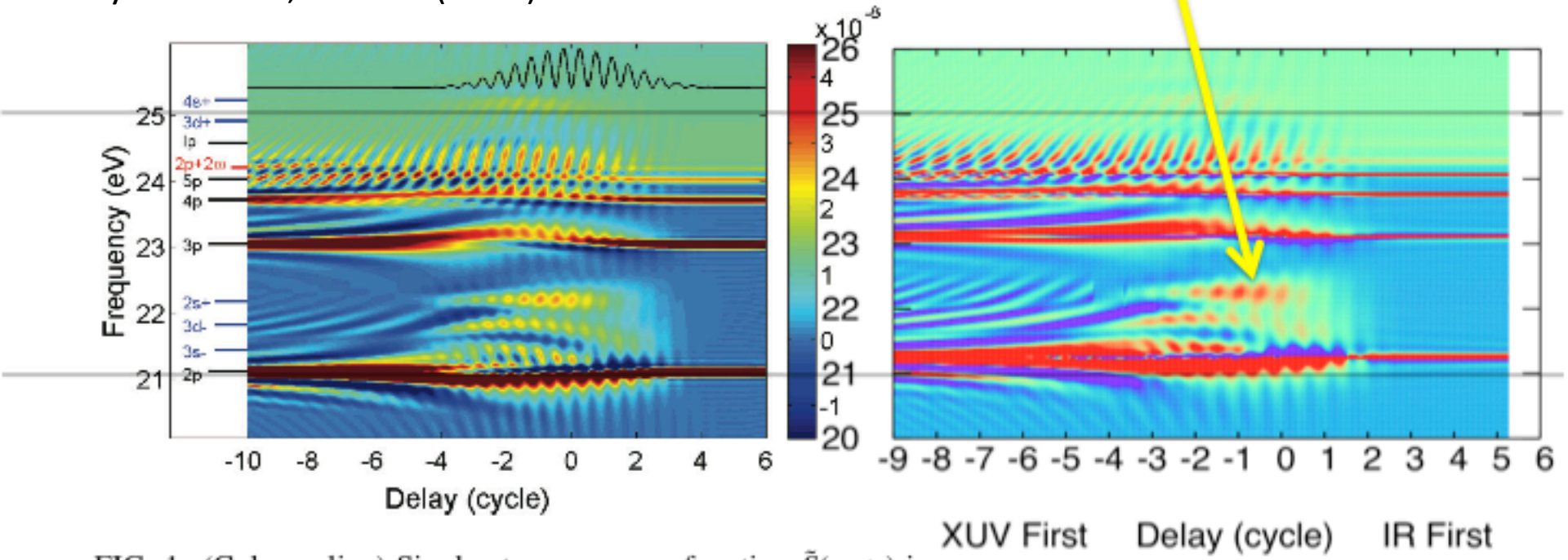

FIG. 1. (Color online) Single atom response function $\tilde{S}(\omega,t_d)$ in helium where t_d is the time delay in IR cycles between the IR laser pulse (800 nm, 3×10^{12} W/cm^2, 4 cycles, cos^2 envelope, sine-like carrier envelope) and the attosecond pulse (330 as, centered at 25 eV). The IR intensity oscillations are shown in black in the top panel.

See also Chen et al,
"Light induced states in attosecond transient absorption spectra of laser-dressed Helium"
Phys Rev A 86, 063408 (2013)

WE WANT TO DECOMPOSE THE SIGNAL FROM A NONLINEAR LASER EXPERIMENT INTO ITS CONTRIBUTIONS FROM DIFFERENT NUMBERS OF PHOTONS ABSORBED/EMITTED FROM EACH LASER USED IN THE EXPERIMENT.

Efficient Calculation of Time- and Frequency-Resolved Four-Wave-Mixing Signals

MAXIM F. GELIN, DASSIA EGOROVA, AND
WOLFGANG DOMCKE*

ACCOUNTS OF CHEMICAL RESEARCH ■ 1290-1298 ■ September 2009 ■ Vol. 42, No. 9

There exist two conceptually different approaches to the calculation of the nonlinear polarization. In the standard perturbative approach to nonlinear spectroscopy, the third-order polarization is expressed in terms of the nonlinear response functions. As the material systems become more complex, the evaluation of the response functions becomes cumbersome and the calculation of the signals necessitates a number of approximations.

Herein, we review alternative methods for the calculation of four-wave-mixing signals, in which the relevant laser pulses are incorporated into the system Hamiltonian and the driven system dynamics is simulated numerically exactly.

TWO DIFFERENT APPROACHES

1) DO PERTURBATION THEORY (NEED TO IDENTIFY STATES)
2) SOLVE TIME-DEPENDENT SCHRODINGER EQUATION

Domcke's method for wave mixing performs decomposition in terms of NET number photons absorbed/emitted.

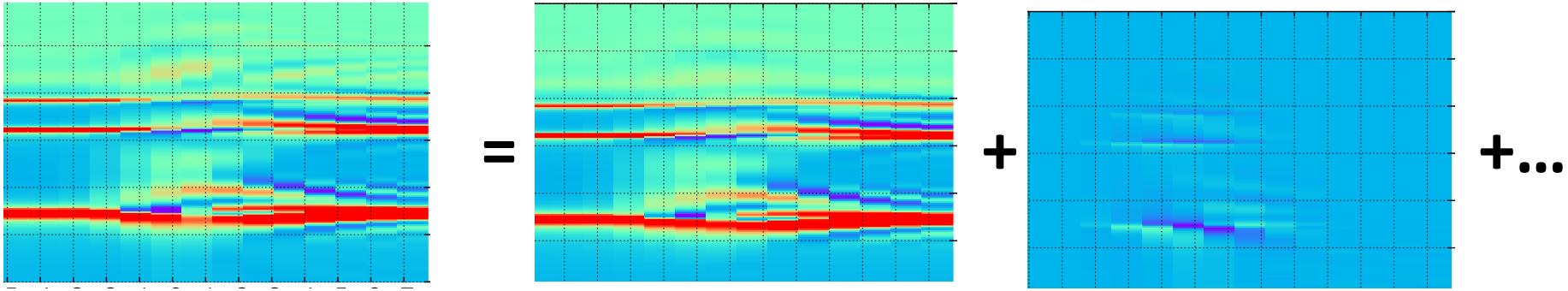

L. Seidner, G. Stock, and W. Domcke. J. Chem. Phys. **103**, 3998 (1995)
S. Meyer and V. Engel. Appl. Phys. B **71**, 293 (2000)
H. Wang and M. Thoss. Chem. Phys. **347**, 139 (2008)

A complex-valued generalization of Domcke's method gives VERY PROMISING RESULTS but is GAUGE-DEPENDENT.

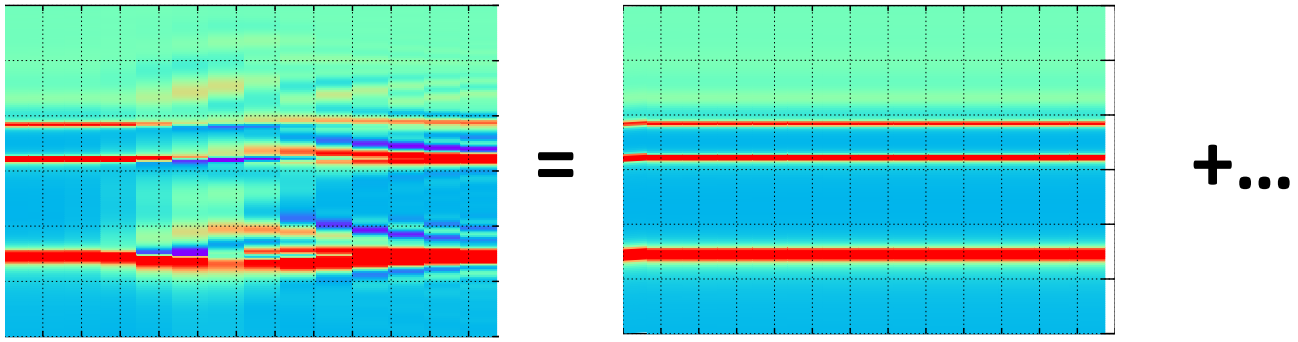

Opposite circular polarization

No feature if opposite circular polarizations

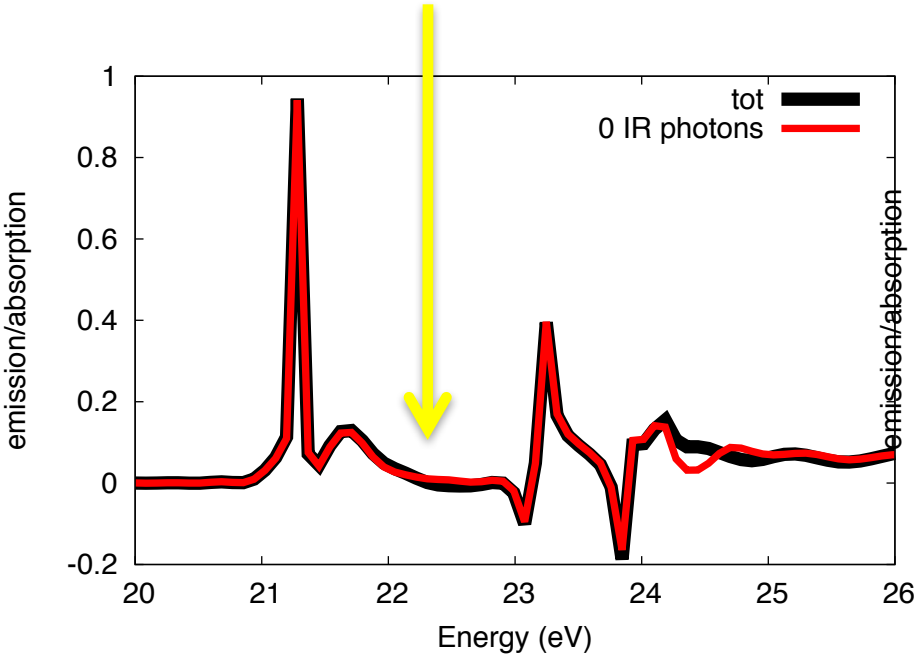

Same circular polarization

This feature is He 1s2s + 1 IR photon

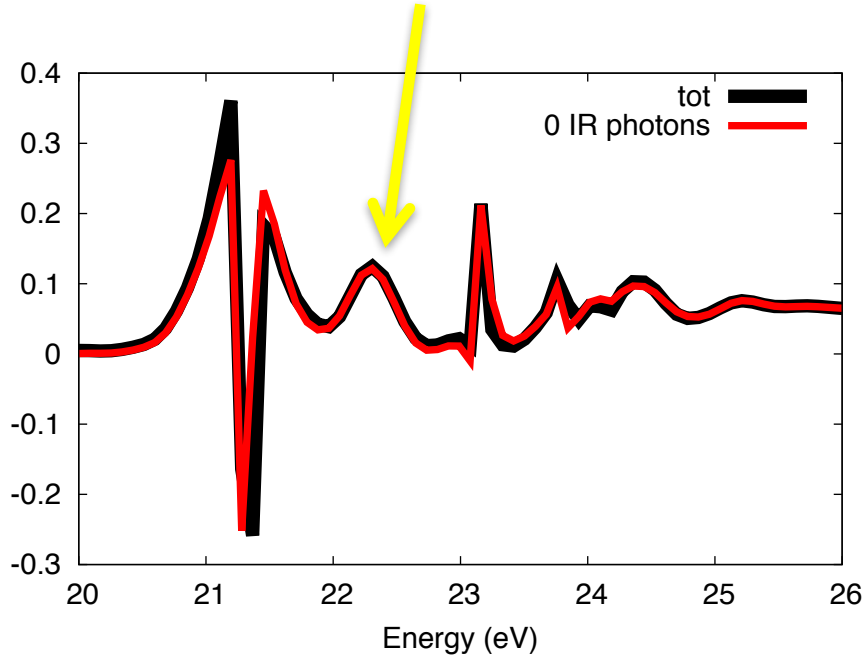

"Circular polarization gives you more information."

At ~22.2eV it absorbs XUV and emits IR

22.2-1.6 = 20.6 He 1s2s

Since it is an S state, polarizations must be the same

(waving his hands saying)

Multi-fragment vector correlation imaging. A search for hidden dynamical symmetries in many-particle molecular fragmentation processes

Mol Phys 110, 1863 (2012)

F Trinter, L.Ph.H Schmidt, T Jahnke, M.S. Schöffler, O Jagutzki, A Czasch, J Lower, T.A Isaev, R. Berger, A.L. Landers, Th. Weber, R. Dörner, H. Schmidt-Böcking